



THE UNIVERSITY OF  
**WAIKATO**  
*Te Whare Wānanga o Waikato*

**Research Commons**

<http://researchcommons.waikato.ac.nz/>

## **Research Commons at the University of Waikato**

### **Copyright Statement:**

The digital copy of this thesis is protected by the Copyright Act 1994 (New Zealand).

The thesis may be consulted by you, provided you comply with the provisions of the Act and the following conditions of use:

- Any use you make of these documents or images must be for research or private study purposes only, and you may not make them available to any other person.
- Authors control the copyright of their thesis. You will recognise the author's right to be identified as the author of the thesis, and due acknowledgement will be made to the author where appropriate.
- You will obtain the author's permission before publishing any material from the thesis.

**INFLUENCE OF VEGETATION COVER ON  
COASTAL AQUIFER FLUCTUATIONS AND  
SAND TRANSPORT ON MATAKANA ISLAND**

A thesis  
submitted in partial fulfilment  
of the requirements for the degree  
of  
**Master of Science in Earth and Ocean Sciences**  
at  
**The University of Waikato**  
by

**JOSHUA MÜLLER**



The University of Waikato

2011



# ***ABSTRACT***

---

The Bay of Plenty beaches on the east coast of the North Island, New Zealand are of significant physical, ecological and economic importance. Over the previous century, anthropogenic development and the introduction of non-indigenous coastal plant species has lead to a degradation of many of the Bay of Plenty regions' coastal dune environments. Restoring these sections of coastline to their natural state strengthens the barrier they provide between coastal developments and the coastal ocean, whilst also promoting the growth of native plant species and improving habitat for local macro-invertebrate species.

The influence of vegetation on aquifer levels and aeolian sediment transport in the dune and foredune was investigated at Matakana Island in the Western Bay of Plenty. Monitoring of the water table between March and November 2010 was undertaken at two adjacent sample sites, with different dominant overlying vegetation, *Ammophila arenaria* and *Spinifex sericeus*. During this time, aeolian sediment transport rates were also monitored through the deployment of sediment traps and two small climate stations.

Results showed that aquifer levels beneath the dune face were highly variable. Fluctuations occurred at a range of time scales, stemming from variations in tide, rainfall and profile shape. Short-term fluctuation was primarily linked to tidal forcing. Tidal fluctuations were observed in the aquifer, and differed from tidal fluctuations directly offshore in their shape and amplitude, with some lag between tide and aquifer fluctuations also evident. Aquifer fluctuation shape and lag, and differences between sample sites were linked to the beach drainage capability through aquifer porosity and permeability; hydraulic conductivity; and transmissivity. Long-term change in beach profile shape further influenced aquifer levels, with an accreting beach resulting in an elevating average aquifer level and an eroding beach resulting in a diminishing aquifer level.

Aeolian sediment deposition varied greatly across the cross-shore profile. Transport rates were limited by a small beach width when high tides combined with storm surge and wave run-ups limiting the source area. Rainfall further reduced transport potential when coinciding with high wind speed events.

Sediment deposition was evenly distributed in the *Spinifex* dominated dune system, whilst deposition in the *Ammophila* dune primarily occurred at the seaward limit of vegetation growth. This pattern of deposition is linked to the characteristics of each species, primarily their average height and growth density.

Sediment deposition differences between sites explain variances in sediment compaction which alters dune porosity and permeability at each site. Greater porosity and permeability in the *Spinifex* dominated dune saw the aquifer draining more readily. Lower beach aquifer levels aid accretion and greaten the source for onshore aeolian sediment transport. *Spinifex* dominated dunes are therefore suggested to provide healthier beach states on Bay of Plenty beaches.

## ***ACKNOWLEDGEMENTS***

---

First and foremost my primary thanks go to my supervisor Dr Willem deLange. Your support, help, patience, guidance and realistic approach with this project has been greatly appreciated. Thanks for allowing me a project that involved field work in an area I am passionate about, and that maximised my beach hours.

Thanks to Walter Stahel, Witana Murray and Pim deMonchy at Bay of Plenty Regional Council for initially suggesting the site and allowing me to dig holes in the sand dunes. I also wish to thank Greg Jenks at Woodlands Consultants for your help, enthusiasm and suggestions during the initial stages of this project.

A massive thank you to Steve, Harry and Geoff at Blakely Pacific for allowing me the use of your barge when getting to the Island, for allowing me to be on your land, and for always showing an interest in what I was doing. Big thanks also to the crew of the Skookum for getting me safely to and from the Island whenever I needed to get into the field.

Thanks to Craig Hosking for all your help setting up my sampling stations, dealing with instrument issues and accompanying me on field visits. Thanks also to Chris McKinnon and Annette Rodgers for all your help with work in both the field and the lab. Thanks to Josh Mawer for your help in the field. To those that dwelled in the dungeon, thanks for riding this train with me and always managing a smile. Thanks go to James for letting me bounce ideas off you, for sharing a realistic approach to this task and always having time for a laugh. Thanks also go to Bryna for your suggestions and advice, help with Matlab, and for putting up with the grief that I gave you.

Thank you to Kelly, your constant support, encouragement, proofing and ability to not get bored with my ramblings over the past 18 months has been invaluable.

Last but not least, thank you to my friends and family for your support. Most of all to Mum and Dad, thank you for your encouragement, help and support, and for being the continual inspiration behind my studies.

*“Ehara taku toa, he taki tahi, he toa taki tini”*



# ***TABLE OF CONTENTS***

---

|                         |     |
|-------------------------|-----|
| Abstract .....          | iii |
| Acknowledgements .....  | v   |
| Table of Contents ..... | vii |
| List of Figures .....   | xi  |
| List of Tables.....     | xv  |

## **CHAPTER ONE**

|                                  |   |
|----------------------------------|---|
| 1.1 MOTIVATION FOR STUDY .....   | 1 |
| 1.2 STUDY SITE DESCRIPTION ..... | 1 |
| 1.2.1 Climate .....              | 3 |
| 1.3 RESEARCH AIMS .....          | 7 |
| 1.4 THESIS OUTLINE .....         | 7 |

## **CHAPTER TWO**

|  |    |
|--|----|
| 2.1 INTRODUCTION .....                         | 9  |
| 2.1 NEW ZEALAND DUNES.....                     | 10 |
| 2.2 DUNE VEGETATION .....                      | 10 |
| 2.2.1 Marram Grass.....                        | 11 |
| 2.2.1 Spinifex .....                           | 12 |
| 2.2.3 Significance of Vegetation.....          | 13 |
| 2.3 WATER TABLE IMPACTS ON BEACH PROFILES..... | 14 |
| 2.3.1 Groundwater.....                         | 14 |
| 2.3.2 Impact of lowering the water table.....  | 18 |
| 2.4 AEOLIAN SEDIMENT TRANSPORT.....            | 18 |
| 2.5 BEACH PROFILES AND EROSION .....           | 21 |
| 2.6 SUMMARY .....                              | 23 |

## **CHAPTER THREE**

|                       |    |
|-----------------------|----|
| 3.1 INTRODUCTION..... | 25 |
|-----------------------|----|

|       |                                |    |
|-------|--------------------------------|----|
| 3.2   | METHODOLOGY .....              | 25 |
| 3.2.1 | Vegetation Sampling .....      | 25 |
| 3.2.2 | Profile Sampling .....         | 26 |
| 3.2.3 | Compaction Sampling .....      | 28 |
| 3.3   | RESULTS .....                  | 29 |
| 3.3.1 | Vegetation Results .....       | 29 |
| 3.3.2 | Profile Results .....          | 30 |
| 3.3.3 | Sediment Characteristics ..... | 31 |
| 3.3.3 | Compaction Results .....       | 32 |
| 3.4   | CLASSIFICATION .....           | 33 |
| 3.4.1 | Vegetation classification..... | 33 |
| 3.4.2 | Profile classification .....   | 34 |
| 3.4.3 | Sediment classification .....  | 34 |
| 3.4.4 | Sediment Compaction .....      | 35 |
| 3.4.5 | Overall Classification .....   | 36 |

## CHAPTER FOUR

|         |   |    |
|---------|---|----|
| 4.1     | INTRODUCTION .....  | 38 |
| 4.1.2   | Expected Outcomes .....   | 38 |
| 4.2     | METHODOLOGY .....   | 38 |
| 4.2.1   | Local Climate .....   | 38 |
| 4.2.2   | Piezometer Placement and Measurement .....  | 41 |
| 4.2.3   | Sampling Limitations .....  | 44 |
| 4.3     | RESULTS .....   | 45 |
| 4.3.1   | General aquifer fluctuation .....   | 45 |
| 4.3.1.1 | Aquifer response to tidal fluctuations .....  | 45 |
| 4.3.1.2 | Aquifer response to rainfall infiltration .....                                     | 48 |
| 4.3.1.3 | Aquifer response to profile evolution .....   | 49 |
| 4.3.2   | Potential aquifer response to sediment compaction and overlying<br>vegetation. .... | 52 |
| 4.4     | DISCUSSION .....  | 54 |
| 4.4.1   | General aquifer fluctuation.....  | 54 |

|        |  |    |
|--------|--|----|
| 4.4.2. | Potential aquifer response to sediment compaction and overlying vegetation. .... | 58 |
| 4.4    | CONCLUSIONS .....  | 60 |

## CHAPTER FIVE

|       |   |    |
|-------|---|----|
| 5.1   | INTRODUCTION.....                         | 62 |
| 5.1.2 | Expected Outcomes.....                    | 62 |
| 5.2   | METHODOLOGY .....                         | 63 |
| 5.2.1 | Vegetation Sampling.....                  | 63 |
| 5.2.2 | Aeolian Sediment Transport Sampling ..... | 63 |
| 5.2.3 | Wind and Rainfall Sampling.....           | 66 |
| 5.2.4 | Sampling Limitations .....                | 68 |
| 5.3   | RESULTS.....                              | 69 |
| 5.3.1 | Vegetation .....                          | 69 |
| 5.3.2 | Wind Sampling .....                       | 69 |
| 5.3.3 | Aeolian Transport Results.....            | 74 |
| 5.3.4 | Aeolian Sediment Characteristics .....    | 89 |
| 5.4   | DISCUSSION .....                          | 91 |
| 5.4.1 | Vegetation and wind interactions.....     | 91 |
| 5.4.2 | Aeolian sediment movement.....            | 92 |
| 5.4.3 | Limitations with Results .....            | 97 |
| 5.4.4 | Further Research .....                    | 97 |
| 5.5   | CONCLUSIONS .....                         | 98 |

## CHAPTER SIX

|     |   |     |
|-----|---|-----|
| 6.1 | INTRODUCTION.....                       | 100 |
| 6.2 | SAND DUNE CLASSIFICATION.....           | 100 |
| 6.3 | SHORT-TERM AQUIFER FLUCTUATION .....    | 101 |
| 6.4 | AEOLIAN SEDIMENT TRANSPORT.....         | 101 |
| 6.5 | SUMMARY .....                           | 102 |
| 6.6 | RECOMENDATIONS FOR FUTURE Research..... | 103 |
|     | REFERENCES.....                         | 106 |

|                    |     |
|--------------------|-----|
| APPENDIX I.....    | 114 |
| APPENDIX II.....   | 116 |
| APPENDIX III ..... | 118 |

## LIST OF FIGURES

---

|   |    |
|---|----|
| <b>Figure 1.1:</b> Map of Matakana Island in the Western Bay of Plenty region. Inset shows Island's position in relation to the North Island (Te Ika a Maui) of New Zealand. Taken from Shepherd <i>et al</i> (1997).   | 2  |
| <b>Figure 1.2:</b> Photographic image showing the Pipeline Road area of Matakana Island. Red box indicates specific location of study site on the Island. Image from Bay of Plenty Regional Council.  | 3  |
| <b>Figure 1.3:</b> 5 year hind cast of wind speeds and directions for stations at Waihi (top) and Tauranga Aero Club (bottom). 0.9% of data is below the calm threshold. Data from CliFlo (2010). Stations plotted are the closest to Matakana Island at a low elevation. | 5  |
| <b>Figure 1.4:</b> Wave climate for Matakana Island. Adapted from Shepherd <i>et al</i> (1997). Wave data from Harry & Healy (1978).  | 6  |
| <b>Figure 2.1:</b> Marram Grass on Matakana Island foredune, Western Bay of Plenty.   | 11 |
| <b>Figure 2.2:</b> Spinifex on Matakana Island foredune, Western Bay of Plenty.   | 13 |
| <b>Figure 2.3:</b> Foredune profiles formed by their overlying vegetation type, Marram A, Spinifex B and Pingao (c). Adapted from Esler (1970).   | 14 |
| <b>Figure 2.4:</b> The effects of watertable elevation and slope on swash zone deposition and erosion (adapted from Duncan, 1964).  | 17 |
| <b>Figure 2.5:</b> Leatherman's vertical rod sand trap design (Leatherman, 1978).   | 21 |
| <b>Figure 3.1:</b> Vegetation sampling, 2 x 2 m <sup>2</sup> quadrant at sample site B.   | 26 |
| <b>Figure 3.2:</b> Typical beach profile cross section at sample site B identified by the red line.   | 27 |
| <b>Figure 3.3:</b> Vegetation species and their estimated percentage of total cover at sample sites A & B including error bars of 1 standard deviation for sample sites A and B.  | 29 |
| <b>Figure 3.4:</b> Initial profile shape plots recorded on Julian Day 63 for sample sites A and B extending from top of dune to water.  | 30 |
| <b>Figure 3.5:</b> Average sediment compaction results at intervals across cross-shore transects at sites A & B obtained from Scala Penetrometer testing (error bars indicate 1 standard deviation away from mean).   | 32 |
| <b>Figure 4.1:</b> Station set-up at sample site A measuring wind speed, direction and rainfall. Wind speed and rainfall are collected from the top of a 4m tower.  | 39 |
| <b>Figure 4.2:</b> Rainfall at sample site A and Tauranga Aero Club (obtained from NIWA's CliFlo programme) for a 37 day period from early April to early May, 2010.  | 40 |
| <b>Figure 4.3:</b> Piezometer placement in the fore dune of Station B. Red box indicating position of PVC tubing, pressure sensor and waratah.  | 41 |
| <b>Figure 4.4:</b> Profiles for sample sites A & B, showing piezometer location in sample site A (top) and sample site B (bottom).  | 42 |

|  |    |
|--|----|
| <b>Figure 4.5:</b> Regression correlation plot for aquifer depth at sites A & B over an 11 day period beginning late April and ending in early May, 2010.  | 44 |
| <b>Figure 4.6:</b> Aquifer level below surface at sample sites A & B and Matakana Island onsite tide heights (generated via NIWA's Tide Forecaster) for 5 day period in late April to early May, 2010.   | 45 |
| <b>Figure 4.7:</b> Aquifer level below surface at sample site B and rainfall for Tauranga Aero Club (NIWA CliFlo data) over a 100 day period from late March to early July, 2010.  | 47 |
| <b>Figure 4.8:</b> Aquifer level below surface at sample site B over a 100 day period from late March to early July, 2010. Red box indicates a period of elevated minimum aquifer level and is discussed in the text   | 49 |
| <b>Figure 4.9:</b> Beach profiles above mean sea level (MSL) at site B for days 90, 138 and 210, showing beach profile evolution over a 120 day period from late March to late July in 2010. Piezometer location is also displayed.  | 50 |
| <b>Figure 4.10:</b> Beach profiles above mean sea level (MSL) at site A for days 90, 138 and 210, showing beach profile evolution over a 120 day period from late March to late July in 2010. Piezometer location is also displayed.   | 51 |
| <b>Figure 4.11:</b> 12 hourly average aquifer level and sites A & B over a 12 day period from late April to early May, 2010. Also shown is the difference between site A and site B means for the same time intervals.   | 52 |
| <b>Figure 4.12:</b> 12 hourly average aquifer level and sites A & B over a 5 day period in April, 2010. Also shown is the difference between site A and site B means for the same time intervals. Lines of best fit have been applied to the three data sets.  | 53 |
| <b>Figure 5.1:</b> Aeolian trap unit design modified from Leatherman (1976) showing total length of trap, length of sampling slit and length of unit which was buried under sand. Entire trap specifications are discussed in the above paragraph.   | 63 |
| <b>Figure 5.2:</b> Photo of sample site B on Matakana Island. Red line A and B shows the position (dune crest) of sediment traps arranged linearly during the first and second periods of aeolian sediment sampling. Red line (C) shows the position (foredune) of linearly arranged sediment traps during the third period of deployment. | 64 |
| <b>Figure 5.3:</b> Wind instruments at sample site B sampling wind speed and direction at average plant height (0.8m).   | 65 |
| <b>Figure 5.4:</b> Comparative wind speeds at site A and site B over a 5 day period in 2010. Site A wind speeds were measured at a height of 4 metres above dune. Site B wind speeds were measured at a height of 0.8 metres above dune.   | 69 |
| <b>Figure 5.5:</b> Correlation between wind speeds at site A and site B. Site A wind speeds were measured at a height of 4 metres above dune. Site B wind speeds were measured at a height of 0.8 metres above dune. R squared value and equation of the line of best fit are displayed on the figure.                                     | 70 |
| <b>Figure 5.6:</b> Correlation between wind directions at site A and site B. Site A wind directions were measured at a height of 4 metres above dune. Site B wind  |    |

directions were measured at a height of 0.8 metres above dune. R squared value and equation of the line of best fit are displayed on the figure. 71

**Figure 5.7:** Comparative wind speed and direction plot for Matakana Island showing cross-shore and long-shore components. Inset A is a wind rose showing wind speed and direction at sample site B for the duration of the study. 25.8% of wind is below the ‘calm’ threshold. Inset B is a wind rose showing average wind conditions for nearby Tauranga Aero Club. 0.5% of wind is below the ‘calm’ threshold. North is indicated by 0 on both inset plots. 72

**Figure 5.8:** Images showing the deposition of sand around piezometers over a period of this study from the 15<sup>th</sup> of June to the 16<sup>th</sup> of October 2010. Top image shows initial sand level at site A piezometer 15<sup>th</sup> June. Bottom image shows sand level at site A piezometer 16<sup>th</sup> October after some sand has been dug away. 74

**Figure 5.9:** Volumes of sediment collected from sediment traps deployed 3 metres landward of the dune crest at sample sites A and B between the 15<sup>th</sup> June and the 29<sup>th</sup> of July 2010. 75

**Figure 5.10:** Images showing the deposition of sand around sediment traps following the first period of their deployment from the 15<sup>th</sup> of June to the 29<sup>th</sup> of July 2010. Top image shows site B, deposition amongst *Spinifex* plants. Bottom image shows site A, deposition around *Ammophila* plants. 76

**Figure 5.11:** Sample site wind speeds during the first wave of sand trap deployment. Red boxes (a, b, c, and d) highlight wind speed events greater than 5 m.s<sup>-1</sup> and are discussed in the text. 77

**Figure 5.12:** Wind rose plots showing wind speed and direction for four identified wind events during the course of initial sediment trap deployment from 15<sup>th</sup> June to the 29<sup>th</sup> July. Plots A, B, (c) and (d) correspond to the sections A, B, (c) and (d) identified in Figure 5.11. 78

**Figure 5.13:** Volumes of sediment collected from sediment traps deployed 3 metres landward of the dune crest at sample sites A and B between the 29<sup>th</sup> of July and the 6<sup>th</sup> of October 2010. 80

**Figure 5.14:** Sample site wind speeds during the second wave of sand trap deployment. Red boxes (a’, b’, c’, d’ and e’) highlight wind speed events greater than 5 m.s<sup>-1</sup> and are discussed in the text. 81

**Figure 5.15:** Wind rose plots showing wind speed and direction for five identified wind events during the course of secondary sediment trap deployment from the 29<sup>th</sup> July to the 6<sup>th</sup> of October. Plots (a’), (b’), (c’), (d’) and (e’) correspond to the sections (a’), (b’), (c’), (d’) and (e’) identified in Figure 5.14. 82

**Figure 5.16:** Volumes of sediment collected from sediment traps deployed in the foredune, landward of the dune crest at sample sites A and B between the 6<sup>th</sup> of October and the 12<sup>th</sup> of November 2010. 84

**Figure 5.17:** Sample site wind speeds during the third wave of sand trap deployment between the 6<sup>th</sup> of October and the 12<sup>th</sup> of November 2010. Red

boxes (a'', b'' and c'') highlight wind speed events greater than  $4 \text{ m}\cdot\text{s}^{-1}$  and are discussed in the text. 85

**Figure 5.18:** Wind rose plots showing wind speed and direction for three identified wind events during the course of the third sediment trap deployment from the 6<sup>th</sup> of October to the 12<sup>th</sup> of November. Plots (a''), (b'') and (c'') correspond to the sections (a''), (b'') and (c'') identified in Figure 5.17. 86

**Figure 5.19:** Comparative wind speeds at site B and Tauranga Aero Club over a 10 day period in 2010. Site B wind speeds were measured at a height of 0.8 m above dune. Aero Club wind speeds were measured at a height of 4 m above mean sea level. 87

**Figure 5.20:** Wind speed (black) and rainfall (gray) comparison from the 2<sup>nd</sup> of April to the 9<sup>th</sup> of May 2010. Rainfall data is from Niwa's CliFlo station at Tauranga Aero Club. Wind speed data is from sample site B. 88

## ***LIST OF TABLES***

---

|  |    |
|--|----|
| <b>Table 3.1:</b> Equilibrium associations between beach state and Deans parameter (Wright <i>et al</i> , 1985).   | 31 |
| <b>Table 3.2:</b> Sediment grain size descriptive statistics for samples collected across the profile at sample sites A & B.                                       | 31 |
| <b>Table 4.1:</b> Aquifer flow velocities ( $\text{m.h}^{-1}$ ) under various sediment porosity and hydraulic conductivity values.                                 | 46 |
| <b>Table 5.1:</b> Sediment grain size descriptive statistics for samples collected across the profile at sample sites A & B.                                       | 89 |
| <b>Table 5.2:</b> Average Sediment grain size descriptive statistics for samples collected from sediment traps at sample sites A & B on the 29 <sup>th</sup> July. | 89 |



# **CHAPTER ONE**

## **INTRODUCTION**

---

### **1.1 MOTIVATION FOR STUDY**

The Bay of Plenty is home to some of New Zealand's most popular beaches. Coastal development in the region has led to the destruction of dune and beach systems, with housing literally being built on top of old sand dunes in Mount Maunganui. Many of the coastal settlements see a large influx of people over the summer months, placing additional strain on these coastal areas. Dune alteration, combined with vegetation destruction, and failure to restrict people to tracks, have further contributed to the degradation of sand dunes. For the majority of the regions coastal settlements, beach and dune systems are relied on for protection from coastal processes. Protection of these systems is therefore paramount to ensure the coastal regions in the Bay of Plenty and around New Zealand will continue to provide resources for future generations.

### **1.2 STUDY SITE DESCRIPTION**

Matakana Island is a 24 km long Holocene sand barrier island that encloses the Tauranga Harbour in the Western Bay of Plenty (Shepherd *et al*, 1997; Smale *et al*, 2003) (Figure 1.1). The Island is comprised of an older area of tephra covered Pleistocene terraces and a large Holocene barrier to the seaward side (Figure 1.1). The Island has been used extensively for exotic forestry since the 1920s, modifying drainage, topography, soils and vegetation. The north-eastern (open coast) side of the Island houses an approximately 200 m wide strip of vegetated sand dunes, which separate plantation forests from the ocean. Local dunes support low growing sand dune communities of spinifex, pingao and marram grass, woodland and unmanaged radiata pine forest (Smale *et al*, 2003).

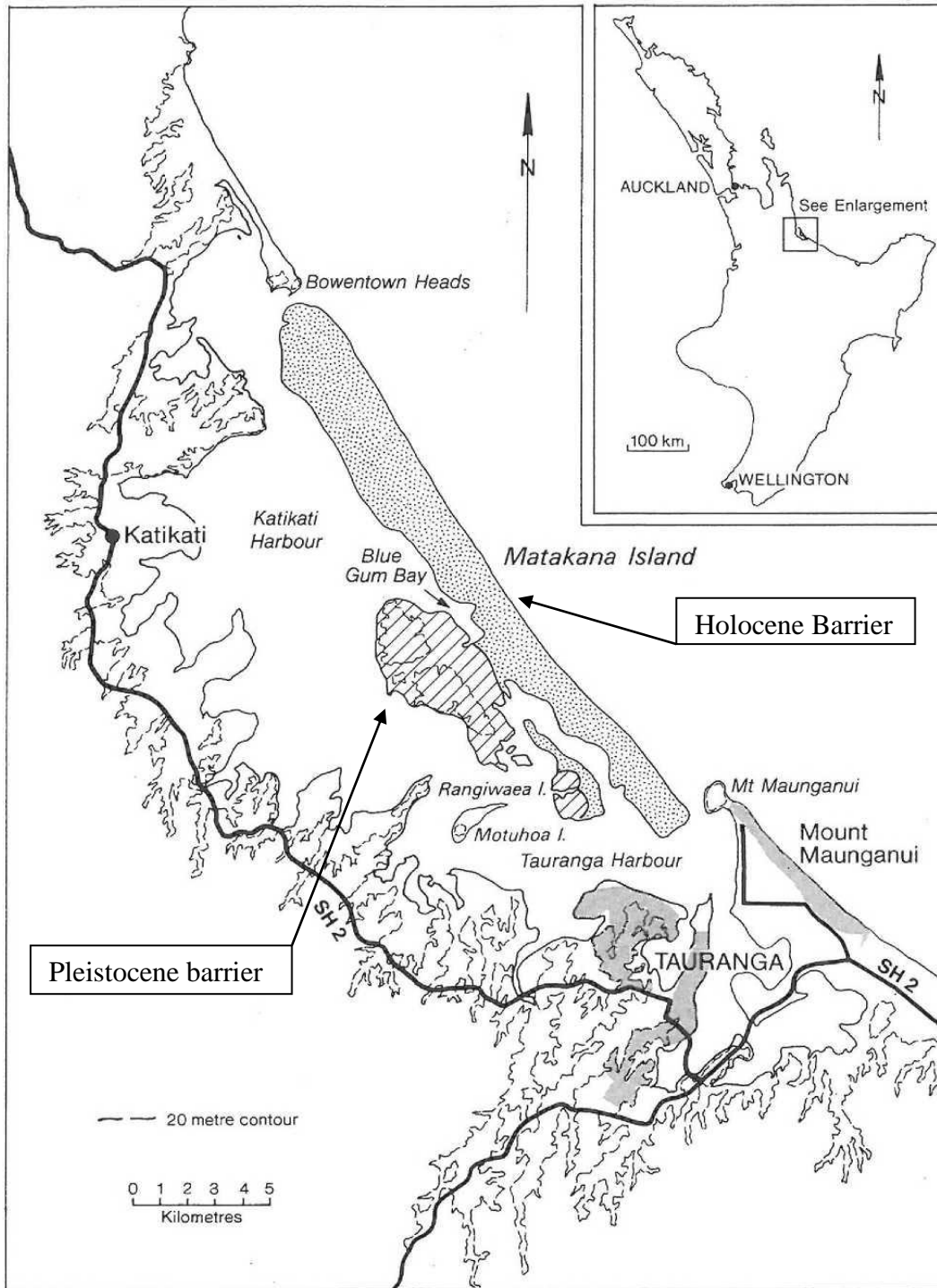


**Figure 1.1:** Map of Matakana Island in the Western Bay of Plenty region. Inset shows the Island's position in relation to the North Island (Te Ika a Maui) of New Zealand. Taken from Shepherd *et al* (1997).



**Figure 1.2:** Photographic image showing the Pipeline Road area of Matakana Island. Red box indicates specific location of study site on the Island. Image from Bay of Plenty Regional Council.

For the purposes of this study, a specific area of interest on Matakana Island was identified. A rectangular zone encompassing the dune and running parallel to the shoreline, approximately 350 m long and 40 m wide, was selected as it provided adjacent sections of native and exotic species of sand binding dune plants (Figure 1.2).

### 1.2.1 Climate

Matakana Island's climate is mild, with a moderate rainfall range between 1300 and 1400  $\text{mm.yr}^{-1}$  compared with 2500 – 2600  $\text{mm.yr}^{-1}$  that falls on the nearby

topographical highs of the Kaimai Ranges (Munro, 1994). The Western Bay of Plenty is sheltered from New Zealand's dominant westerly rain winds by these ranges. A large proportion of the area's rainfall is accounted for by periods of north to north east (onshore) airstreams travelling over the Pacific Ocean. Air flowing onto the Island under these conditions is very humid, resulting in high intensity rainfall events (Munro, 1994).

The wind climate is characterised by westerly and south westerly winds that predominate the area (Figure 1.3). Whilst north-easterly gales are infrequent, they are, along with characteristic south-westerlies, sufficiently strong to initiate the development of blowout and parabolic dunes following vegetation disturbance (Shepherd *et al*, 1997).

The wave climate of the region is illustrated in Figure 1.4. Due to its prevailing south westerly winds and north easterly aspect, the Western Bay of Plenty coastline has a lower energy wave climate when compared to most other New Zealand coasts. Healy *et al* (1977) classified the Bay of Plenty wave climate as a "mild-meso energy swell wave environment", also stating offshore and near-shore significant wave heights as 1.5 m and 0.6 m respectively. Macky *et al* (1997) expressed similar findings stating mean significant wave height in 34 m water depth at the north western inlet end of Matakana Island was 0.8 m.

Macky *et al* (1997) further calculated the long-shore wave energy flux suggesting that the direction of littoral drift fluctuates regularly. In the three year period during El Niño conditions in which their study was undertaken, it was suggested that there was a small net drift in the northwest direction. However, it was recognised that this may not be typical of the long-term climate. In comparison, Healy *et al* (1977) calculated a wave approach resultant of 4° north of normal to the coast. From this, they suggested net littoral drift was in the southeast direction, estimating net littoral drift along Matakana to be at least 40 000 m<sup>3</sup> per year, based on observations of longterm progradation at the south-eastern point of the Island (Shepherd *et al*, 1997).

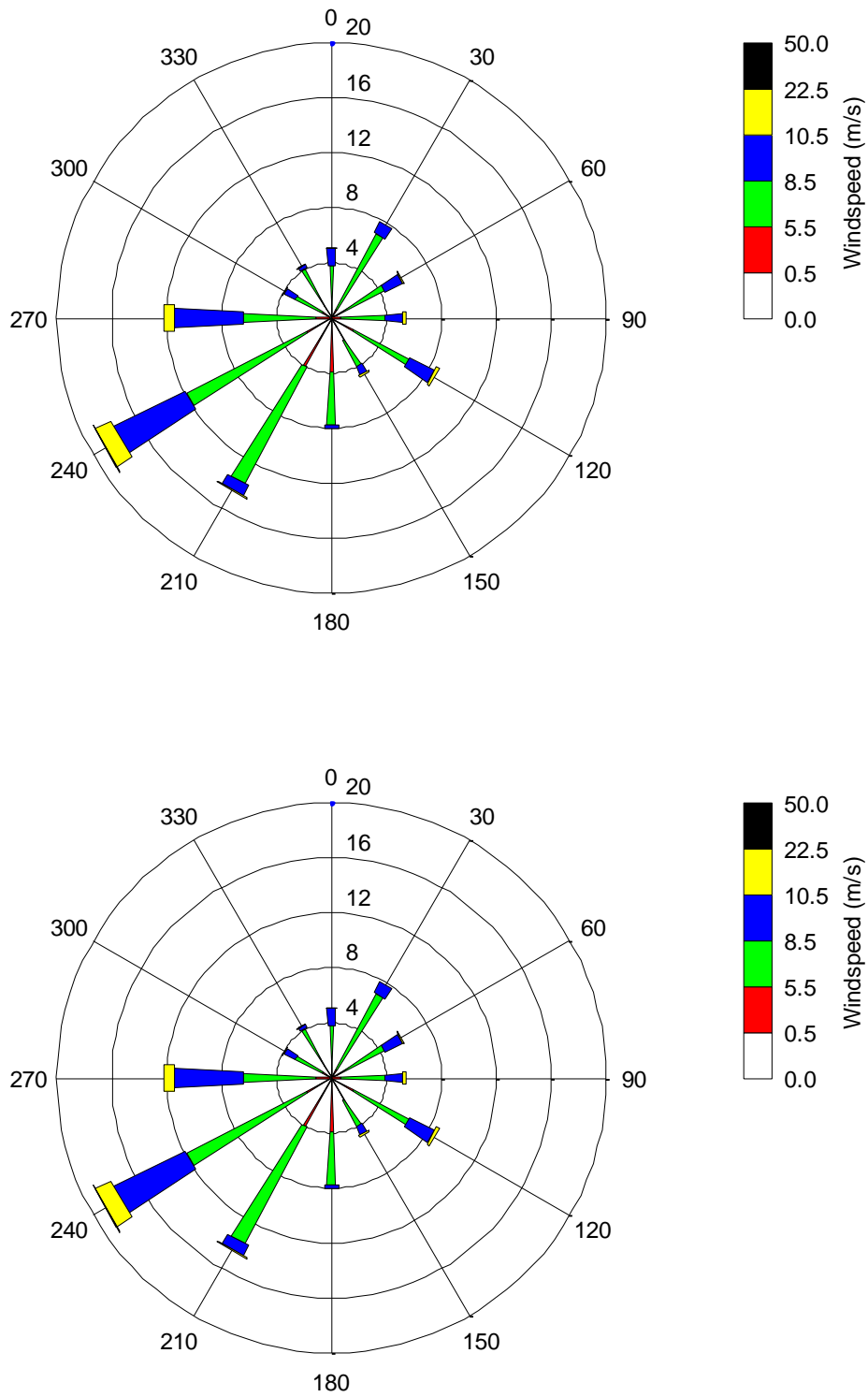


**Figure 1.3:** 5 year hind cast of wind speeds and directions for stations at Waihi (top) and Tauranga Aero Club (bottom). 0.9% of data is below the calm threshold. Data from CliFlo (2010). Stations plotted are the closest to Matakana Island of a low elevation.

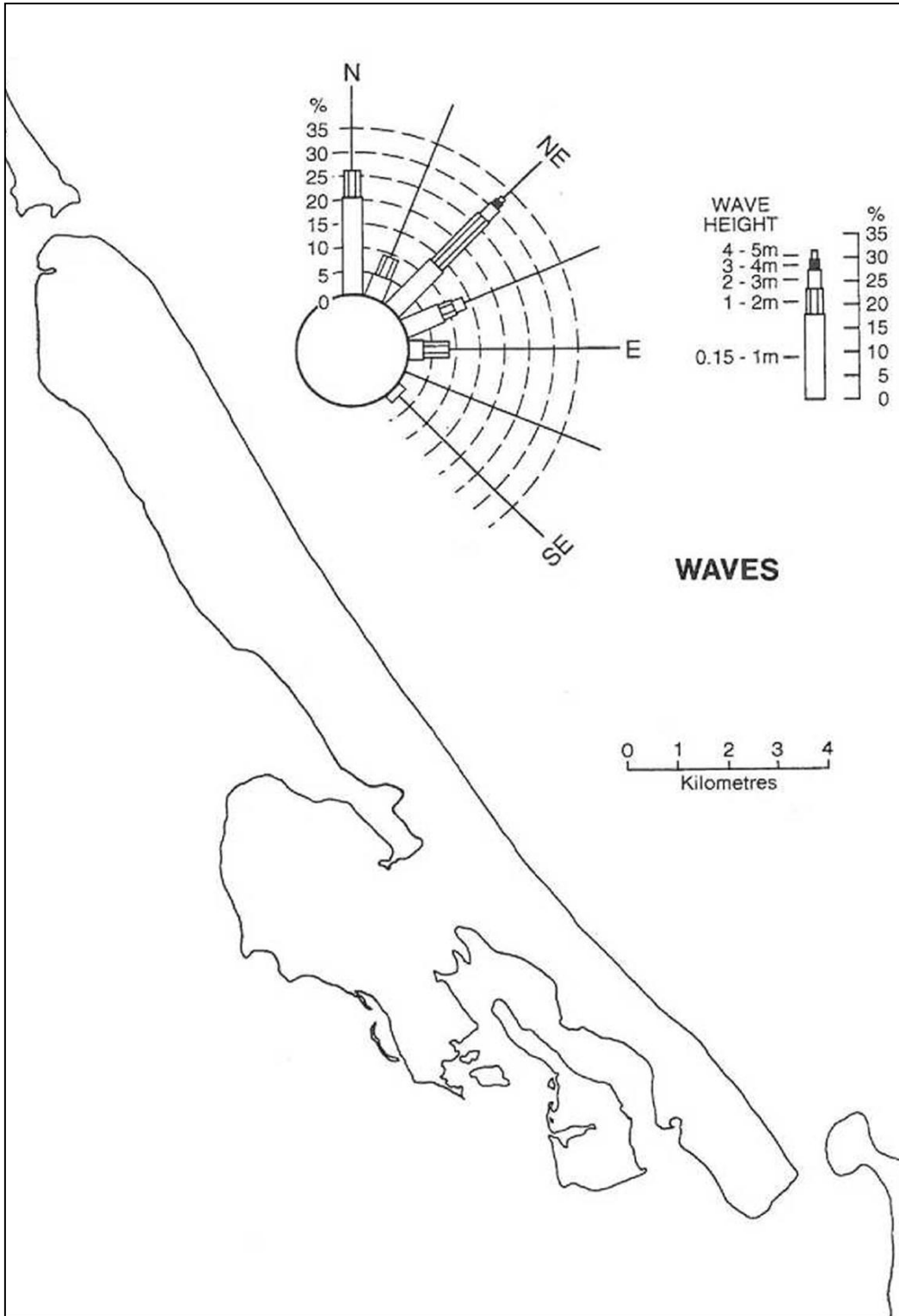


**Figure 1.4:** Wave climate for Matakana Island. Adapted from Shepherd *et al* (1997). Wave data from Harry & Healy (1978).

### **1.3 RESEARCH AIMS**

The primary aim of this research is to establish the impact different species of dune vegetation have on unconfined coastal aquifers, primarily during, and directly following seasonal short term storm events on Matakana Island in the Bay of Plenty, New Zealand. A secondary aim of establishing differences in sediment movement between two neighbouring dune systems comprised of different vegetation species is also investigated. These two research aims are further broken down into the following objectives:

1. To describe the beach and dune type and geomorphology through beach profiling, vegetation sampling and sediment sampling.
2. To quantify short term variation in local aquifer levels in response to storm events and determine the impact vegetation species present on overlying dune have on aquifer levels.
3. To determine the volume of beach sediment shifted through the dunes over short term storm events, identifying differences between neighbouring dune sites with respect to the vegetation species overlying the dune.
4. To establish the foundation for further research surrounding this topic whilst providing a stronger case for dune replanting with native species as a form of coastal management across New Zealand's beaches.

### **1.4 THESIS OUTLINE**

After this chapter, this thesis is separated into five further chapters based on the time scale of the analysis and the components investigated.

#### **Chapter 2: Literature Review**

Relevant literature is explored and summarised in Chapter 2 regarding the significance of New Zealand's dunes and dune vegetation, water table impacts on beach profiles, aeolian sediment transport and beach profiles and erosion. The literature review provides a basis of current research required when discussing the results of this thesis in the following chapters.

### **Chapter 3: Sand Dune Classification**

In order for a comparison between study sites, a description and classification of each sample site was required. A classification is presented based upon vegetation, profile, sediment and sediment compaction type for the two sample sites investigated.

### **Chapter 4: Short term Aquifer Fluctuations**

Chapter 4 presents the analysis of short-term aquifer fluctuations beneath the fore dune of the sandy beach, Matakana Island. The various forcings responsible for short term fluctuation are identified. Comparisons between sample sites are made, with differences identified. Differences between sites are linked to the site classifications.

### **Chapter 5: Aeolian Sediment Transport**

An analysis of wind regime for the area is presented, coupled with the measurement of sediment movement through the sand dune. Again, comparisons between sample sites are made, with differences identified and those between sites are linked to the site classifications.

### **Chapter 6: Conclusions and Recommendations**

A summary of all the results and key findings summarising short term aquifer fluctuation and aeolian sediment transport on the sandy beach, Matakana Island is provided in Chapter 6. This chapter also outlines suggestions for further research in order to better understand the role of native and exotic species of sand binding dune plants on the health of New Zealand's sandy beaches.

# **CHAPTER TWO**

## **LITERATURE REVIEW**

---

### **2.1 INTRODUCTION**

Dune vegetation can provide a classification measure for dune systems, but more importantly influences the movement of wind and sediment within the system. Vegetation can affect the morphodynamic shape of beaches and their response to short term storm events (Horn, 2002; Bauer *et al*, 2009), whilst also affecting the local hydrology.

When discussing the hydrology of coastal regions in relation to coastal processes it is generally groundwater that is the main point of focus. It is coastal groundwater's role in swash zone dynamics of sandy beaches that most studies have focused on (Horn, 2005). The movement of groundwater in estuarine environments, coastal barriers and gravel beaches as well as its effect on aeolian sediment transport has been studied, with local climate and rainfall shown to be contributors to groundwater levels and flow.

Local weather further plays a part in beach geomorphology through the role of wind on sediment flux (List, 2005). Coastal features that are poorly stabilised by vegetation are prone to sediment losses whilst good sand binding vegetation can greatly increase sediment accretion and aid the formation of dunes on sandy beaches. Rainfall also plays a role with sediment mobilisation by wind heavily affected by any saturation at the source.

This literature review provides some background on the influence of coastal hydrology and aeolian sediment transport on sandy beach profiles, providing a framework for this thesis, which attempts to identify the relationship between species of coastal dune grass, coastal hydrology and aeolian sediment transport.

## 2.1 NEW ZEALAND DUNES

The health of New Zealand's dune systems has undergone a large decline since the first arrival of humans. Prior to the 1900's large sections of dune were burned by Māori people to aid the growth of bracken fern for food, and sections forest in the back dune cleared to make way exotic forest grown for timber (Jamieson, 2010). A more widespread disturbance of New Zealand's dunes followed the settlement of Europeans (Taylor & Smith, 1997). Disturbances to dune vegetation cover by fire and grazing triggered the expansion of some dune lands and the loss of adjacent agricultural lands (Hilton *et al*, 2000). Cockayne suggested in his 1911 report on the Dune areas of New Zealand that Marram grass (*Ammophila arenaria*) be planted to stabilize shifting sand and prevent this loss. With the aid of intentional planting, *Ammophila* quickly succeeded in invading many of the country's natural dune areas displacing native sand binding plants and altering physical and ecological characteristics of these areas (Jamieson, 2010).

Population growth in coastal regions has placed additional strain on our fragile and highly modified dune environment, with recreational activities and foot traffic impacting on growth of dune plants and increasing the risk of beach erosion (Milne & Sawyer, 2002). New Zealand's dunes now occupy less than 30% of their initial coverage with native vegetated dunes now classified as endangered ecosystems (Hilton *et al*, 2000; Sawyer, 2004; Hilton, 2006). Restoration and sustainable management of these significant national assets is vital for the protection of our cultural heritage and biodiversity.

## 2.2 DUNE VEGETATION

Through New Zealand and the rest of the world, plant communities now contain great proportions of exotic species introduced indirectly or directly by humans (King & Wilson, 2006). Regardless of where these plants come from, the impact of their establishment varies upon the niche they inhabit. New Zealand is home to a variety of coastal species both indigenous and exotic. Occupation of the dune

and fore dune by sand-binding dune plants plays a large role in the ecological and physical health of the local dune system. Throughout the North Island three main species of sand binding dune plant are present, Marram grass (*Ammophila arenaria*), Spinifex (*Spinifex sericeus*) and Pingao, formally named *Desmoschoenus spiralis* and recently changed to the more appropriate *Ficinia spirialis* (Muasya & de Lange, 2010). *Ammophila* and *Spinifex* are the main focus of this thesis and are discussed further in sections 2.2.1 and 2.2.2.

### 2.2.1 Marram Grass

*Ammophila arenaria*, Marram grass, was introduced to New Zealand from Europe beginning in the late 1800's as a means of protecting coastal farmland from windblown sand encroachment (Moore & Davis, 2004). Known for its excellent sand binding ability, *Ammophila* has been shown to be a highly invasive species that threatens the ecology of active dune systems outside its natural range (Hilton *et al*, 2005), adversely affecting indigenous dune flora and habitat diversity through dune stabilisation and vegetation succession (Buell *et al*, 1995; Hertling & Lubke, 1999b).



**Figure 2.1:** Marram Grass on Matakana Island foredune, Western Bay of Plenty.

*Ammophila* is a coarse, perennial, rhizomatous grass growing in small stout tufts extending up to 120 cm tall (Figure 2.1). The plant is native to the sandy coastlines of the North Sea, the Baltic Sea, the Black Sea and the Mediterranean

Sea. Today it is common along North America's Pacific coast, South East Australia, Chile, South Africa and New Zealand (Buell *et al*, 1995; Hertling & Lubke, 1999b; Hilton *et al*, 2005). Establishment of the plant takes place through seedlings and vegetative reproduction, most often through regeneration from pieces of rhizome removed during periods of erosion and washed ashore via winds and high tides (Buell *et al*, 1995).

*Ammophila* has been shown to grow most vigorously on sites characterised by the fresh deposition of sand by wind (Van der Putten *et al*, 1989), with the plant thriving in the wind blown foredune above the high tide line. The plant, however, soon becomes feebler and degenerates when sand drift diminishes (Marshall, 1965; Willis, 1965; Hope-Simpson & Jefferies, 1966; Huiskes, 1980). The extension of leaves up into the wind column diminishes wind speed allowing sand to be deposited around the plant. The accumulation of this windblown sand is thought to provide the nutrients *Ammophila* requires to enable the plants to renew their root system and escape competition, as few other plant species can withstand strong sand accretion (Van der Putten *et al*, 1989).

### **2.2.1 Spinifex**

*Spinifex sericeus*, is a coastal sand dune grass which occurs along coasts of New Zealand, Eastern Australia and New Caledonia. Growth is most vigorous on the dynamic incipient foredunes (Figure 2.2), appearing less vigorous in more stabilized established dunes (Maze & Whalley, 1990; Maze & Whalley, 1992). Spinifex is a stoloniferous dioecious, perennial grass with its stoloniferous habit making it an excellent dune stabilisation species (Maze & Whalley, 1990). This stabilization property has made the species a popular choice for dune reclamation and rehabilitation programmes (Clements *et al*, 2010).



**Figure 2.2:** Spinifex on Matakana Island foredune, Western Bay of Plenty.

*Spinifex* is a rhizomatous grass with erect stems extending up to 60 cm tall. The plant is adapted to survive within the active sand zone (incipient dune), moving with and loosely holding shifting sands (Clements *et al*, 2010). *Spinifex* naturally colonises this zone from seed washed on shore during spring tides, with seaward growth of *Spinifex* rhizomes producing a gradual relocation of aeolian sand deposition, eventually forming a second more seaward dune (Clements *et al*, 2010; Maze & Whalley, 1992).

### 2.2.3 Significance of Vegetation

Vegetation is one variable responsible for different types of dune, with dune type also dependent on local wind climate, pore water pressure as well as sediment supply. Both *Ammophila* and *Spinifex* effectively trap sand in their roots and vegetation promoting accretion through the dune. Dunes created by the introduced *Ammophila*, tend to have a much steeper foredune than dunes created by the native species *Spinifex* and Pingao (*Ficinia spirialis*) (Figure 2.3) (Esler, 1970). The key difference is that the lower profiled dunes created by native vegetation are able to infiltrate wave run-up more effectively and accrete sand following erosion events, where infiltration rates are limited in steep foredunes created by the introduced *Ammophila* and sand accretion post erosion events is reduced due to foredune vegetation losses (Hilton *et al*, 2005; Maze & Whalley, 1992). Dunes created by native species are therefore likely to provide a more effective barrier against coastal ocean processes.

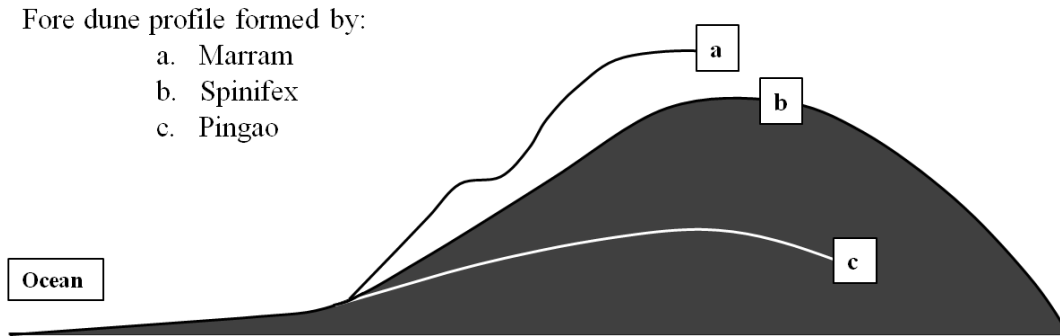


**Figure 2.3:** Foredune profiles formed by their overlying vegetation type, Marram A, Spinifex B and Pingao (c). Adapted from Esler (1970).

## 2.3 WATER TABLE IMPACTS ON BEACH PROFILES

To understand beach profile evolution and the physical health of sand dunes, it is necessary to understand the interaction between groundwater and surface flow in the swash zone (Horn, 2002). Pore water pressure in the beach is one variable that can affect a beach's state. Current research suggests that the internal flow within the beach, driven by hydraulic gradients as a result of fluctuations in water table levels and swash zone infiltration/exfiltration, may influence sea bed stability and promote sediment transport (Duncan, 1964; Horn, 2002). Understanding beach and swash zone groundwater dynamics will lead to greater accuracy when predicting the profile evolution of beaches. Currently, most shoreline prediction models do not include sediment processes in the swash zone (Horn, 2002).

### 2.3.1 Groundwater

The beach groundwater system is highly dynamic. Interactions between the swash/backwash flows and the beach water table can influence the sediment budget on the intertidal face of beaches (Chappel *et al*, 1979). The beach water table is an unconfined aquifer, its levels primarily affected by oceanographic and atmospheric forcing (Turner & Nielsen, 1997; Horn, 2006). These include: propagation of shelf waves, coastal storms, wave set-up, barometric pressure changes and ocean tides (Clarke and Eliot, 1987; Turner & Nielsen, 1997; Urish

and McKenna, 2004). Isla & Bujalesky (2005) showed that the beach water table is also affected by beach composition (grain size sorting and porosity).

Xun *et al* (2006) showed that coastal aquifers respond to tidal fluctuations as far as 2.3km from the coast demonstrating that coastal impacts on water tables are not limited to the confined coastal region.

Pore water pressure is the fluid pressure of groundwater within the pores between sediment grains relative to atmospheric pressure. The water table is an equilibrium surface where pore water pressure is equal to atmospheric pressure (Horn, 2002).

The flow of groundwater in the beach is driven by hydraulic gradients. Since the 1940s a number of studies have described the shape and elevation of the beach water table as a function of beach morphology and tidal state (Horn, 2002).

Duncan (1964) summarised beach groundwater behaviour (Figure 2.4), observing deposition over erosion being greatest during the rising tide (period when the landward-sloping beach water table is steepest). The same observation is supported by Chappel *et al*, (1979) and Lanyon *et al*, (1982), who also suggested that the proportion of time a water table slopes in a given direction relates to net beach change (Steele, 1995).

The beach water table surface is generally not flat as seen in observations of its behavior. Several studies have shown that slope of the water table changes with tide, sloping landward on a rising tide and seaward on a falling tide (Turner, 1998). Tides produce an asymmetric water table elevation, as the water table rises abruptly but drops off slowly. This process is due mainly to the fact that the beach fills more easily than it drains, causing a decoupling to occur between the tides and the water table (Horn, 2002).

Decoupling results in a seepage face forming during the ebb tide. The seepage face occurs between the exit point of the water table and the swashzone. It also separates a lower saturated region of groundwater effluence and an upper unsaturated region of potential swash infiltration (Baird & Horn, 1996). This exit point marks a divergent point between zones of erosion and accretion and

sometimes explains the distinct break in slope often observed on large tidal range beaches (Horn, 2002). On the upper unsaturated profile swash infiltration on the rising tide enhances steepening. Promotion of offshore transport occurs in the lower saturated zone due to the water table sloping seaward on the ebb tide, causing a hydraulic gradient which results in fluidization of sediment, which then becomes easily entrained by backwash (Figure 2.5) (Baird & Horn, 1996; Horn, 2002). A similar process occurs during short period wave forcing, where if there is a low water table, there is room for infiltration so less water in the backwash to move sediment, so accretion can occur (Vesterby, 2000; Eliot & Clarke, 1988).

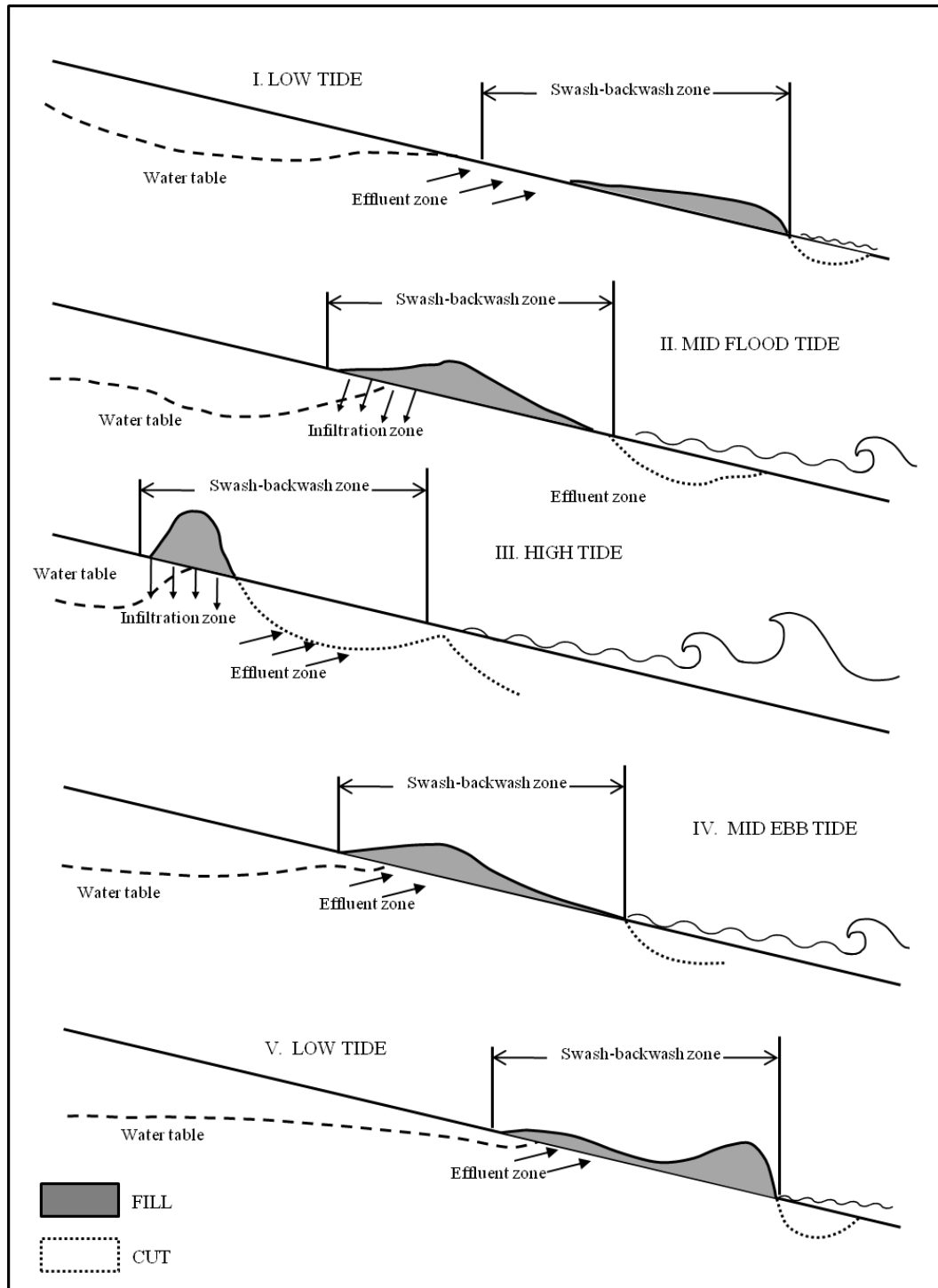


**Figure 2.4:** The effects of watertable elevation and slope on swash zone deposition and erosion (adapted from Duncan, 1964).

### **2.3.2 Impact of lowering the water table**

Elevation of the beach water table has been linked to beach erosion and accretion, with studies demonstrating a higher beach water table relative to mean sea level can enhance offshore sediment transport leading to erosion (Li *et al*, 1997; Turner, 1998).

Artificial manipulation of beach water tables such as beach drainage, is an example of one type of 'soft' engineering, as a solution to coastal erosion (Turner & Leatherman, 1997). Wesiman *et al* (1995) showed that coastal water table manipulation is effective at promoting beach accretion under both accretive and erosive wave climates. Further literature however, shows that not all the physical mechanisms linking groundwater elevation and coastal erosion/accretion are fully understood (Turner & Leatherman, 1997; Bruun, 1989), and the lowering of beach water tables are less effective during storm events (Bruun, 1989). There is however significant promise in the manipulation concept with further research.

## **2.4 AEOLIAN SEDIMENT TRANSPORT**

Aeolian sediment transport is one of many important processes that occur in the foredune ridge in terms of sediment transport (Rhew & Yu, 2009). The basic physics of aeolian sediment transport have been relatively well understood for the last 70 years, with many of the principles established by Bagnold (1941) remaining basically valid today (Pye, 1993).

Aeolian sediment transport is the mobilisation of sediment by wind and is best described by Bagnold (1941). Bagnold (1941) defined two thresholds for sand transport: the fluid and the impact thresholds. Wind at any point on a beach requires certain strength to initiate sand transport over a loose dry surface: this wind strength is deemed the fluid threshold. If wind strength decreases after sand transport has begun, transport can be sustained at wind strengths below the fluid threshold (McEwan & Willetts, 1993). Hence, another threshold, defined as the impact threshold is observed, below this sand transport ceases.

In a natural dune environment, moisture and vegetation act to stabilize the dunes. Vegetation reduces wind strength near the surface, with the wind velocity profile a logarithmic function of height, increasing the velocity needed to mobilise sediment. Vegetation also reduces the strength of wind carrying mobilised sediment to below the impact threshold, resulting in the deposition of sand around the vegetation (Carter & Wilson, 1993). Plants reduce wind speeds through frictional forces, the magnitude of which are a function of the surface area of their stems and leaves and the density of their growth. Bressolier & Thomas (1977) recognised the impact of vegetation and suggested that plant roughness was not controlled by plant height alone, but that further factors such as vegetation density and the natural characteristics of the species such as stem and leaf distributions must be taken into account.

Svasek and Terwindt (1974) showed that with increased moisture content, the fluid threshold for sediment entrainment is increased, a feature further exemplified by Arens (1996). Arens showed that during wet conditions (prolonged rainfall), sediment transport by wind declined to zero, regardless of wind strength. Arens also recognised that sand content of wind decreases exponentially with height.

It is widely accepted that onshore and offshore aeolian sediment transport plays a role in dune sediment budgets and their formation (Wal & McManus, 1993). While this is the case, aeolian sediment transport is complex to the degree where ideal conditions, on which many sediment transport 'equilibrium' theories are based, are rarely encountered on natural beaches. Sediment flux at any point on the beach surface is dependent on grain size, wind stress, and available sediment supply (Bauer *et al*, 2009). Other complicated factors such as sand surface moisture content, sorting, bed roughness, vegetation cover and beach slope, impact the application of equilibrium models (Sherman & Hotta, 1990). Understandably, aeolian transport is hard enough to measure, let alone predict.

Several studies such as Rhew & Yu (2009) and Aagaard *et al* (2004) have looked at methods of simply measuring in-situ transport rates, while others like McEwan

(1993) and Gillette *et al* (1998) have attempted to predict aeolian transport rates through physical and numerical models.

Attempting to accurately account for all variables in a system that is fundamentally unstable proves difficult (Baas, 2007). Arens (1994) showed that actual rates of transport deviate considerably from potential rates predicted by transport equations, citing the main cause of this deviation as the absence of transport during very wet conditions, regardless of wind speed and the variation of threshold velocity with time. Potential transport in this instance can then be defined as optimum transport.

The aeolian transport process on a beach has been simulated in a boundary layer wind tunnel (Okoli, 2003). However, Arens & van der Lee (1995) imply that the relationship between sand concentration and height within the wind column vanishes as wind passes up and over the foredunes, a process that is much more difficult to simulate in wind tunnels. It is suggested that sand traps provide an alternative to simulation by measuring on site sediment transport conditions. Many types of traps have been described in the literature, with Leatherman (1978) providing a simple cost effective design for sediment traps.

Leatherman (1978) recognised that total sand flow over a surface can only be approximated, as the presence of collection devices interfere with the air stream. Leatherman further suggested that a streamlined collector that offers a narrow front to the wind would result in saltation grains unable to follow the deflected wind path and will therefore pass into the mouth of the collector. Leatherman's sand trap design consisted of a section of PVC pipe with slits cut in one end. The trap is buried so the base of the slits sits flush with the ground (Figure 2.5). One slit serves to collect sediment, while the other is covered with 65  $\mu\text{m}$  screening to provide flow through of wind. All sediment material is collected in an inner sleeve (Figure 2.5).

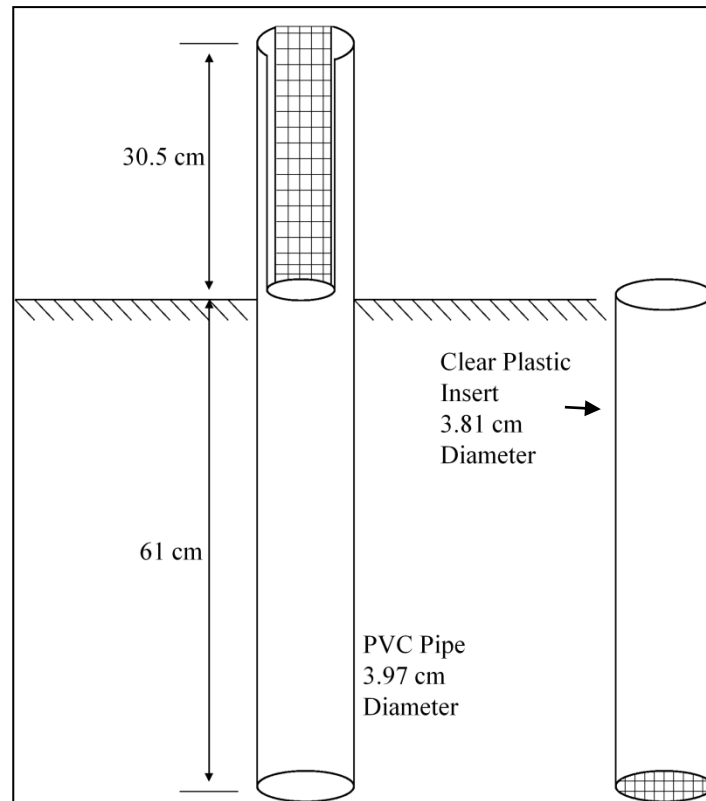


**Figure 2.5:** Leatherman's vertical rod sand trap design (Leatherman, 1978).

## 2.5 BEACH PROFILES AND EROSION

Beach profiles are one of the most studied features of coastal morphology (Kraus, 2005). Profile shape can be used to predict a beach's response to storms and its extent as a usable resource, as well as providing an indicator of the physical health of a beach. Understanding how beach profiles change in response to environmental forcing is essential when determining the state of the beach for conservation and rehabilitation purposes.

Many studies have recognised that stable equilibrium forms of beach profile can be achieved for given wave height, water level and sediment characteristics (Kriebel & Dean, 1985), with beaches constantly adjusting towards an equilibrium shape (Dean, 1977). Based on Deans equilibrium profile characteristics, if a given point on the profile increased in water depth (during a storm surge), it is generally accepted a resulting increase in offshore sediment will occur. This offshore sediment flux is classified as short term erosion or short-term

change, and may involve sediment loss from the foredunes. In this sense, dunes act as a bank for sediment. Should sediment be returned to the dunes by long period waves in between storms, the dunes require an effective measure to help collect and bind the sediment (in natural environments, vegetation).

Erosion reduces a beach's ability to act as a buffer against storms (Anthony, 2005), negatively impacting low lying areas and coastal communities. Short term erosion, or change, is commonly part of the morphodynamic cycle of the beach as it adjusts to seasonal and non-seasonal changes in wave conditions (Bird, 2008). Seasonal patterns commonly show an eroded winter profile induced by storms and an accreting summer profile brought about by calmer weather. It is also important to recognise that any short-term variability in beach profile may be imbedded in longer term changes involving net sediment gains or losses to the area (Anthony, 2005). That dunes are eroded during storms to replenish beach levels has been well known since the mid-nineteenth century (Carter, 1991). Dune erosion often occurs during storm surges, when onshore winds, high tides and low barometric pressure coincide (Carter, 1991). Vegetation plays a role in accumulating sand following erosion events. The degree of vegetation stabilisation is a factor in how quickly the system responds, and is reflected in the morphodynamic classification of coastal foredunes, or beach state (Short & Hesp, 1982).

The beach state at any given time is an indicator of the three-dimensional morphology of the beach and surf zone, dominant surf processes and also influences the mechanisms and possibility of accretion or erosion (Wright & Short, 1985). Wright & Short (1985) analysed 6.5 years of daily observations to produce six classifications for beach state ranging from dissipative through to reflective, with four different intermediate stages. Dissipative beaches display the classic forms of 'winter' beach profiles (Sonu & Van Beek, 1971) commonly wide and flat they are also often comprised of finer grain size. Dissipative beaches often have a substantial sediment volume and at least one offshore bar. A key point to note is wave energy is commonly dissipated over the offshore bar (Sherman, 2005). Reflective beaches are systems where minimal wave energy is dissipated by breaking and is hence reflected (Sherman, 2005). They display the classic

‘summer’ beach profile indicative of a short, steep beach, and are commonly associated with coarse sediment (Sonu & Van Beek, 1971).

Landward aeolian sediment transport is dependent on the beach topography (state) and aerodynamic flow across that topography (Short & Hesp, 1982). Aeolian sand transport rates are potentially lowest on reflective beaches, with more moderate flow on intermediate beaches through to highest flows on dissipative beaches (Short & Hesp, 1982). Short & Hesp (1982) showed that frequency of beach or dune erosion, rates of aeolian sand transport and foredune morphology and volume can explain the nature and morphology of any landward occurring, large scale dune systems. Their study pointed out that dissipative beaches are commonly characterised by large-scale transgressive dunes; intermediate, by a trend from large parabolic dunes to small-scale blowouts; and reflective, by little dune development. Therefore, the state of a beach will impact vegetation diversity and stabilisation.

## **2.6 SUMMARY**

Sandy beaches and dunes are highly dynamic environments prone to large changes in characteristics as a result of a multitude of environmental forcing. Coastal regions of New Zealand are of particular importance due to the physical and ecological strains we place on them, the cultural identity they represent and the protection they provide.

The ability of *Ammophila* to trap windblown sediment and stabilise mobile sand dunes made the plant a popular choice for preventing sand encroachment in coastal regions of the countries it has been introduced to. *Ammophila*'s establishment has led to the decline of native species of sand binders *Spinifex* and Pingao in many areas of New Zealand's coastline. *Ammophila* may be effective at stabilising dunes but its impact on the ecological diversity of the coastline poses a threat to the overall biodiversity of the country. *Spinifex* is shown to be an effective sand binder, but more important is the type of sand dune

it forms. The lower dune formed by *Spinifex* allows increased swash infiltration across the profile promoting accretion by aiding the deposition of sediment.

Beach state (morphodynamic shape) is shown to influence how beaches respond to storm events, the vegetation that inhabits their dunes, aeolian sand transport rates and the type of dunes present. A healthy beach state with well developed sand dunes provides a sediment buffer for extreme storm events.

Dunes play an important role in regulating coastal groundwater. More permeable dune systems support a freshwater lens which provides a barrier to landward salt intrusion (Carter, 1991). Precipitation regime and the geometry of the dune system affect the size of this lens. The potential for vegetation to impact the permeability of the dune has received little attention in the literature, giving rise to the nature of this thesis.

# **CHAPTER THREE**

## **SAND DUNE CLASSIFICATION**

---

### **3.1 INTRODUCTION**

New Zealand's dune systems can be characterised by the vegetation present and the overall shape and properties of the dune/beach. This chapter identifies the vegetation types, beach characteristics and beach shapes, used to classify the two sample sites. Classification between sites allows for the explanation of the relationship between sites, differences in water table levels and sediment transport. This is explored in the following chapters.

### **3.2 METHODOLOGY**

#### **3.2.1 Vegetation Sampling**

An assessment of vegetation overlying the sand dune at each sample site was used to classify the sites into two categories characterised by the dominant vegetation species, Marram grass (*Ammophila arenaria*) (sample site A) and Spinifex (*Spinifex sericeus*) (sample site B). Sampling was conducted in 2x2 m<sup>2</sup> quadrants at randomly selected intervals, across 15 m transects running through both sample sites (Figure 3.1). Transect lines ran from the fore dune through to a belt in the back dune where the swale vegetation ended. Species of vegetation present were identified by visual observation, and assigned a percentage of ground cover relative to the quadrant being sampled. An average across quadrants at each sample site was used to estimate vegetation species present and the percentage of cover for the entire dune at each specific sample site. Bare sand was recorded as bare ground cover, and also assigned a percentage value to establish vegetation density.



**Figure 3.1:** Vegetation sampling, 2 x 2 m<sup>2</sup> quadrat at sample site B.

### **3.2.2 Profile Sampling**

Sampling of the beach profile shape was undertaken on most site visits to establish general beach shape and changes to the profile during the course of the study. Profiles were taken using a Nikon 302 Series Total Station and measured from the dune, seaward to the water's edge (Figure 3.2). Reference pegs were placed in the dune at each sample site as a starting point for each profile, ensuring the same section of profile was sampled each time. Profiles were plotted in a Microsoft Excel spreadsheet, where data was adjusted to Mean Sea Level (MSL) using tide data from NIWA. The initial profile shapes at sample sites A and B were recorded on Julian Day 63 (March 4<sup>th</sup> 2010).



**Figure 3.2:** Typical beach profile cross section at sample site B identified by the red line.

Average beach slope is defined as the average slope between the berm and offshore bar. Where no offshore bar was visible due to high tides, slope was estimated as average slope between berm and water level at the time. Slope is used as an indicator of current beach state.

Dean's Parameter values were calculated to classify the beach state as per Wright & Short (1984) (Equation 3.1).

$$\Omega_{Db} = \frac{H_b}{w_s T}$$

Equation (3.1)

$H_b$  is breaking wave height (m) with  $H_b = H_{rms}$  (root mean square wave height (m)), which is used to categorise wave height in shallow water.  $w_s$  is settling velocity of local sediment and  $T$  is wave period (s). Stokes Law was used to estimate sediment settling velocity.

Sediment samples were collected at sites A and B from three sections in the beach profile, the swash zone, dune face and swale. Samples were run through a laser particle size analyser to determine mean, median, standard deviation, skewness and kurtosis statistics for grain size. Mean grain size diameter of the beach between both sites was applied to Stokes Law when estimating sediment settling velocity.

Wave characteristics for the area, required for Deans Parameter were obtained from Macky *et al*, (1995). Wave measurements made over a three year period from a buoy moored of the coast from the Katikati entrance, at the Northern end of Matakana Island, were used to establish wave climate for the area. Mean significant wave height and mean period were noted as 0.8 m and 10-11 s respectively (Macky *et al*, 1995).

### **3.2.3 Compaction Sampling**

The Scala Drop Cone Penetrometer was used to measure the in situ penetration resistance of beach sediment at samples sites A and B. Sites were sampled across transects which ran from the back dune (where swale vegetation ended) through to the beach face (above berm). Sampling was conducted at regular intervals across each transect. Due to the low cohesiveness of sand, a 'distance per blow' method of measuring penetration was adopted. At each interval a series of drops were

made small distances apart, recording the penetration per one drop. Average penetration at each interval was established for comparisons between sites.

### 3.3 RESULTS

#### 3.3.1 Vegetation Results

Marram grass (*Ammophila arenaria*) was the dominant species present at sample site A with an estimated total ground cover of 72.5% (Figure 3.2). Haretail (*Lagurus ovatus*) was more abundant at site A when compared with site B with 5% of ground cover, while Sea Rocket (*Cakile edentula*) and Shore Bindweed (*Calystegia soldanella*) found in site B were absent at site A. A small number of *Spinifex* plants were found throughout the sample quadrants at site A, with some dead *Ammophila* matter covering a small percentage of the dune. Bare ground cover represented 20.5% of total ground cover at site B, with sections of the back dune/swale remaining free of vegetation.

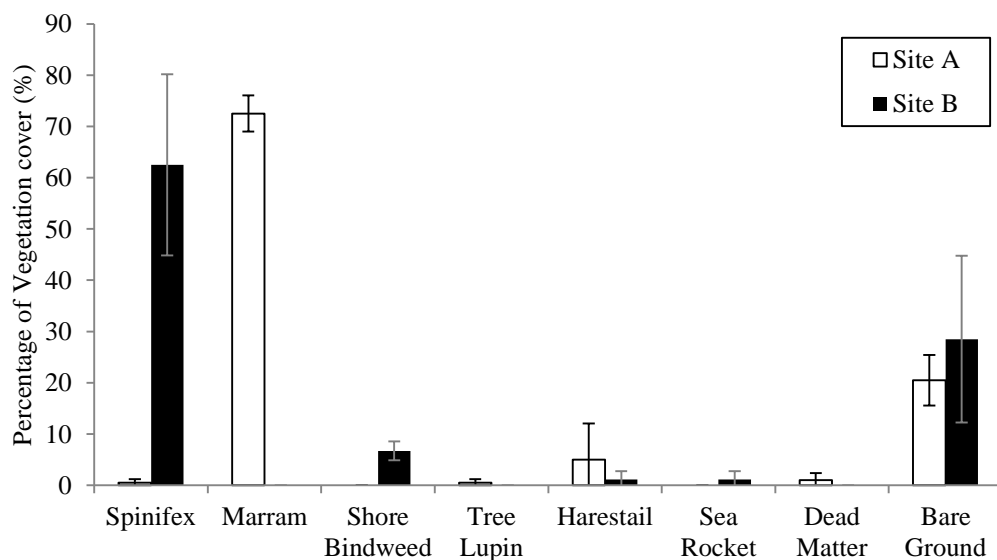


**Figure 3.3:** Vegetation species and their estimated percentage of total cover at sample sites A & B including error bars of 1 standard deviation for sample sites A and B.

*Spinifex* (*Spinifex sericeus*) was the dominant species present at sample site B with an estimated total ground cover of 62.5% (Figure 3.3). Harestail (*Lagurus ovatus*) and Sea Rocket (*Cakile edentula*) were shown to represent a small percentage of groundcover, predominantly found in the swale/back dune area. Shore Bindweed (*Calystegia soldanella*) was also found in limited numbers, accounting for 6.7% of estimated total groundcover at sample site B. This is most likely to be an overestimate, with species numbers being confined to one particular quadrant situated in the swale/back dune and no plants found through the fore dune and dune. Bare ground cover was high (28.5%) while no *Ammophila* was found across the sample site.

### 3.3.2 Profile Results

The initial site profiles recorded on Julian Day 63 show sample site A is steeper between horizontal distance points 2 and 6 m, showing the presence of a steeper foredune at site A (Figure 3.3). Both profiles display a developed berm. Beach width is defined as narrow at high tide with distance between dune toe and berm top small, at between 12 and 13 m.

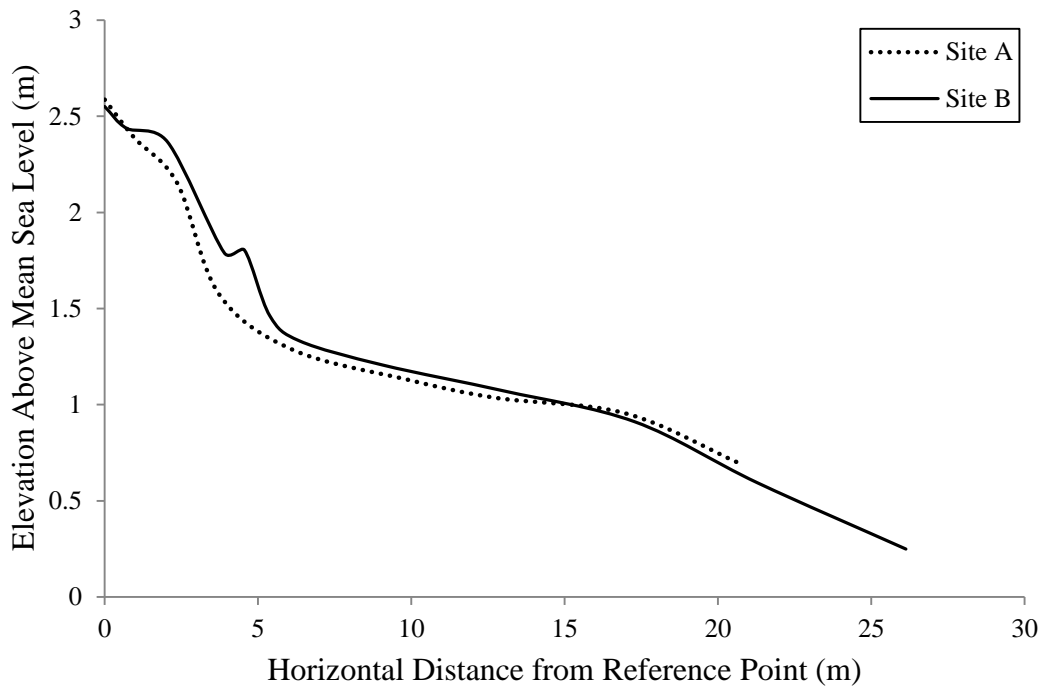


**Figure 3.4:** Initial profile shape plots recorded on Julian Day 63 for sample sites A and B extending from top of dune to water.

Beach slope at sites A and B was the same at the time of initial profile measurement with the measured slope angle at both sites being  $4^\circ$ . Dean's Parameter values for sites A and B were 2.08 and 2.22 respectively, indicating an intermediate state beach, towards the reflective end of the spectrum (Table 3.1).

**Table 3.1:** Equilibrium associations between beach state and Deans parameter (Wright *et al*, 1985)

| Beach State              | $\Omega_e$      |
|--------------------------|-----------------|
| Reflective               | <1.5            |
| Low tide terrace         | $2.40 \pm 0.19$ |
| Transverse bar and rip   | $3.15 \pm 0.64$ |
| Rhythmic bar and beach   | $3.30 \pm 0.76$ |
| Longshore bar and trough | $4.70 \pm 0.93$ |
| Dissipative              | >5.5            |

### 3.3.3 Sediment Characteristics

Sediment size samples undertaken showed mean grain size diameter differing slightly between sites. Mean grain size diameter was greater at site A in all 3 sampled areas (beach, dune face and swale) when compared to site B (Table 3.2).

**Table 3.2:** Sediment grain size descriptive statistics for samples collected

across the profile at sample sites A & B.

| Sample Location  | Median ( $\mu\text{m}$ ) | Mean ( $\mu\text{m}$ ) | Standard Dev ( $\mu\text{m}$ ) | Skewness ( $\mu\text{m}$ ) | Kurtosis ( $\mu\text{m}$ ) |
|------------------|--------------------------|------------------------|--------------------------------|----------------------------|----------------------------|
| Site A Beach     | 353.63                   | 394.15                 | 195.55                         | 0.90                       | 0.38                       |
| Site A Dune Face | 224.49                   | 239.91                 | 87.07                          | 0.92                       | 0.85                       |
| Site A Swale     | 252.06                   | 274.98                 | 114.27                         | 1.03                       | 1.03                       |
| Site B Beach     | 285.59                   | 315.00                 | 139.83                         | 1.03                       | 0.96                       |
| Site B Dune Face | 218.14                   | 232.02                 | 81.80                          | 0.86                       | 0.64                       |
| Site B Swale     | 236.53                   | 253.01                 | 92.58                          | 0.93                       | 0.84                       |

The sediment at all three sampled sections at site B were more well-sorted than samples from site A, with skewness values indicating near symmetrical skewness at both sites.

Dahm (1983) discussed the general textural and mineralogical characteristics of local sediments, identifying quartz, plagioclase feldspars, rhyolitic rock fragments, shell and pumiceous material as the major constituents of the sediment. Dahm also identified little spatial variation with mineral ratios being relatively uniform throughout the area.

### 3.3.3 Compaction Results

Sediment compaction results were similar across the profile transects. Intervals in the swale, fore dune and beach showed differences between sites of 0.67, 6.66 and 6.66mm respectively (see Appendix I). Significant differences occurred at sample intervals 4 and 6.2 through the dune section of each transect (Figure 3.3).

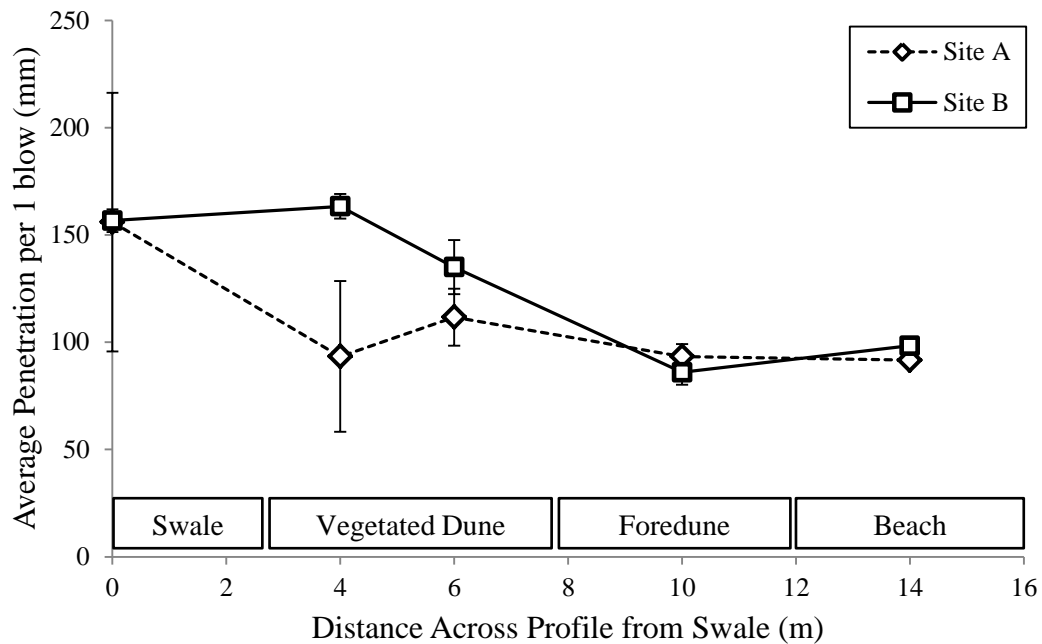


**Figure 3.5:** Average sediment compaction results at intervals across cross-shore transects at sites A & B obtained from Scala Penetrometer testing (error bars indicate 1 standard deviation away from mean).

Sample intervals 4 and 6.2 showed differences in average penetration of 70 and 23 mm respectively. Greatest variation was observed at the 4 m interval (vegetated section of dune) where a maximum penetration of 200 mm was achieved at sample site B, whilst a minimum of 90 mm was reached at sample site A.

### 3.4 CLASSIFICATION

#### 3.4.1 Vegetation classification

Vegetation between sample sites varied greatly, allowing each site to be classified by the dominant species present. Sample site A is characterised by the dominance of Marram grass (*Ammophila*) with an estimated total ground cover of 72.5%, whilst sample site B is characterised by the dominance of *Spinifex* grass with an estimated total ground cover of 62.5%. Based on this abundance at each sample site, it is assumed that sample site A, provides a reliable representation of typical Marram grass dune systems around New Zealand, while sample site B provides a reliable representation of typical *Spinifex* grass dune systems. Site B exhibited an average of 8% more ‘bare ground’ cover than that recorded at site A. The difference in bare ground cover reflects differences the growth densities

between the two species, with Marram having the densest growth. Gadgil (2002) showed that the growth of spinifex across the sand surface traps sand grains more evenly across the surface of the dune.

The classification of each site into A (*Ammophila* dominated dune) and B (*Spinifex* dominated dune) allows for between site comparisons to be made in following chapters.

### **3.4.2 Profile classification**

Site profiles and Dean's Parameter values show both sample sites A and B represent intermediate beach states, towards the reflective end of the scale. Beach width is small at high tide with a developed berm at both sample sites. Profile shapes vary slightly with site A only having a steeper foredune than seen in site B. Proximity between sites reduces any potentially large differences in profile shape, with any upper beach profile differences attributed to differences in vegetation between sites.

### **3.4.3 Sediment classification**

Local sediment is classified as medium sand, comprised of quartz, plagioclase feldspars, rhyolitic rock fragments, shell and pumiceous material.

Slight differences occur in the sediment characteristics between sample sites with site A displaying:

- Sediment that is more poorly sorted than site B.
- A mean grain size diameter greater than that at site B

As there is no other sediment source in the direct vicinity of the sampling area, sediment sorting and grain size differences could be attributed to three factors:

1. Sample site B is 50 metres to the southeast of sample site A. Assuming, as stated by Healy *et al* (1977) (refer to Chapter 1.2.1), that net littoral drift is in the southeast direction, sample site B is further from the source and hence is expected to exhibit sediment comprised of a smaller mean grain size that is better sorted than sediment closer to the source. However, the

influence of proximity to the source is considered negligible as the sample sites are only 50 m apart.

2. Fresher and more evenly distributed aeolian sand deposited at site B, due to different dominant vegetation species, is responsible for the smaller, better sorted sediment present.
3. A combination of factors 1 and 2 are responsible for variations in mean grain size and sorting between sites.

The possibility of aeolian sediment deposition being responsible for the differences in mean grain size and sorting observed between sites is examined in Chapter 5.

#### **3.4.4 Sediment Compaction**

Sediment compaction was similar across the profile transects. Intervals in the swale, fore dune and beach showed little differences between sites. Significant differences occurred at sample intervals through the dune section of each transect, with differences ranging between 20 and 70 mm (Figure 3.3), indicating more compaction at site A.

It is suggested that differences in sediment compaction observed between sites are linked to differences in mean sediment grain size and sorting. Poorly sorted sediments have a reduced porosity with smaller grains filling in the pores between larger grains. It is therefore assumed that sediment in the vegetation section of the dune at site A is less porous than that at site B, based on mean grain size and sorting, reducing the penetration achieved with the scala drop cone penetrometer during sampling. However, textural differences are small and it is more likely that penetration is linked to the mode of sediment deposition. In this case, aeolian sediment transport.

Differences in dune porosity between sites have the potential to impact the movement of groundwater in the dune, resulting in variations between sites. Aquifer level variations between sites, as a result of differences in porosity are explored in the following Chapter 4.

### 3.4.5 Overall Classification

Overall classification of the dune system at each sample site is as follows:

#### Site A

- Narrow intermediate beach comprised of medium sand.
- Sediment is more poorly sorted (standard deviation of 87.07 $\mu\text{m}$ ) with a larger mean grain size (239.9 $\mu\text{m}$ ) when compared to site B.
- Sediment porosity less than site B
- Incipient foredune dominated by *Ammophila arenaria*.

#### Site B

- Narrow intermediate beach comprised of medium sand.
- Sediment is better sorted (standard deviation of 81.80 $\mu\text{m}$ ) with a smaller mean grain size (232.02 $\mu\text{m}$ ) when compared to site A.
- Sediment porosity greater than site A.
- Incipient foredune dominated by *Spinifex sericeus*.

The two key differences between sites A and B are sediment porosity and predominant dune species. The potential link between these characteristics is explored in the following chapters. Chapters 4 and 5 further attempt to investigate and establish differences in aquifer fluctuation and aeolian sediment transport between sample sites, linking these variations back to the two key differences between sample sites identified in this chapter.

***CHAPTER FOUR***  
***SHORT TERM AQUIFER FLUCTUATIONS***

---

## 4.1 INTRODUCTION

Fluctuations in the levels of aquifers underlying coastal sand dunes are influenced by several factors. A sloping water table changes with the rising and falling of the tide, while also responding to wave run-up and rainfall infiltration. Higher aquifer levels will enhance erosion rates, illustrating the role coastal aquifer levels play in local sediment budgets.

In this chapter, a case for the influence of overlying vegetation on underlying aquifer levels is presented, based on comparing levels between sites.

### 4.1.2 Expected Outcomes

This chapter examines the following hypotheses relating to local short term aquifer fluctuations:

- The aquifer will respond to both forcing from tidal fluctuation and rainfall events. Tidal fluctuations will be seen in the aquifer with diminished amplitude and some lag, increasing with distance from the ocean. Rainfall events will be seen in the aquifer as an increase in mean aquifer level.
- Differences in aquifer fluctuation will occur between sample sites A and B, with the aquifer at sample site B will draining more readily than the aquifer at sample site A, due to differences in dune porosity and permeability, as a result of the varying vegetation types present at each site.

## 4.2 METHODOLOGY

### 4.2.1 Local Climate

An assessment of weather conditions as well as aquifer water levels required the installation of a temporary weather station and two piezometers at sample sites A and B. One primary station, Station A, was installed in the *Ammophila* dune section (identified in Chapter 3). A secondary station, Station B, was installed 50

m to the South East of Station A in the *Spinifex* dune section. Wind vanes and anemometers were installed in both samples sites (A & B). At site A these were attached to the top of a 4 m station tower, to reduce any obstruction to wind speed and direction resulting from low lying vegetation cover on the dunes (Figure 4.1). At site B both wind vane and anemometer were positioned at a height of 1 m to gauge wind speed and direction at plant level. The wind vanes at both stations were orientated with north corresponding to zero degrees. A rain gauge was installed atop a levelled structure, 1.5 m above ground level, at site A to reduce rain obstruction through wind turbulence as a result of the surrounding vegetation. On site wind and rainfall data were compared with data obtained through NIWA's CliFlo programme, to ensure on site stations were recording comparable outcomes with those obtained for Waihi Beach and Tauranga Aero Club (the 2 closest NIWA stations that are still currently recording).



**Figure 4.1:** Station set-up at sample site A measuring wind speed, direction and rainfall. Wind speed and rainfall are collected from the top of a 4m tower.

Issues with the onsite rain gauge resulted in a large amount of onsite rainfall data missing or unusable. From early data that were usable, it was deduced that rainfall

data obtained from NIWA's CliFlo station at the Tauranga Aero club provided a reasonable estimation of onsite rainfall conditions (Figure 4.2).

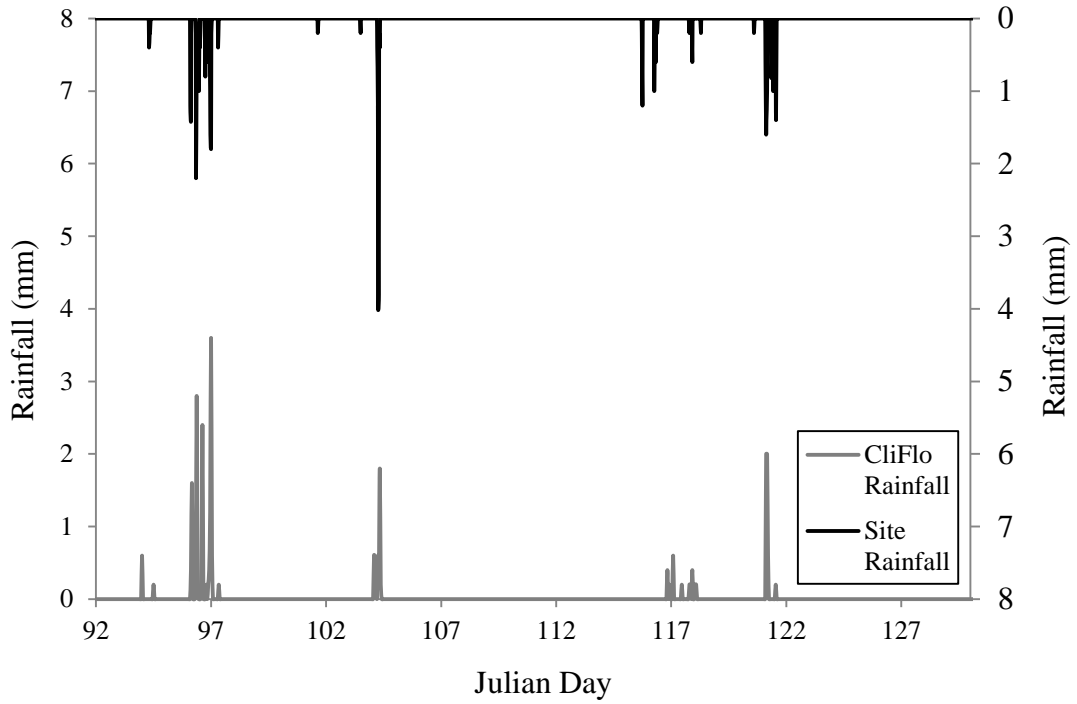


**Figure 4.2:** Rainfall at sample site A and Tauranga Aero Club (obtained from NIWA's CliFlo programme) for a 37 day period from early April to early May, 2010.

#### 4.2.2 Piezometer Placement and Measurement

A single piezometer was placed in the fore dune of sites A & B (Figures 4.3 & 4.4). The foredune section of the swale to MSL cross shore transect was deemed most appropriate for placement due to it being the lowest point of surface elevation within the dune still incorporating the overlying vegetation.



**Figure 4.3:** Piezometer placement in the fore dune of Station B. Red box indicating position of PVC tubing, pressure sensor and waratah.

A soft sediment auger was used to dig holes at both stations down to the water table. 2.5 m lengths of PVC (Polyvinyl chloride) tubing, 40 mm in diameter were inserted in the holes. The tubing had to be pushed and twisted down to sit 0.5 m below the water table, as sediment below this point was liquefied and could not be removed with the auger, and it was not assumed that water table level was as its minimum. 0.4 m of tubing was left protruding above the dune surface.

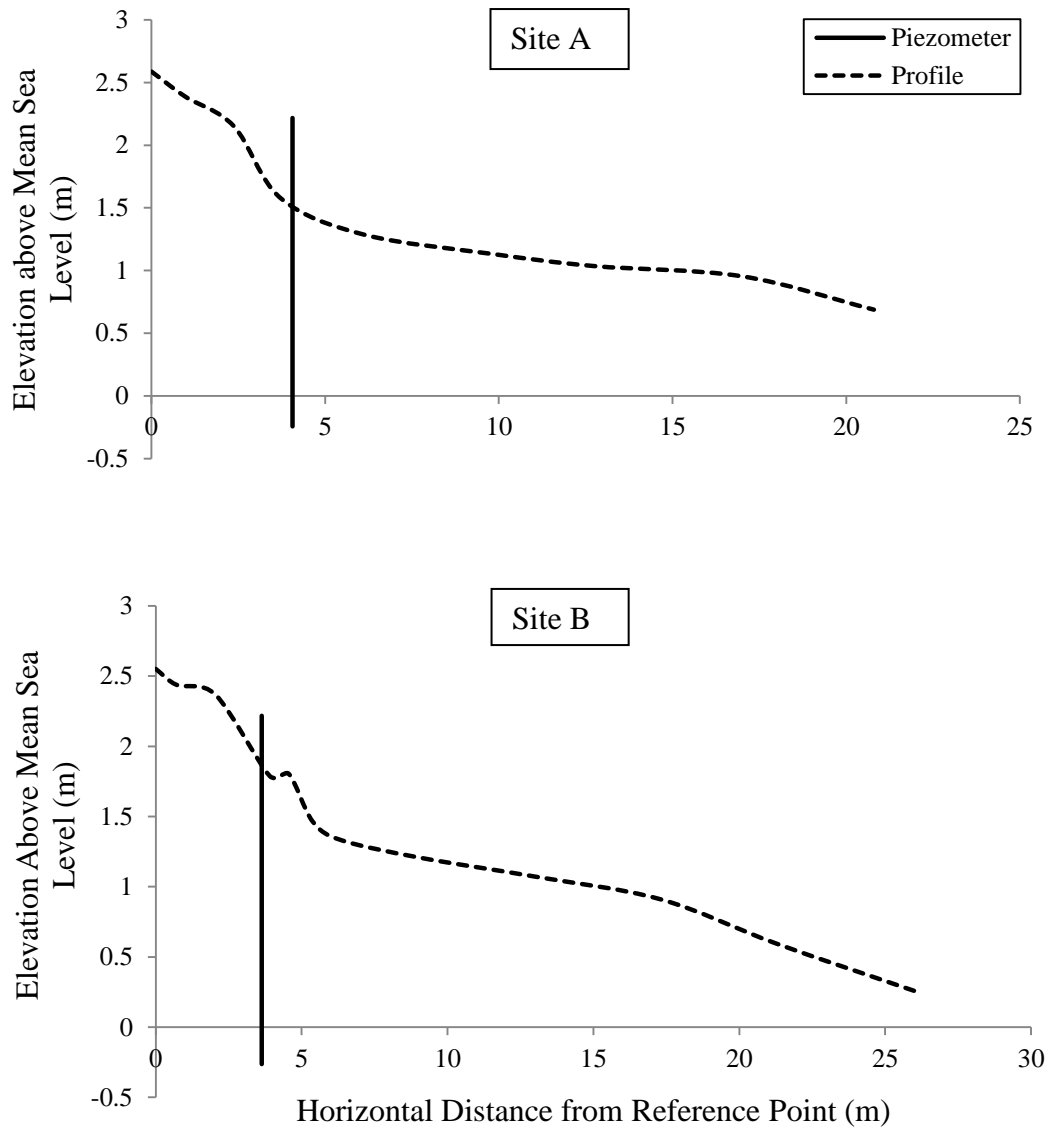


**Figure 4.4:** Profiles for sample sites A & B, showing piezometer location in sample site A (top) and sample site B (bottom).

The PVC had several horizontal slits cut into the lower 150 mm of its length. These slits were then covered with a fine mesh plastic fabric, which was taped around the tubing to prevent sediment from entering, whilst still allowing water to pass through. The tubing was sealed at the bottom end with a PVC cap and silicone. A Hydrological Services WL 1000 Pressure Transducer was inserted into the tubing at each station and positioned 20 mm up from the bottom. The sensors were completely submerged below the water table and self corrected to atmospheric pressure via an outlet at the top end of the sensor cable. Both sensors were calibrated in the lab and in the field using an external pipe with a known

water level. Dip well measurement were also taken to ensure sensors were reading accurately. Sensors were attached to a stable waratah driven into the dune next to the tubing. This was to ensure sensors remained in the same position if some vertical movement of the PVC tubing occurred. Both sensors recorded to separate CR10X data loggers, measuring the water level in the tubing every 10 minutes and recording 30 minute averages.

### **4.2.3 Sampling Limitations**

Several problems affected the collection of data at sample site A over the duration of this study and are identified as the following:

- Failure of the pressure transducer measuring water table levels at site A resulted in large chunks of the water table data for the site being unusable.
- Strong winds during May managed to twist the sampling tower at sample site A by a considerable amount. As the solar panel charging the battery at site A was attached to the sampling tower, it was also rotated away from its north facing aspect. As a result, the battery only gained enough charge to power instruments for a couple of hours in the afternoon on sunny days. As a result, little data were available for site comparisons beyond the 11<sup>th</sup> of May.
- Aquifer level was only measured at a single location. Several measuring points would provide a more detailed interpretation of aquifer fluctuations.

### 4.3 RESULTS

#### 4.3.1 General aquifer fluctuation

Aquifer depth at sample sites A and B was observed and compared to establish any difference between sites. As a general observation, aquifer fluctuation both spatially and temporally at one site, was reflected in fluctuation at the second site. Figure 4.5 illustrates this relationship, with a regression comparison of aquifer depth between sites giving a high  $R^2$  value of 0.999.

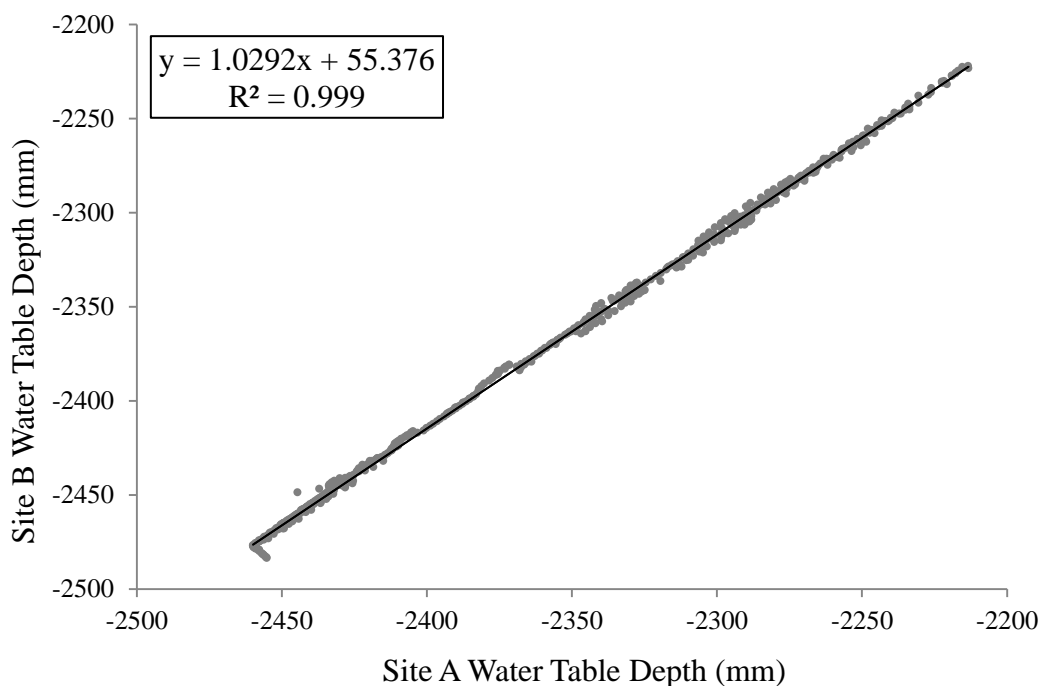


**Figure 4.5:** Regression correlation plot for aquifer depth at sites A & B over an 11 day period beginning in late April and ending in early May, 2010.

##### 4.3.1.1 Aquifer response to tidal fluctuations

Aquifer depth at sites A and B responded to local tidal fluctuations. NIWA's Tide Forecaster (<http://.niwa.co.nz/our-services/online-services/tides>) was used to generate tide peaks and troughs at co-ordinates: 37° 32'57"S, 176° 04'01"E, an area just offshore of sample site locations on Matakana Island. Time difference between forecasted tidal peaks for Matakana Island data was 12.48 hours, matching the time difference of 12.48 hours between peaks and troughs in aquifer

depth at sites A and B. The relationship between aquifer depth fluctuation and tidal fluctuation is illustrated in Figure 4.6. The two most notable points in Figure 4.6 are: the time delay, or lag, between peaks or troughs of tidal level and aquifer depth and the asymmetric shape of the tide represented in the aquifer. On average, peaks or troughs in aquifer depth lag 2.16 hours behind peaks or troughs in tidal fluctuation. Tidal fluctuations are apparent in aquifer levels throughout the entirety of the data set, irrelevant of any fluctuations in aquifer depth as a result of other forcing.

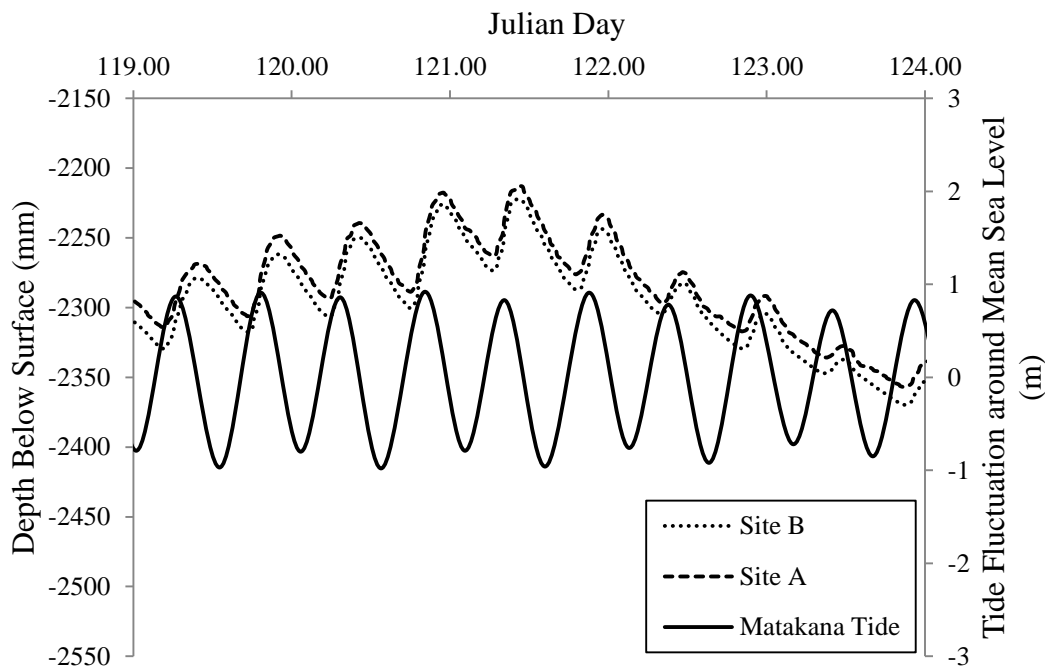


**Figure 4.6:** Aquifer level below surface at sample sites A & B and Matakana Island onsite tide heights (generated via NIWA’s Tide Forecaster) for 5 day period in late April to early May, 2010.

Medium moderately sorted sand has a hydraulic conductivity ( $K$ ) range from 5 to 20  $\text{m.d}^{-1}$  and an assumed porosity of 40% (Curry *et al*, 2004). The flow rate of water through unconfined aquifers,  $Q$ , is given by Darcy’s Law (Li *et al*, 1997):

$$Q = -K \frac{\partial h}{\partial x}$$

Equation (4.1)

Where  $K$  is hydraulic conductivity ( $\text{m.h}^{-1}$ ),  $h$  is hydraulic head (m) and  $x$  is the distance (m). Darcy's Law was applied to the fluctuation of aquifer height at the piezometer, giving flow rate values ranging from 0.2 to 0.8  $\text{m.h}^{-1}$ , relative to the range of hydraulic conductivity used (Table 4.1). A  $\partial h/\partial x$  ratio of 1 was used as  $\partial h$  is considered equal to  $\partial x$  when assuming only vertical movement of the aquifer. The pore velocity is related to the Darcy flux ( $Q$ ) by sediment porosity ( $n$ ), pore velocity flow rate,  $v$ , can therefore be given by the equation (Rehbinder, 1978):

$$v = \frac{Q}{n}$$

Equation (4.2)

Where  $n$  is sediment porosity and  $Q$  is Darcy flux. A range of hydraulic conductivity and sediment porosity values were applied under optimum tidal forcing conditions recorded at sample sites, with an assumed static aquifer level (Table 4.1). The application of these conditions was used to assess potential water movement through the sediment, accounting for the lag between tidal fluctuations and aquifer fluctuations

**Table 4.1:** Aquifer flow velocities ( $\text{m.h}^{-1}$ ) under various sediment porosity and hydraulic conductivity values

| Hydraulic Conductivity<br>( $K$ ) | Sediment Porosity |             |            |             |            |             |            |
|-----------------------------------|-------------------|-------------|------------|-------------|------------|-------------|------------|
|                                   | <b>0.3</b>        | <b>0.35</b> | <b>0.4</b> | <b>0.45</b> | <b>0.5</b> | <b>0.55</b> | <b>0.6</b> |
| <b>5</b>                          | 0.69              | 0.60        | 0.52       | 0.46        | 0.42       | 0.38        | 0.35       |
| <b>10</b>                         | 1.39              | 1.19        | 1.04       | 0.93        | 0.83       | 0.76        | 0.69       |
| <b>15</b>                         | 2.08              | 1.79        | 1.56       | 1.39        | 1.25       | 1.14        | 1.04       |
| <b>20</b>                         | 2.78              | 2.38        | 2.08       | 1.85        | 1.67       | 1.52        | 1.39       |

Potential aquifer flow velocities in response to tidal fluctuations ranged from as little as 0.35, through to, 2.78  $\text{m.h}^{-1}$ . The distance between the piezometers and swash zone varied between 15 and 65 m dependent on the phase of the tide. Based on an average flow velocity of 1.56  $\text{m.h}^{-1}$  and an average distance between piezometers and swash zone of 40 m, it would take the flood tide peak 25.6 hours to be observed at the piezometer, much greater than the 2.16 hour lag suggested in Figure 4.6

A further point to note is that the tidal peak is often seen in the aquifer peak at site B between 20 and 30 minutes earlier than it is seen at site A.

#### 4.3.1.2 Aquifer response to rainfall infiltration

Aquifer depth at sample sites A and B responded to rainfall events as well as tidal fluctuations. The relationship between rainfall and aquifer depth is illustrated in Figure 4.7. Mean aquifer levels elevate in response to rainfall events, with levels diminishing following rainfall events. Rainfall data was obtained from NIWA's CliFlo station at the Tauranga Aero Club and was used as a measure of on site rainfall conditions. The response time of aquifer fluctuation following rainfall events varied, with an average 10 hour lag due to the time taken for rainwater to infiltrate the sediment and percolate down to the present water table level. A point to note illustrated in Figure 4.7 is in a few select instances, minimum aquifer levels begin to elevate when no rainfall events are occur. Following this, minimum aquifer levels drop in some instances following large rainfall events. These discrepancies may be linked to CliFlo station positioning and profile evolution.

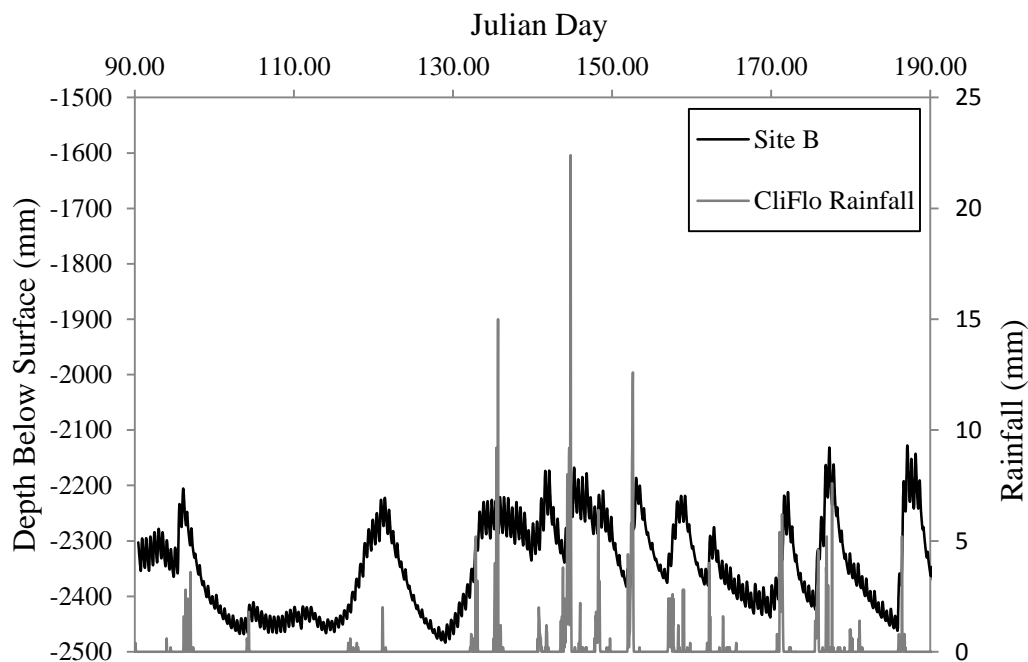


**Figure 4.7:** Aquifer level below surface at sample site B and rainfall for Tauranga Aero Club (NIWA CliFlo data) over a 100 day period from late March to early July, 2010.

#### **4.3.1.3 Aquifer response to profile evolution**

During the winter months it was expected that there would be an increase in minimum aquifer levels at both sites A and B as a result of an increase in rainfall occurrence duration and quantity. Figure 4.8 illustrates an elevation in minimum aquifer level on day 94, 2010. Following this, aquifer levels fall to more than 100mm lower than what they were prior to the rainfall event (red box a). Around day 130, an elevation in aquifer level occurred over a 5 day period that preceded any rainfall event, brings minimum aquifer levels back to a similar level to what they were at day on day 90 (red box b).

Figure 4.8 illustrates a steady decline in minimum aquifer levels (red box c) from day 150 through to day 190 (winter months) despite frequent rainfall during this period (Figure 4.7). Minimum aquifer levels return to low levels exhibited earlier in the year (red box d).

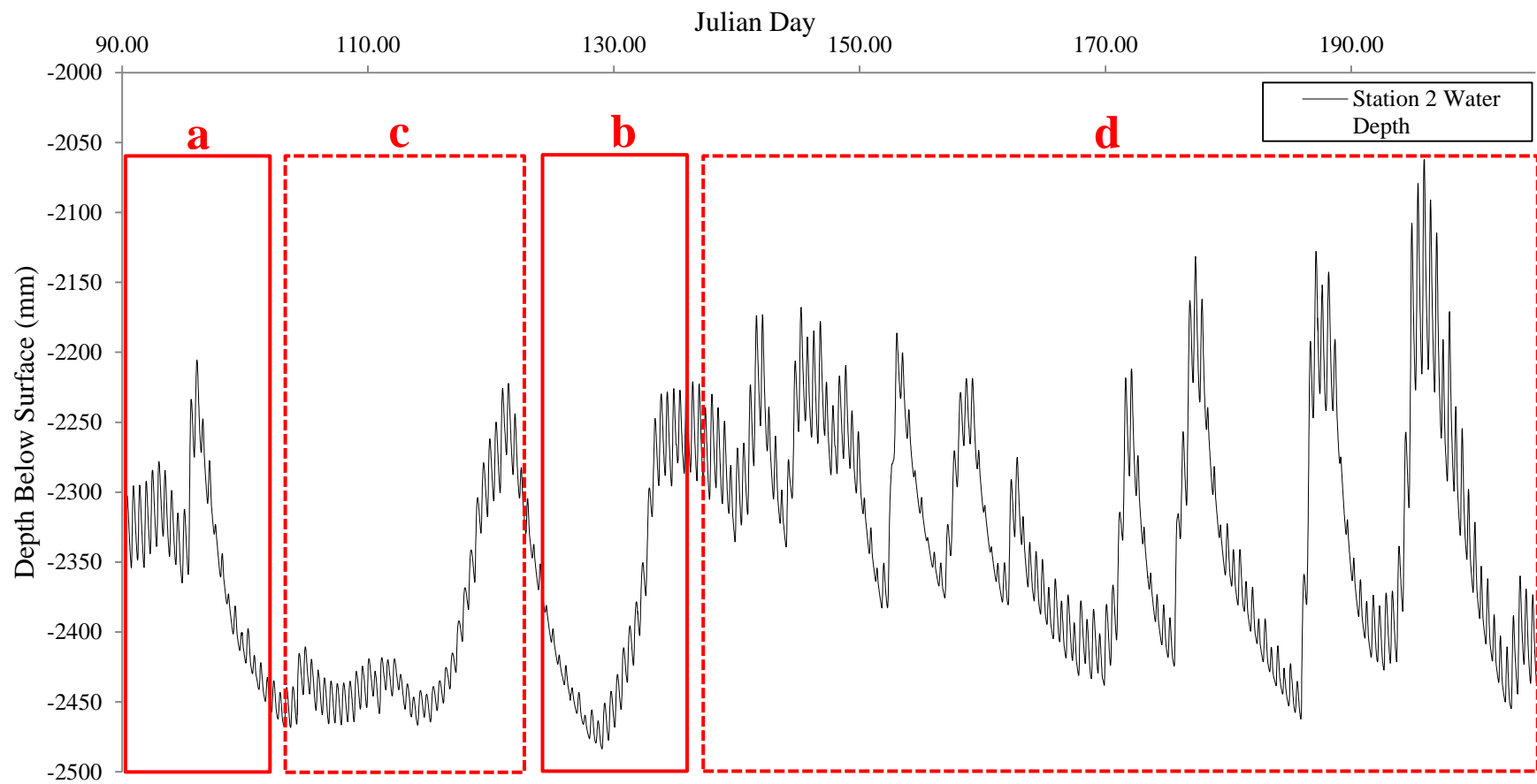


**Figure 4.8** Aquifer level below surface at sample site B over a 100 day period from late March to early July, 2010. Red boxes a, b, c and d indicate periods of elevated and low minimum aquifer level and are discussed in the text.

During the aquifer level changes outlined in Figure 4.8, beach morphodynamic shape (profile) moved through a series of phases (Figures 4.9 & 4.10). During times when the minimum aquifer level was high (red boxes a & b Figure 4.8) the beach profile shape was similar. Profile shape at day 138 has a more eroded beach face, but more sediment in the upper beach close to the foredune. Profile shape at day 138 has a more eroded beach face, but more sediment in the upper beach close to the foredune.

During periods when minimum aquifer levels were low or declining (red box c Figure 4.8) profile shape differed, displaying a more eroded profile. In comparison with beach profile on day 138, beach profile on day 210 illustrates a more eroded upper and lower beach, with the relocation of the berm seaward.

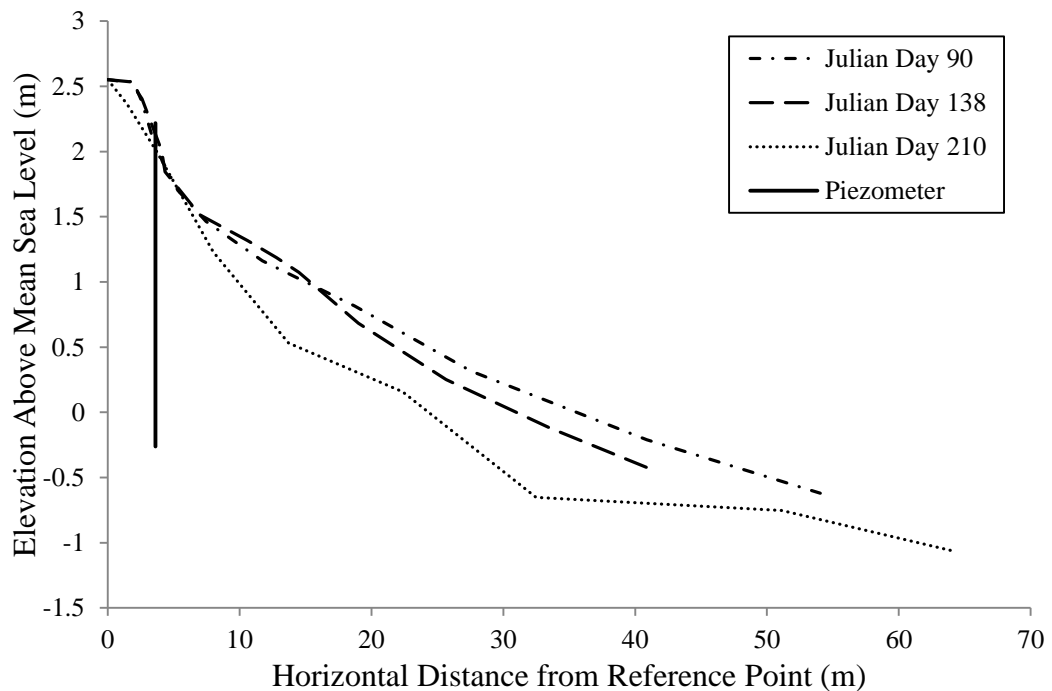


**Figure 4.9:** Beach profiles above mean sea level (MSL) at site B for days 90, 138 and 210, showing beach profile evolution over a 120 day period from late March to late July in 2010. Piezometer location is also displayed.

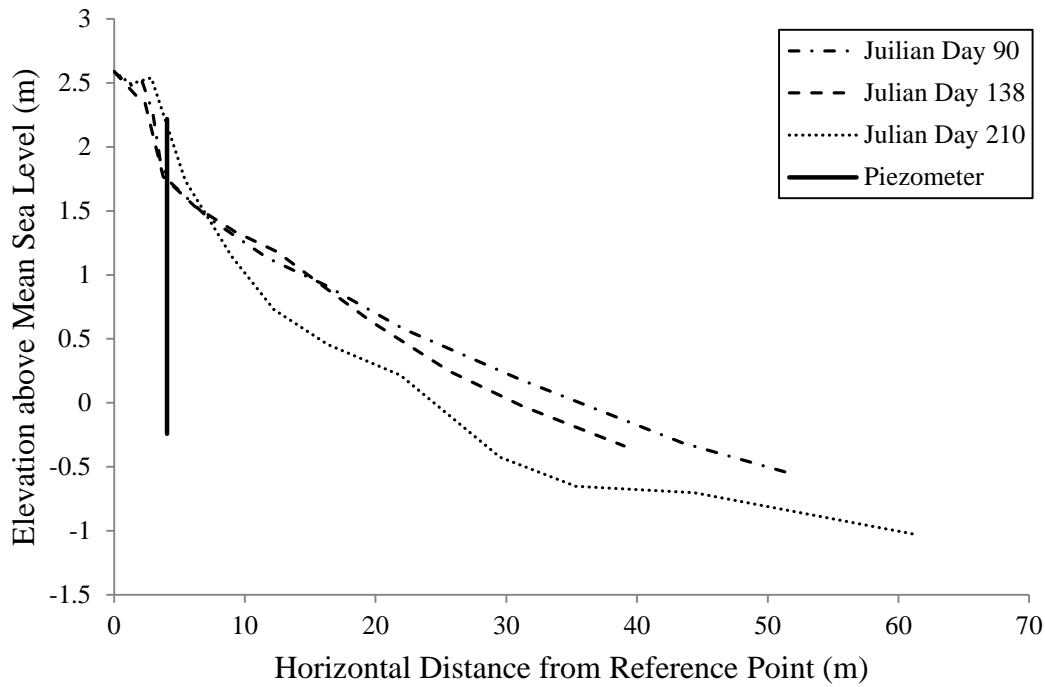


**Figure 4.10:** Beach profiles above mean sea level (MSL) at site A for days 90, 138 and 210, showing beach profile evolution over a 120 day period from late March to late July in 2010. Piezometer location is also displayed.

#### 4.3.2 Potential aquifer response to sediment compaction and overlying vegetation.

12 hour mean aquifer levels for site A and B were calculated to remove tidal fluctuations, allowing the overall trend in response to rainfall and profile evolution to be easily identified. Figure 4.11 illustrates 12 hour mean aquifer levels for sites A & B over a 12 day period, incorporating their response to a small rainfall event. The difference between site A and B means is also plotted. The key point to note from Figure 4.11 is that as aquifer levels increase, the difference between them decreases and as the aquifer levels decrease the differences between them increases.

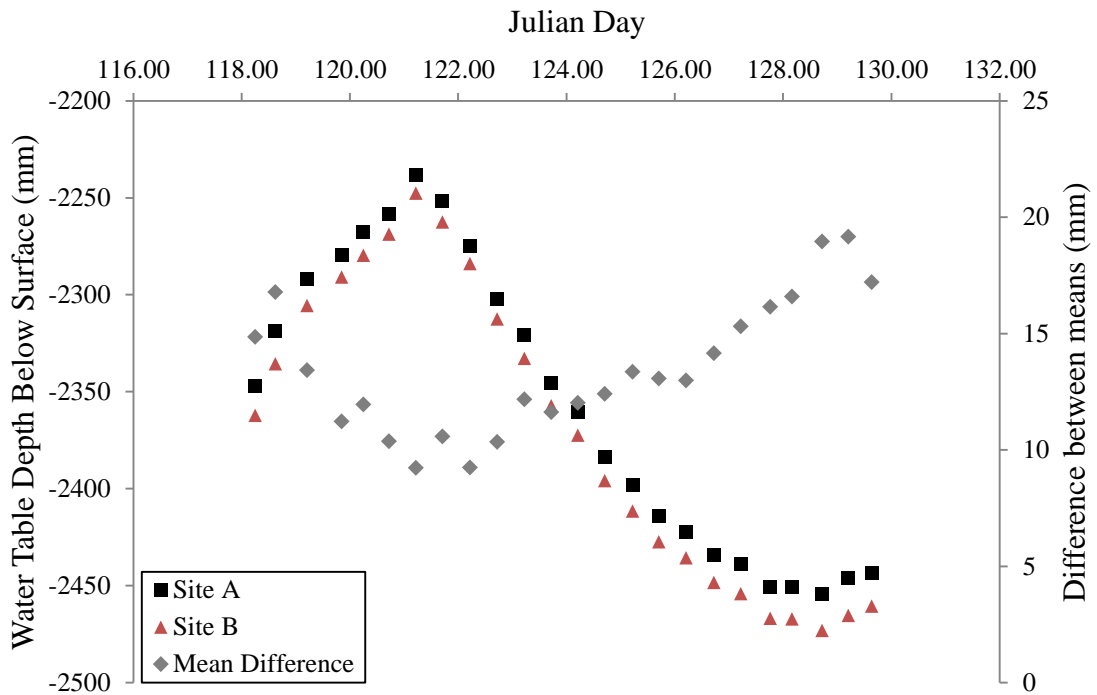


**Figure 4.11:** 12 hourly average aquifer level and sites A & B over a 12 day period from late April to early May, 2010. Also shown is the difference between site A and site B means for the same time intervals.

The same trend exhibited in Figure 4.11 is also illustrated in Figure 4.12. The plot shows aquifer levels responding to a rainfall event earlier in the year (days 99 to 104), with levels dropping following the event. Lines of best fit have been applied to each data set to show the general trend for the displayed timeframe. As previously exhibited in Figure 4.11, Figure 4.12 also shows that as aquifer levels drop following a rainfall event, the difference between aquifer levels greatens.

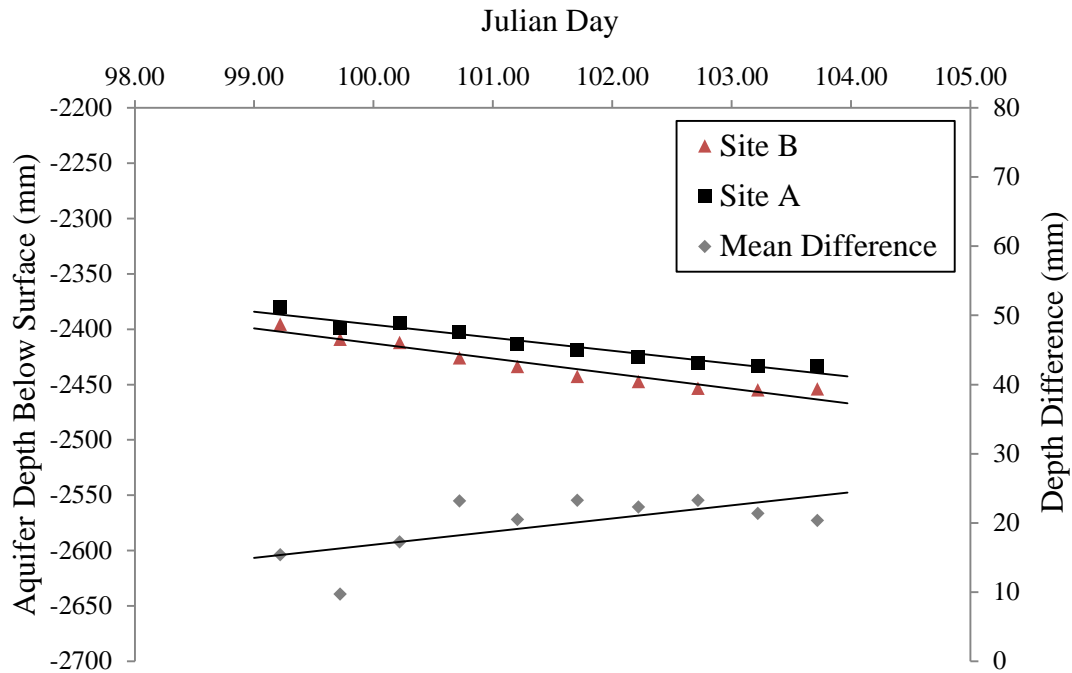


**Figure 4.12:** 12 hourly average aquifer level and sites A & B over a 5 day period in April, 2010. Also shown is the difference between site A and site B means for the same time intervals. Lines of best fit have been applied to the three data sets.

## 4.4 DISCUSSION

### 4.4.1 General aquifer fluctuation

The proximity of site A to site B ensured that any fluctuation in aquifer level at one site was reflected in the other. The relationship between sites A and B was exhibited in Figure 4.5 where a regression analysis showed a strong relationship between the aquifer levels at each site, with an  $R^2$  value of 0.999. The strong relationship reflects the similar response at each site to tidal fluctuations, rainfall and profile change.

Aquifer levels at sites A and B responded strongly to local ocean tidal fluctuations. Tide induced oscillations in aquifer levels landward of the high tide mark have been shown in various studies (Nielsen, 1990; Turner, 1993; Baird & Horn, 1996; Li *et al.*, 2006). In accordance with the literature, a rise and fall of aquifer levels with respect to tidal fluctuations is exhibited throughout the entirety of the data set

(Figure 4.6). Chappell *et al* (2003) showed that water table height variations are coupled with tides and propagate landward as a slow wave of increasing lag and diminishing amplitude.

Agreeing with these results, in this study tidal fluctuations seen in aquifer levels in are shown to lag on average 2.16 hours behind tidal fluctuations predicted directly offshore from the sample sites. Offshore tidal amplitude varied through neap and spring phases and diminished to amplitudes of around 50 mm by the time it propagated to the position of the piezometer. The lag was expected and can be explained by the transmission of water level and pressure through the beach. Piezometers at sites A and B were positioned more than 30 m landward of mean sea level, requiring the tidal movement to pass through beach sediment before it's fluctuation is seen at the piezometers.

The velocity of this movement could be affected by several factors including sediment porosity, hydraulic conductivity (dependent on grain size and sorting and permeability), distance in which the water must travel and the hydraulic head or forcing that is applied. Potential aquifer flow velocities in response to tidal fluctuations ranged from as little as 0.35, through to 2.78 m.h<sup>-1</sup> (Table 4.1). The distance between swash zone and piezometers ranged between 15 and 65 m dependent of the phase of the tide. During an instance of average flow velocities and distance between piezometers and swash zone, it would take the flood tide peak 25.6 hours to be observed at the piezometer, much greater than the 2.16 hour lag suggested in Figure 4.6. Horizontal flow of water into the beach is therefore dismissed as the main driving factor behind aquifer lag, with the transmission of pressure suggested as a more likely reason.

The local ocean and coastal aquifer are hydraulically connected. Rather than flowing into the beach, aquifer levels fluctuate based on the transmission of pressure applied and removed by the rising and falling of the tide at the land/ocean boundary (Xun *et al*, 2006). The pressure induced by a flood tide at this boundary transmits through the aquifer causing the aquifer to elevate into available pore space compensating for the pressure increase. The transmissivity of the aquifer is directly proportional to it's the hydraulic conductivity and thickness (Marui & Yasuhara, 1993). It is therefore suggested that the lag seen between

tidal fluctuation and aquifer fluctuation is a result of the porosity, permeability and hydraulic conductivity of the beach and dune sediment.

Aquifer levels fluctuating in response to tidal forcing are asymmetrical in shape compared to the symmetrical sinusoidal curve expressed by offshore tidal fluctuation (Figure 4.6). The asymmetrical shape is a product of aquifer levels rising more steeply than they fall. The steep slope of the curve expresses the speed of infiltration, with the flatter slope expressing the slower rate of drainage. Steele (1995) showed similar results for Waihi Beach, suggesting the rear slope (slower drainage section of the curve) may be an indication to the amount of groundwater contained in the upper slope profile that must drain past the measured lower position. The rear slope of the fluctuation curve was also indentified as a function of drainage capability. Steele's suggestion is illustrated in this study's results through the pattern of change in the rear slope of aquifer fluctuation (Figure 4.6). As average aquifer levels drop, aquifer fluctuation becomes more asymmetric due to a slower fall rate. In accordance with Steele (1995) it is suggested that this is a result of a diminishing amount of groundwater contained in the upper slope profile.

Aquifer depth at sample sites A and B responded to rainfall events as well as tidal fluctuations (Figure 4.7). The relationship between unconfined coastal aquifers and atmospheric processes (such as rainfall and barometric pressure) is well documented (Turner & Nielsen, 1997; Horn, 2006). The results of this study sit in line with this literature, with mean aquifer levels elevating in response to rainfall events, leaving levels to diminish more slowly following rainfall events. Response time of aquifer fluctuation following rainfall events varied, with an average 10 hour lag due to the time taken for rainwater to infiltrate the sediment and percolate down to the present water table level. The lag between rainfall event and mean aquifer elevation can be attributed to the permeability and porosity of the overlying sediment. As with aquifer flow, rainfall infiltration is affected by sediment porosity and hydraulic conductivity.

An interesting point, is that in a few select instances, minimum aquifer levels begin to elevate prior to rainfall events occurring. Following this pattern, minimum aquifer levels were seen to steadily decline despite frequent rain events

during the winter months. Some of this variation may be reflected in localised rainfall events. The Tauranga Aero Club is approximately 18 km to the south-east of the study site. It is therefore possible that rainfall occurred at the study site and either did not occur at the Tauranga Aero Club CliFlo station, or occurred at a different time, providing some explanation to these aquifer fluctuations. Following further investigation, some of this fluctuation is attributed to profile change.

Figure 4.8 illustrated the rise and fall in minimum aquifer levels at sites A and B during 120 day period in 2010. Red boxes a, b, c and d show periods where minimum aquifers levels rose and fell regardless of tidal and rainfall induced fluctuation. During these periods, significant profile change is identified. Between days 138 and 210 a large amount of upper and lower beach face erosion was observed (Figures 4.9 & 4.10) (red box c). During this time, aquifer level responded to profile change through a diminishing minimum level. Beach erosion induced a landwards migration of shoreline position, steepening the average gradient in aquifer surface between the piezometer location and shoreline position in the shoreward direction. A steepening in average aquifer gradient would explain a greater flux of groundwater propagating in the seaward direction and account for diminishing minimum aquifer levels following erosion events through some drainage of the aquifer.

However, a more short-term relationship between aquifer slope and beach profile is recognised as discussed in the literature (Chappell *et al*, 1979; Lanyon *et al*, 1982). Steele (1995) summarised this relationship, suggesting the following:

- During the early flood tide, aquifer level slopes seaward draining through the beach face as the terrestrial aquifer level is higher than the sea level. This situation is more likely to facilitate erosion in the swash zone as a result of ground water seepage.
- Once sea level has risen above the level of the beach water table, infiltration of sea water into the beach face occurs, causing aquifer surface to slope landwards. The steepest gradient occurs where elevation between sea level and aquifer is greatest. Greatest gradients occur when swash

excursions traverse the steeper more elevated berm slope. Under these conditions, sediment deposition is favoured.

Recognising the impact swash zone mechanics have on short term fluctuation in aquifer levels, it is suggested that profile shape influences aquifer levels over a longer time scale, with average aquifer levels responding to larger scale erosion and depositional events.

#### **4.4.2. Potential aquifer response to sediment compaction and overlying vegetation.**

A lag ranging from 20 to 30 minutes, between aquifer fluctuation at sites A and B was often exhibited throughout the data set. The lag suggests the permeability at site A is less than site B, as indicated by the scala penetrometer measurements, reducing hydraulic conductivity and therefore aquifer pressure transmissivity. Potentially the lag could be explained by the proximity of the piezometer, to the shoreline, and/or difference in profile shape. This potential is dismissed as firstly, there is little difference between profile shapes at each site, and secondly, the piezometer at site A is located 0.42 m closer to the average shoreline position than the peizometer at site B. It would be expected that any fluctuation should therefore be seen first at site A rather than site B.

A lag between sites A and B is also seen in their response to rainfall events. Figures 4.11 and 4.12 simply display this lag. In these figures, 12 hour mean water table levels have been plotted to remove the noise of sinusoidal tidal fluctuations. The figures show the difference in mean aquifer level between sites diminishes as the aquifer rises in response to a rainfall event, and increases as it falls following a rainfall event. This pattern of a decreasing and increasing mean difference is the result of aquifer level at site B rising and falling faster than site A, in response to rainfall events.

The lag between sites A and B is therefore attributed to differences in porosity and permeability between sites. Earlier investigations (refer section 3.3.4 Chapter 3) illustrated the difference in sediment compaction between sites. Through the vegetated section of dune, the sediment at site A is shown to be more compacted than that sampled at site B. Nygard, *et al* (2004) showed that as sediment is compacted, its' porosity and permeability decrease. Decreasing the permeability

of sediment decreases the ease and speed at which groundwater can pass, as well as causing a decrease in transmissivity. It was hypothesised that overlying vegetation effects dune porosity and permeability and hence impacts the movement of groundwater in the dune. The lag in aquifer levels between sites A and B supports this hypothesis. The distinguishing feature between the adjacent study sites (refer to section 3.4.4 Chapter 3) was primarily vegetation type and its influence on sediment compaction. Greater compaction at site A in comparison to site B implies decreased porosity and permeability in the vegetated section of the dune at site A. Decreased porosity and permeability values lead to a decrease in aquifer flow velocities (Table 4.1) and aquifer transmission properties, restricting rainfall infiltration and the propagation of the tide through the beach.

#### 4.4 CONCLUSIONS

Analysis of coastal aquifer levels in the beach system of Matakana Island showed some results typical of sandy beaches worldwide, results which further distinguished between the two beach types characterised in Chapter 3 and results which stress the complexity of the coastal system. The following conclusions have been drawn from the analysis of coastal aquifer fluctuation:

- Matakana Island aquifer levels beneath the dune face were highly variable. Fluctuations were a combination of short-term and long-term change as a result of a range of factors including tide, rainfall and profile shape.
- Short-term cyclical fluctuations in aquifer level occurred as a result of tidal forcing. The cycles were asymmetrical in the aquifer compared to symmetrical offshore as their shape is a function of beach drainage capability and the amount of groundwater contained in the upper slope of the profile.
- Longer term change in the profile of the beach influenced average aquifer levels, with an accreting beach resulting in an elevating average aquifer level and an eroding beach resulting in a diminishing aquifer level.
- Lower sediment permeability in the *Ammophila* dominated dune system hindered the movement of groundwater resulting in the *Spinifex* dominated dune system filling and draining more readily.

The key suggestion surrounding the beach face groundwater dynamics discussed in this chapter is the ability of *Spinifex* to provide more mobile groundwater movement when compared to *Ammophila*, supporting the original hypothesis that *Spinifex* is well equipped to create a more porous and permeable dune. The differences in sediment compaction between sites (which give rise to porosity and permeability differences) as a result of differing vegetation types are discussed in the following chapter.



# **CHAPTER FIVE**

## **AEOLIAN SEDIMENT TRANSPORT**

---

### **5.1 INTRODUCTION**

Sand binding vegetation can greatly increase sediment accretion and enhance the formation of dunes on sandy beaches. Features that are poorly stabilised by vegetation are prone to sediment losses. Sediment mobilisation by wind is heavily affected by any saturation at the source. Local wind and rain therefore, play an important role in the flux of sediment in many coastal regions, (List, 2005).

Analysis of local wind and rain patterns as well as aeolian sediment movement on Matakana Island is undertaken in this chapter. Differences between sample sites are related to the site classification.

#### **5.1.2 Expected Outcomes**

This chapter examines the following hypotheses relating to local wind and rainfall events and aeolian sediment transport:

- The onshore component of aeolian sediment transport will dominate over the offshore component despite the characteristic offshore (south-west) winds of the region. Larger dunes landward of the sample site are vegetated with pine forest, largely sheltering sample sites from offshore winds.
- Aeolian sediment deposition will be more evenly distributed throughout the dune at site B, based on the growth characteristics of *Spinifex sericeus*. Deposition at site A will primarily occur at the seaward edge of dune vegetation due to the density in which *Ammophila arenaria* grows.

It is hypothesised that sediment will be deposited more evenly throughout the dune at sample site B, with deposition at site A predominantly occurring in the foredune. If this hypothesis is correct, the process of aeolian sediment transport may provide some explanation to the between site differences in sediment size

and porosity observed in chapters 3 and 4, further strengthening the linkages between dune vegetation type and local sediment budgets.

## **5.2 METHODOLOGY**

### **5.2.1 Vegetation Sampling**

The method for vegetation sampling is outlined in Chapter 3 (section 3.2.1). This method of sampling was used to identify the main species of sand binding plant present at each sample site and the denseness of its growth.

### **5.2.2 Aeolian Sediment Transport Sampling**

Sampling of aeolian sediment transport was achieved by catching aeolian sands with custom built sand traps during three periods between June and November 2010. An aeolian trap was developed from the device described by Leatherman (1978). Eight sampler units and 16 sampler inserts were constructed. Trap specifications are as follows (Figure 5.1):

- The body of each sampler unit was constructed from 106 cm lengths of PVC piping, each with a diameter of 10 cm.
- 9.8 cm and 6.3 cm wide slits were cut to extend 45 cm down from the top of the tube. The centre of each slit was orientated on directly opposite sides of the tubing. A 1cm strip of tubing was left at the top of each tube to preserve structural integrity (Figure 5.1).
- The larger slit was covered with 50  $\mu$ m screening, whilst the smaller slit remained open and served as an entry for sediment.
- The base is covered with 50  $\mu$ m screening and reinforced with tape to allow rainwater to pass through and prevent each unit from shifting, should groundwater reach the base of units.
- Inserts were constructed from 55 cm lengths of PVC piping, each with a diameter of 9 cm.
- The base of each insert was covered in 50  $\mu$ m screening to allow water to pass whilst still collecting sediment.
- Rubber sealers and tape were used to create a ring around the top of each insert and ensured a tight seal between inserts and trap units once units were in place.

- String was attached to the top of each insert so they could be removed without altering the position of the trap unit.

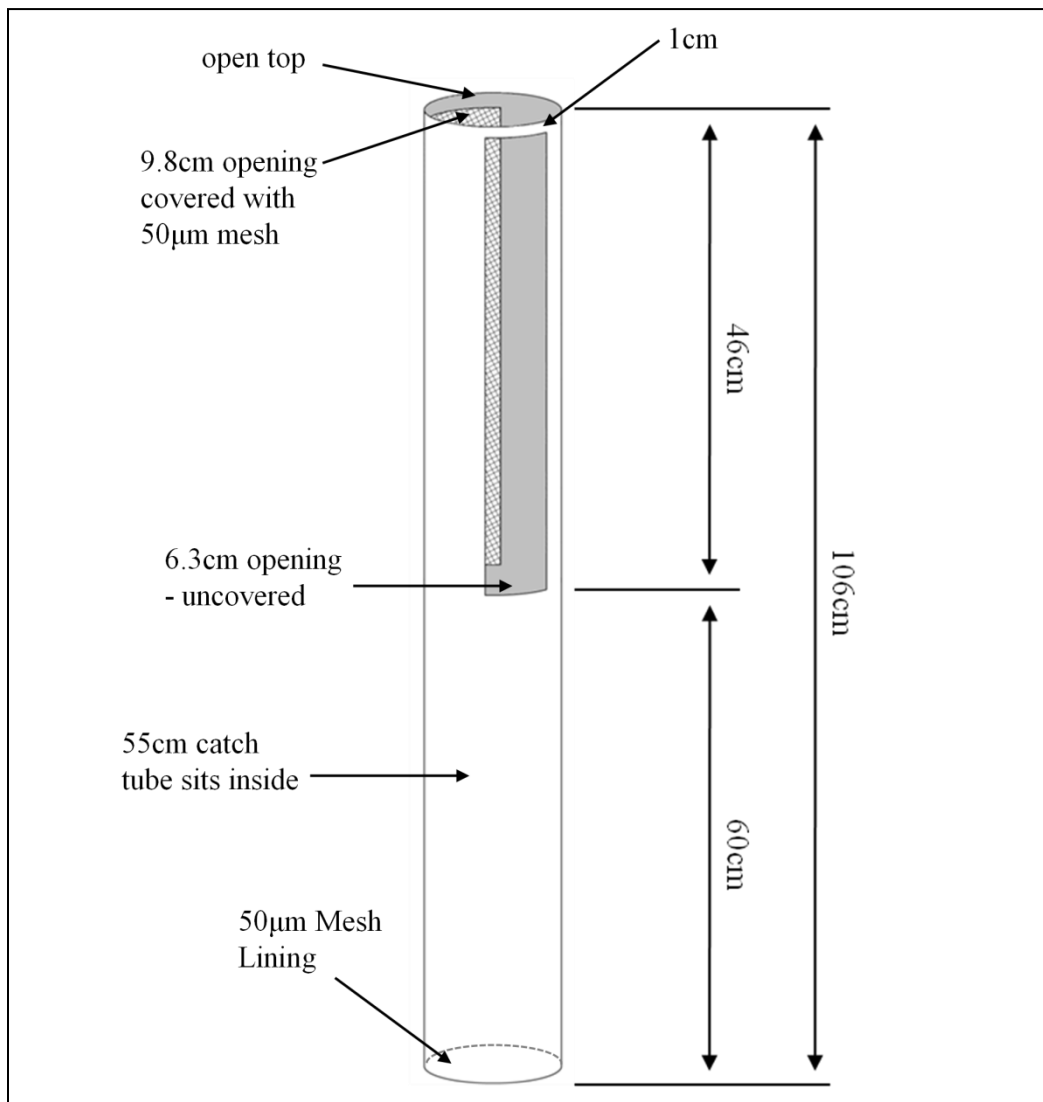


**Figure 5.1:** Aeolian trap unit design modified from Leatherman (1978) showing total length of trap, length of sampling slit and length of unit which was buried under sand. Entire trap specifications are discussed in the above paragraph.

Aeolian traps were arranged in two sets of four, with one set deployed at each sample site. Traps were arranged parallel to the shore with alternating onshore and offshore aspects: traps 1 and 3 at each site orientated in the southwest direction (offshore); while traps 2 and 4 were orientated in the northeast direction (onshore). Sampling was implemented over three periods. During the first period (15<sup>th</sup> June to the 29<sup>th</sup> July) traps at both sample sites were arranged 3 m landward of the dune crest (Figure 5.2, line A). During the second period (29<sup>th</sup> July to the 6<sup>th</sup> October)

traps remained in the same position (Figure 5.2, line B) and during the third period (6<sup>th</sup> October to the 12<sup>th</sup> November) traps at both sample sites were shifted into the foredune (Figure 5.2, line C)



**Figure 5.2:** Photo of sample site B on Matakana Island. Red line A and B shows the position (dune crest) of sediment traps arranged linearly during the first and second periods of aeolian sediment sampling. Red line (C) shows the position (foredune) of linearly arranged sediment traps during the third period of deployment.

At the end of each period of deployment, trap inserts were removed and replaced with fresh ones. Removed inserts were brought back to the lab where the volume of sediment collected in each trap was calculated and sediment samples from each trap removed. Sediment samples were then run through a Malvern Laser Seizer to calculate mean grain size and sorting for each individual trap.

During the sediment removal process, several species of insects were found in sediment trap inserts from both sample sites. Considerable numbers of *several* unidentifiable beetles and weevils were recorded, as well as Wolf Spiders (*Anopterus sp.*), Slaters, Sand Hoppers (Amphopods), unidentifiable centipedes, Scarab Beetles (*Coleoptera scarabaeidae*), Bumble Bees (*Bombus sp.*) and several types of unidentifiable larvae.

### 5.2.3 Wind and Rainfall Sampling

During the aeolian trap deployment phase, onsite rainfall wind speed and wind direction were collected to identify the likely wind events responsible for initiating periods of aeolian sediment transport. As outlined in Chapter 4, issues with the onsite rain gauge resulted in a large amount of onsite rainfall data missing or unusable. From early data that was usable, it was deduced that rainfall data obtained from NIWA's CliFlo station at the Tauranga Aero club provided a reasonable estimation of onsite rainfall conditions (refer to Chapter 4, section 4.2.1).

Wind sampling was conducted by way of three wind vane and anemometer set-ups. One set recorded wind speeds and direction atop a 4 m tower to mitigate the impact of obstruction on the wind data caused by vegetation. A second sampling set was placed at a height of 1 m amongst the vegetation at sample site A to measure speeds at vegetation top height (Figure 5.3). The third set was placed at a height of 0.8 m at sample site B to again, measure speeds at vegetation top height.



**Figure 5.3:** Wind instruments at sample site B sampling wind speed and direction at average plant height (0.8 m).

Each anemometer was orientated north and recorded direction in degrees, with both 0 and 360 degrees corresponding to north. All anemometers recorded speed and direction every 10 minutes, logging 30 minute averages to two onsite CR10X data loggers. Data was collected on each site visit, compiled and analysed back in the lab.

Wind speed and direction for specific wind events on site were used to calculate potential rates of transport and sand deposition based on the following simple equations suggested by Hsu (1974) and Davidson-Arnott & Law (1996):

$$q = 1.16 \times 10^{-4} U^3$$

Equation (5.1)

Where:  $q$  = rate of sand transport ( $\text{g.cm}^{-1}\text{s}^{-1}$ ),  $U$  = wind speed at a height of 2–10m ( $\text{m.s}^{-1}$ )

$$Q_D = 0.1q \cos \alpha$$

Equation (5.2)

Where:  $Q_D$  = rate of sand deposition ( $\text{kg.m}^{-1}\text{s}^{-1}$ ),  $\alpha$  = angle of wind approach from shore perpendicular.

Before beach sediment is transported by wind, the boundary layer shear stress must be increased above a threshold value. Bagnold (1941) described the critical shear stress, in terms of the shear velocity, as the following:

$$V_{*t} = A \sqrt{\frac{(\rho_s - \rho_a)gD}{\rho_a}}$$

Equation (5.3)

Where:  $A$  = a dimensionless constant ( $A = 0.118$ ),  $\rho_s$  = the mass density of the sediment,  $\rho_a$  = the mass density of the air,  $g$  = acceleration of gravity, and  $D$  = mean sediment grain diameter.

Based on Bagnold's threshold equation, Livingstone & Warren (1996) suggested a threshold of around 6-6.5 m.s<sup>-1</sup> recorded at a height of 2 m for sediment across both sites A and B. A similar threshold of around 6-7.5 m.s<sup>-1</sup> recorded at a height of 2 m was suggested in the Coastal Engineering Manual (2008). Bagnold's (1941) equation shows that at the surface transport threshold values for sites A and B are as low as 0.3-0.4 m.s<sup>-1</sup>. The transport threshold based on site wind speeds is likely to be less than suggested by Livingstone & Warren and the Coastal Engineering Manual, but greater than that suggested by Bagnold due to the following:

- Site wind speed was recorded at a height of 0.8 m, which falls between the surface to 2 m height range covered by Livingstone & Warren and Bagnold.
- Vegetation surrounding anemometer reduces wind speed, lowering recorded values.

It was therefore assumed that threshold velocity based on recorded site wind speed could reach as little as 4 m.s<sup>-1</sup>. Wind events where speeds reached greater than 4 m.s<sup>-1</sup> were therefore considered potential aeolian transport events and have been designated contributors to aeolian sediment transport rates in the results section of this chapter.

#### **5.2.4 Sampling Limitations**

Several problems hindered the collection of data at sample site A and included the following:

- Strong winds during May managed to twist the meteorological tower at sample site A by a considerable amount. As a result, wind direction data was unusable following Julian Day 131.
- The solar panel charging the battery at site A was attached to the sampling tower, it was also rotated away from its north facing aspect. As a result, the battery only gained enough charge to power instruments for a couple of hours in the afternoon on sunny days.

These instrument problems resulted in the wind station at sample site B being used as an estimate of wind speed and direction at both sample sites during the deployment of aeolian sediment traps. This also made a comparison of vegetation

height winds speeds between sites impossible as most of the wind data from the 4 m tower was lost and no data from the 1 m tower was recorded.

## 5.3 RESULTS

### 5.3.1 Vegetation

Vegetation results are outlined in greater detail in Chapter 3 (refer Chapter 3, 3.3.1). The key results are summarised as the following:

- *Ammophila arenaria* was shown to be the dominant species present at sample site A with an estimated total ground cover of 72.5%
- *Spinifex sericeus* was shown to be the dominant species present at sample site B with an estimated total ground cover of 62.5%
- Site B exhibited an average of 8% more 'bare ground' cover than that recorded at site A. The difference in bare ground cover reflects the differences of growth densities between the two species.

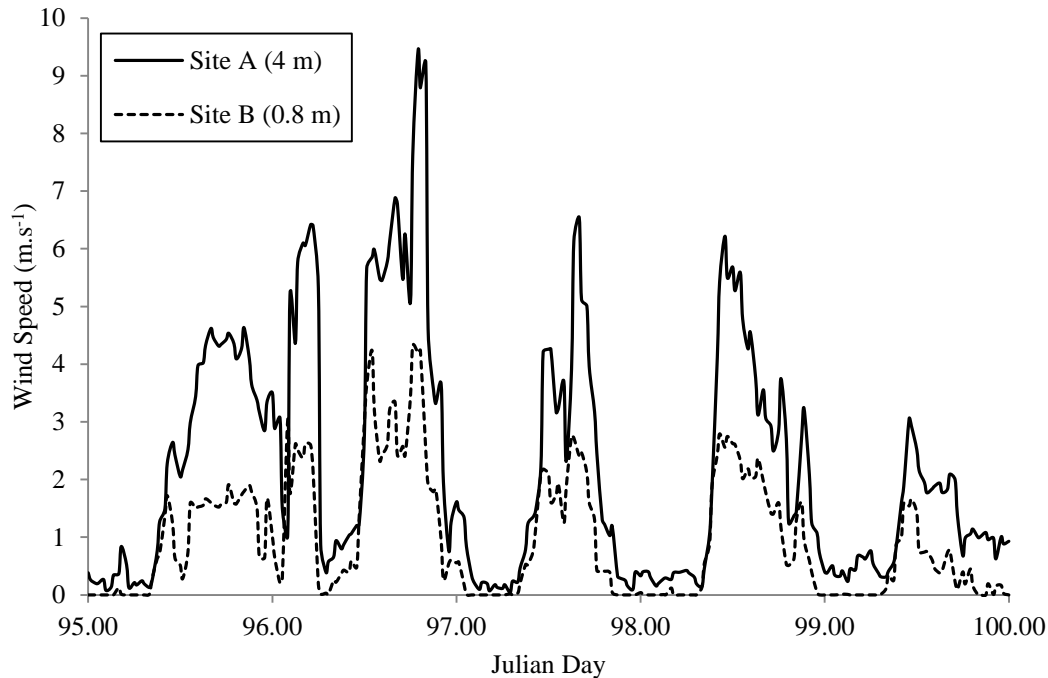
Sample site A was therefore classified as an *Ammophila* type sand dune, whilst sample site B was classified as a *Spinifex* type.

A point to note is that observations made during the course of the study, show seawards development of new plants at both sample sites A and B extending on average 1 m further seaward than when sampling began. This in turn lead to a slight seaward development of the foredune.

### 5.3.2 Wind Sampling

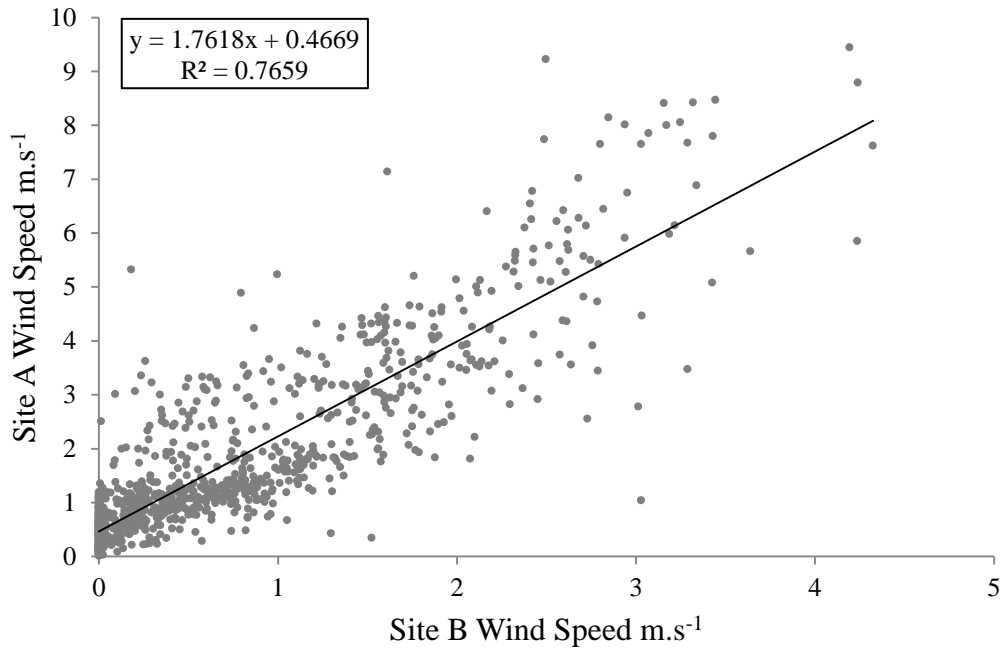
Early usable data for sample site A allowed for comparisons in wind speed and direction between sites to be made. Figure 5.4 illustrates differences in site wind speeds due to the difference in elevation between sampling devices. The sampling device at sample site A is positioned at a height of 4 m above surface. At sample site B positioning is 0.8 m above surface. Wind speeds at both sites follow a similar pattern. Speeds are greatest in the afternoon and evening (sea breeze) and at their lowest in the early morning. Although wind speeds at both sample sites exhibit a similar pattern, rises and falls in wind speed are greater at sample site A compared to sample site B. During peak wind speed events, wind speed at sample site B ranges between 3 and 5 m.s<sup>-1</sup> slower than wind speed at site A. The pattern

exhibited at both sites is further illustrated in Figure 5.5. No data was obtained from the sampling device at site A recording wind speed at 1 m.



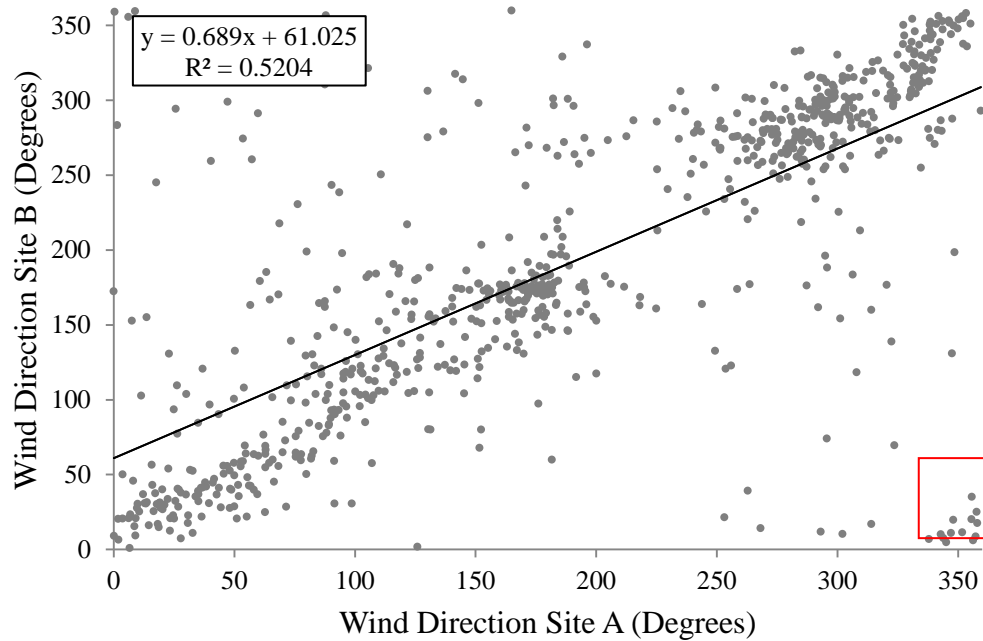
**Figure 5.4:** Comparative wind speeds at site A and site B over a 5 day period in 2010. Site A wind speeds were measured at a height of 4 m above dune. Site B wind speeds were measured at a height of 0.8 m above dune.

Figure 5.5 illustrates the relationship between wind speeds at each sample site through a linear regression correlation. The correlation is not strong showing that there is some difference in the overall pattern between sites. However, a trend is apparent with rises in wind at one site, a reasonable predictor of rises in wind at the second site. It is in the magnitude of the rise in wind speed that parts of the data differ. A line of best fit has been applied to the data that shows wind speed at any one point is approximately twice as fast at site A relative to site B. This difference is most likely due to station height and influence of ground cover and is explored in the discussion section of this chapter.



**Figure 5.5:** Correlation between wind speeds at site A and site B. Site A wind speeds were measured at a height of 4 metres above dune. Site B wind speeds were measured at a height of 0.8 m above dune.  $R^2$  value and equation of the line of best fit are displayed on the figure.

Following an apparent trend in the relationship between wind speeds at sample sites, a correlation between wind directions across sites is explored. Figure 5.6 illustrates the regression correlation between wind directions of sample sites A and B. Wind direction was recorded in degrees with both  $0^\circ$  and  $360^\circ$  corresponding to north. The data is plotted accordingly. It is paramount to note that the wind direction data for sample site A has been adjusted by 30 degrees. This adjustment was made to account for an approximate 30 degree rotation to the west of north of the sampling tower in the field. The original unadjusted plot is displayed in Appendix II. Several data points have also been removed from the data due to instrument malfunction at sample site A. During a period where site B recorded wind directions ranging between 200 and 250 degrees, site A recorded values of 0, indicating instrument error. As a result of removing these data point there is gap in the data plot between the 200 and 250 degrees mark for both sites. This may have weakened the correlation between sites.



**Figure 5.6:** Correlation between wind directions at site A and site B. Site A wind directions were measured at a height of 4 metres above dune. Site B wind directions were measured at a height of 0.8 metres above dune. R squared value and equation of the line of best fit are displayed on the figure.

Although the correlation in wind direction between sites is not strong, there is an apparent trend in the data. The red box in the bottom right hand corner highlights a small cluster of points well removed from the trend line. Although the points appear as obvious outliers this is not necessarily the case. The points are clustered around the 350 degree mark at site A and below the 50 degree mark at site B. Therefore, the difference between wind directions of points in the cluster is less than 40 degrees. This difference may be due to human error in the orientation of each sampling station in the field or the difference in elevation and vegetation obstruction between sites. These errors may also be responsible for the general scatter of many of the data points across the plot. A case for these errors is explored in the discussion section of this chapter.

Assuming that there is a relationship between wind speed and direction at each site, site B is used as an approximation for wind characteristics of both sample sites at an elevation of 0.8 m above the surface.

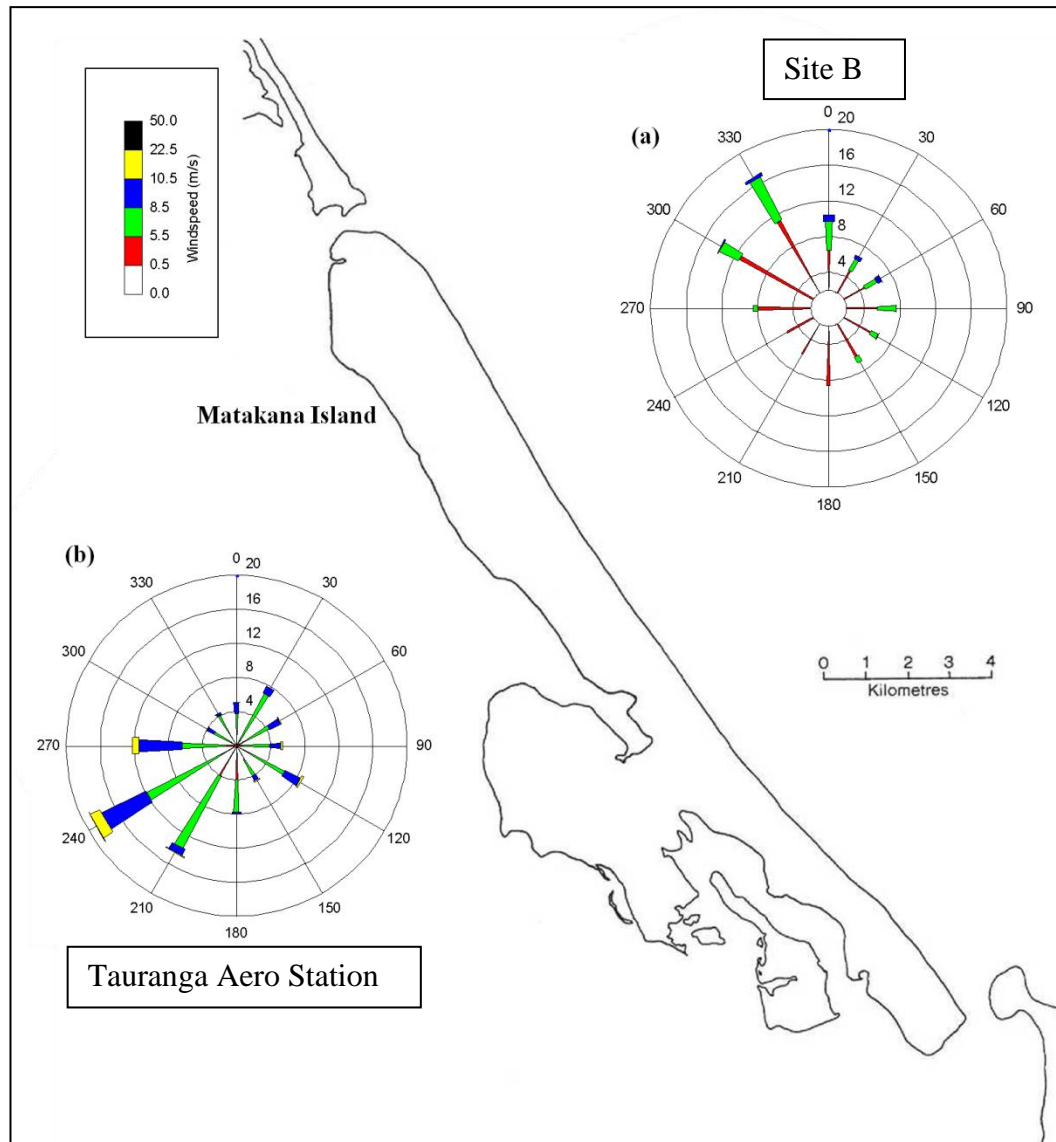


**Figure 5.7:** Comparative wind speed and direction plot for Matakana Island showing cross-shore and long-shore components. Inset A is a wind rose showing wind speed and direction at sample site B for the duration of the study. 25.8% of wind is below the ‘calm’ threshold. Inset B is a wind rose showing average wind conditions for nearby Tauranga Aero Club. 0.5% of wind is below the ‘calm’ threshold. North is indicated by 0 on both inset plots.

Figure 5.7 illustrates the differences in wind speed and direction between the Matakana Island sample site and the Western Bay of Plenty region. The key difference to note is the directional component of the wind rose plots A and B. Inset B shows the main component of average wind for the area coming from the south-west, heading in the offshore direction. This average is not reflected in the site data, inset A, which shows the main component of onsite wind coming from the north, north-east direction. Average wind heads in the long-shore (south-east)

direction with very little offshore component recognised in the study site rose plot. Inset A also shows that the strongest wind speeds are recorded coming from the north through to north-east direction. The directional difference is a result of pine trees landward of the sample site, sheltering the site from winds from the south to west direction (Figures 1.2 & 5.8).

### **5.3.3 Aeolian Transport Results**

Aeolian sediment transport was measured over three separate periods during the course of this study. During this time, the beach underwent a series of small short term erosion events (refer to Chapters 3 & 4). A general trend of foredune accretion associated with seaward growth of the dune vegetation was noted over the duration of the study. This trend is illustrated in Figure 5.8 which shows the accumulation of sand around the piezometer at sample site A. Sediment has built up significantly around the piezometer to the point where on final retrieval the top of the pipe was completely covered by sand.



**Figure 5.8:** Images showing the deposition of sand around piezometers over a period of this study from the 15<sup>th</sup> of June to the 16<sup>th</sup> of October 2010. Top image shows initial sand level at site A piezometer 15<sup>th</sup> June. Bottom image shows sand level at site A piezometer 16<sup>th</sup> October after some sand has been dug away.

## 5.3.3.1 First sediment trap deployment

The initial deployment of sediment traps recorded the most significant aeolian sediment movement event observed over the duration of this study. During this phase of deployment, traps were located 3 m landward of the dune crest and were surrounded by the dominant species of dune vegetation at each site. Figure 5.9 illustrates the directional orientation of sediment traps at sample sites A and B as well as the volumes of sediment collected. At both sample sites, the traps orientated to the north-east collected greater volumes of sediment than those orientated towards the south-west. All traps at sample site B collected vastly greater amounts of sediment than traps at sample site A.

An important point to note is that volumes of sediment in all traps at site B represent a minimum value, compared to the true value seen in traps from site A. This is due to the vast deposition of sand at site B which completely filled the trap inserts, half the sediment trap, and then overflowed to the surrounding area (Figure 5.10). It is expected that the true volume value of sediment caught at site B would be greater than that illustrated in Figure 5.9.

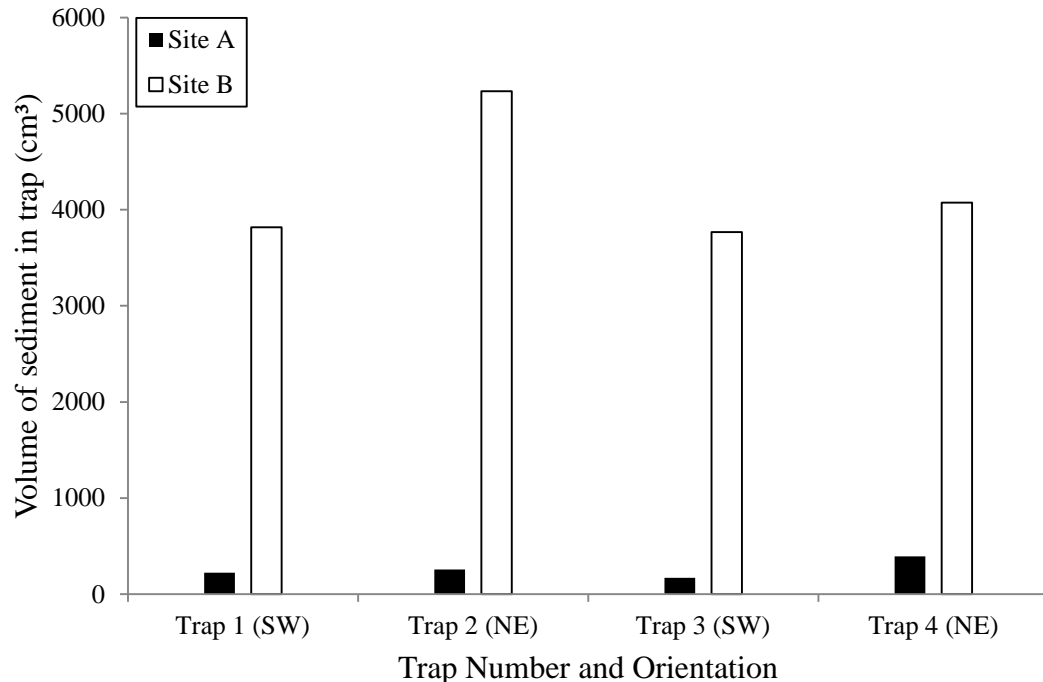


**Figure 5.9:** Volumes of sediment collected from sediment traps deployed 3 metres landward of the dune crest at sample sites A and B between the 15<sup>th</sup> June and the 29<sup>th</sup> of July 2010.



**Figure 5.10:** Images showing the deposition of sand around sediment traps following the first period of their deployment from the 15<sup>th</sup> of June to the 29<sup>th</sup> of July 2010. Top image shows site B, deposition amongst *Spinifex* plants. Bottom image shows site A, deposition around *Ammophila* plants.

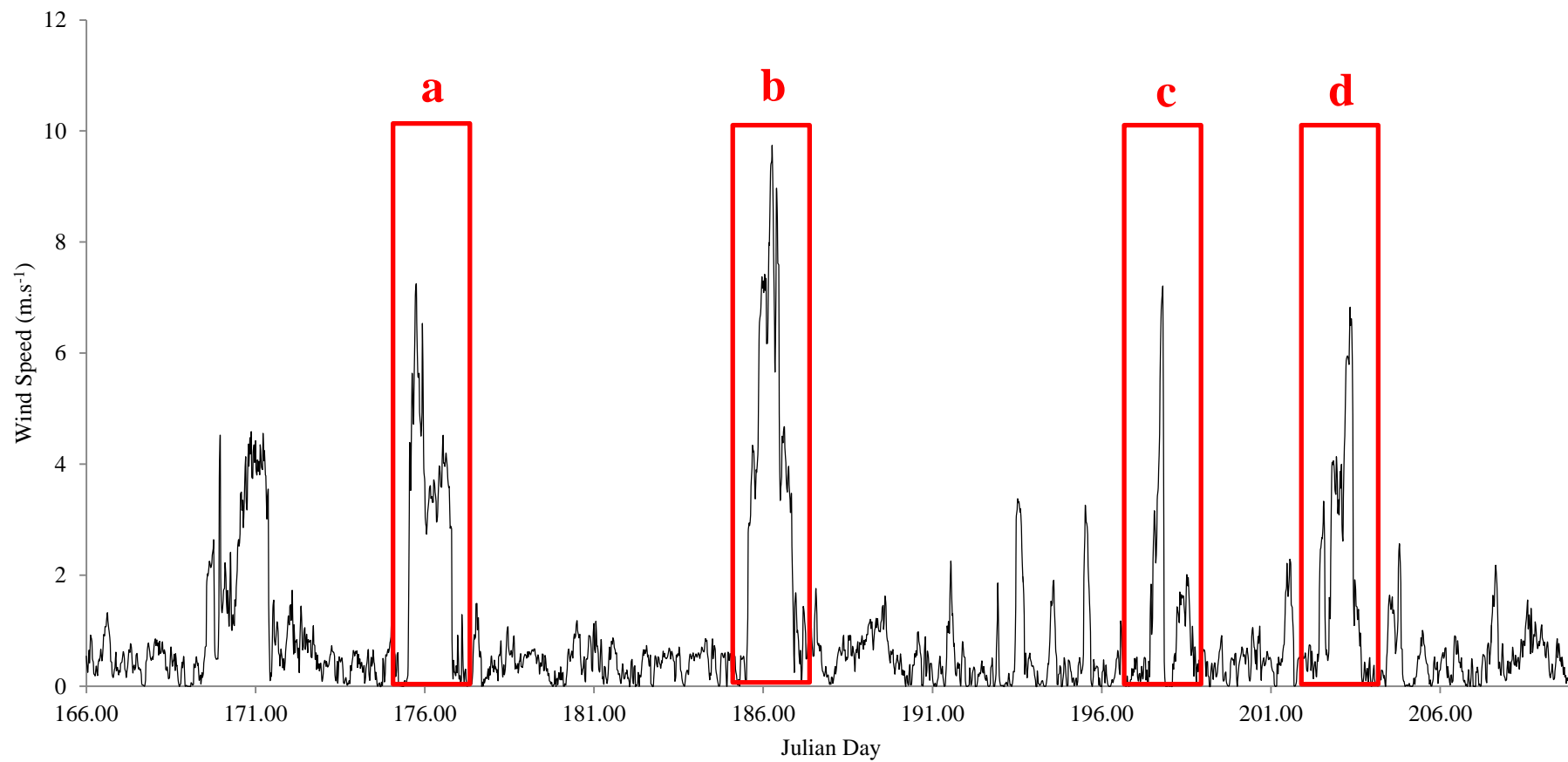


**Figure 5.11:** Sample site wind speeds during the first wave of sand trap deployment. Red boxes (a, b, c, and d) highlight wind speed events greater than  $4 \text{ m}\cdot\text{s}^{-1}$  and are discussed in the text.

On several occasions during initial sediment trap deployment, site wind speeds exceeded  $4 \text{ m.s}^{-1}$ , with speeds reaching close to  $10 \text{ m.s}^{-1}$  in some instances. Four instances of high wind speeds have been identified in Figure 5.11 by the red boxes A, B, (c) and (d). These areas have been selected as possible wind events which exceed the specific site threshold velocity ( $4 \text{ m.s}^{-1}$ ) for initiating sediment movement. The primary direction of these wind events are outlined in Figure 5.12.

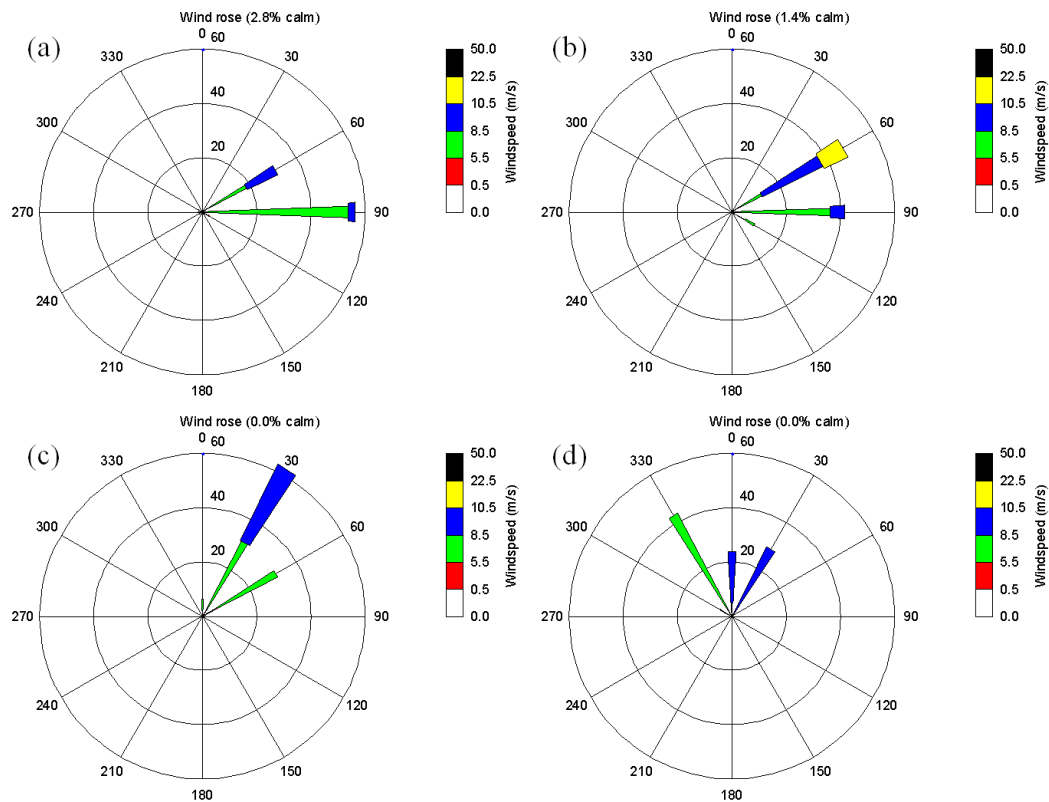


**Figure 5.12:** Wind rose plots showing wind speed and direction for four identified strong wind events during the course of initial sediment trap deployment from 15<sup>th</sup> June to the 29<sup>th</sup> July. Plots A, B, (c) and (d) correspond to the sections A, B, (c) and (d) identified in Figure 5.11.

Red box B (Figure 5.11) and inset B (Figure 5.12) illustrate the most significant wind event identified over the course of sediment trap deployment. During this event, average wind direction was 60 degrees (East-north-east) (directly onshore) with wind speeds reaching close to  $10 \text{ m.s}^{-1}$ . Wind speed remained strong for the longest duration during this event, with onshore wind speeds remaining above  $4 \text{ m.s}^{-1}$  for around 19 hours. Average predicted sediment deposition rate during this

event was  $15.4 \text{ kg}\cdot\text{m}^{-1}\text{hr}^{-1}$ . In accordance with Figure 5.7 inset A, Figure 5.12 shows the strongest winds as north-easterlies, with these onshore winds dominating the cross-shore component during short term wind events.

#### 5.3.3.2 Second sediment trap deployment

The second sediment trap deployment recorded the least amount of aeolian sediment movement. During this phase of deployment, traps were again located 3 m landward of the dune crest, having only their inserts replaced following the initial deployment. The traps were raised following their partial burial during initial deployment so that the catchment slit was again flush with the surface sediment. At site A, the traps were surrounded by the dominant species of dune vegetation (Figure 5.10). Following the large deposition of sediment at sample site B during the initial deployment of sediment traps, the majority of plants in the direct vicinity of the traps had been buried (Figure 5.10). Figure 5.13 illustrates the directional orientation of sediment traps at sample sites A and B as well as the volumes of sediment collected. At both sample sites, the traps orientated to the north-east collected greater volumes of sediment than those orientated towards the south-west, as seen during the initial deployment. During this phase of deployment all traps at sample site A collected greater amounts of sediment when compared to sample site B. This is in direct contrast to observations made during initial trap deployment.

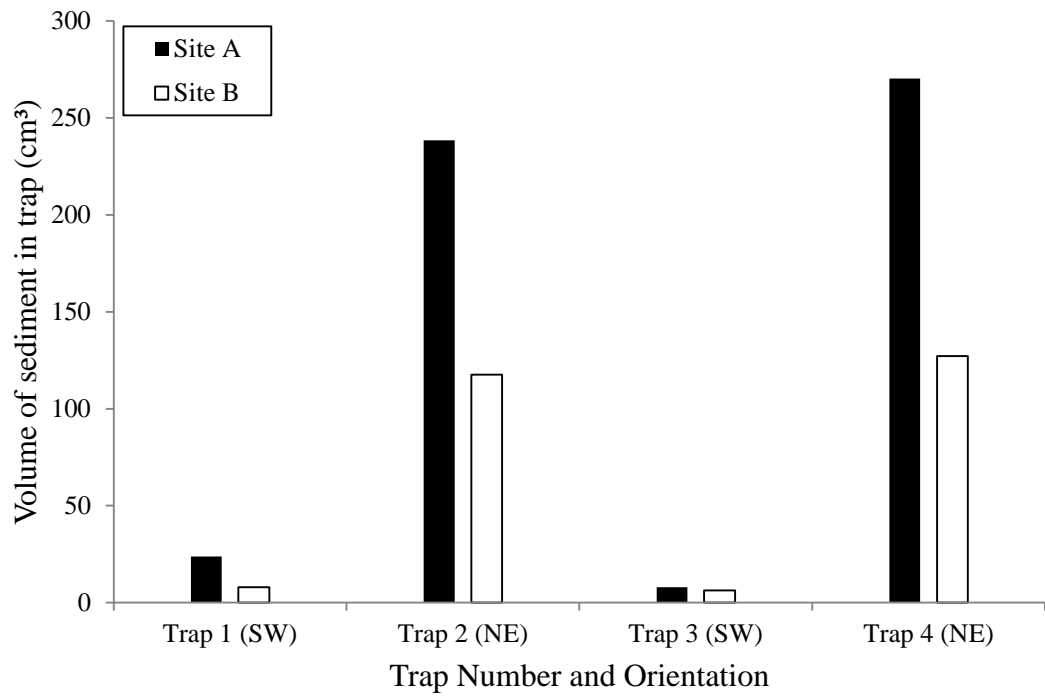


**Figure 5.13:** Volumes of sediment collected from sediment traps deployed 3 m landward of the dune crest at sample sites A and B between the 29<sup>th</sup> of July and the 6<sup>th</sup> of October 2010.

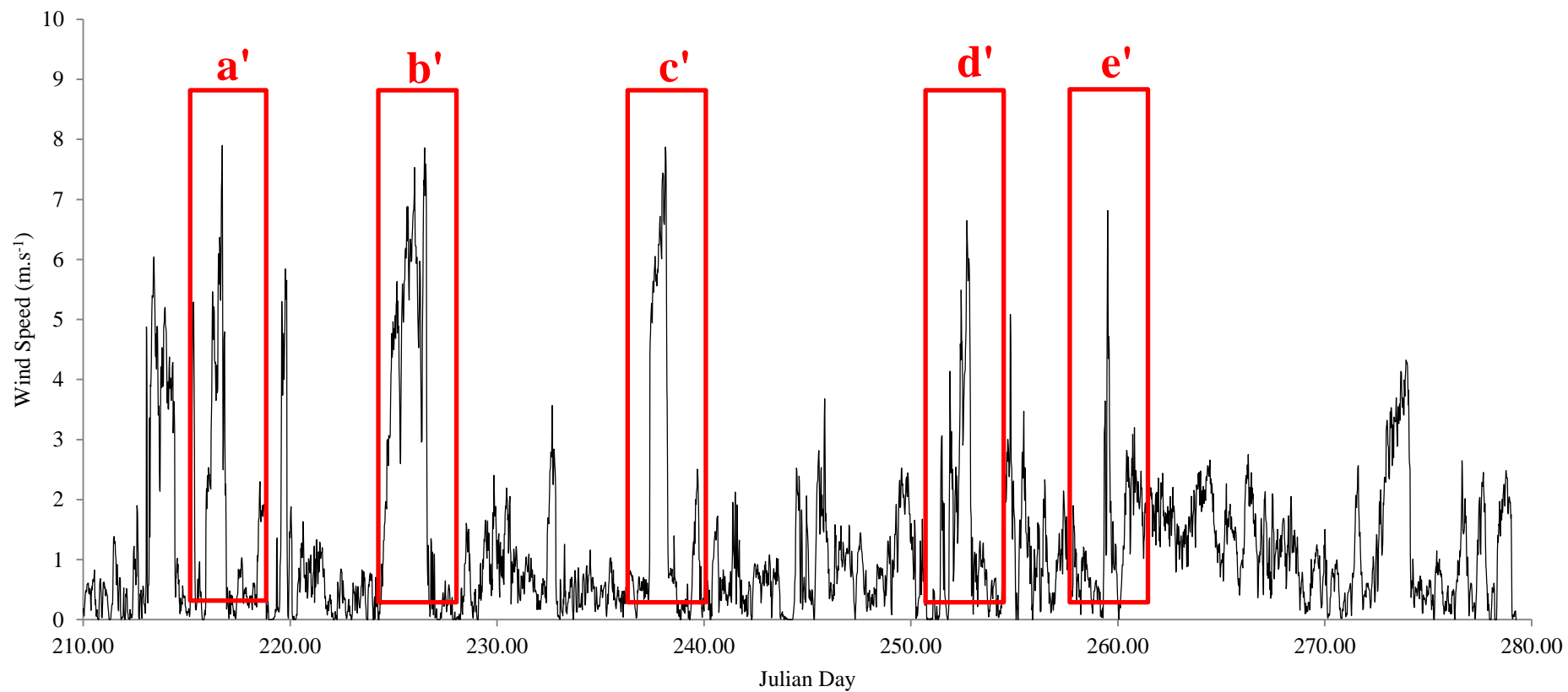


**Figure 5.14:** Sample site wind speeds during the second wave of sand trap deployment. Red boxes (a', b', c', d' and e') highlight wind speed events greater than  $4 \text{ m}\cdot\text{s}^{-1}$  and are discussed in the text.

On several occasions during the second phase of sediment trap deployment, site wind speeds exceeded  $4 \text{ m.s}^{-1}$ , with speeds reaching close to  $8 \text{ m.s}^{-1}$  in some instances. Five instances of high wind speeds have been identified in Figure 5.14 by the red boxes (a'), (b'), (c'), (d') and (e'). These areas have been selected as possible wind events which exceed the specific site threshold velocity ( $4 \text{ m.s}^{-1}$ ) for initiating sediment movement. The primary direction of these wind events are outlined in Figure 5.15.

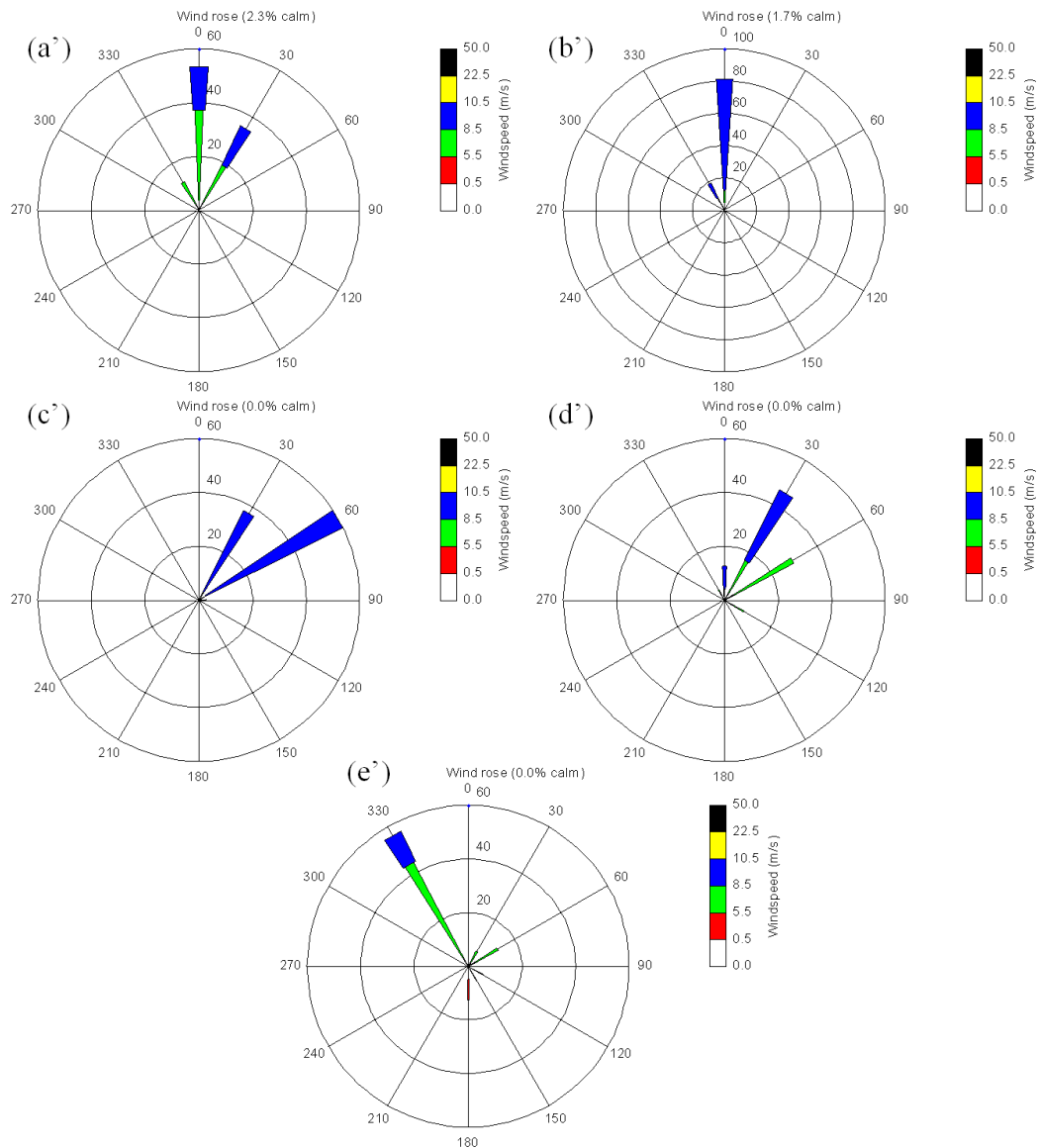


**Figure 5.15:** Wind rose plots showing wind speed and direction for five identified wind events during the course of secondary sediment trap deployment from the 29<sup>th</sup> July to the 6<sup>th</sup> of October. Plots (a'), (b'), (c'), (d') and (e') correspond to the sections (a'), (b'), (c'), (d') and (e') identified in Figure 5.14.

Red boxes (b') and (c') (Figure 5.14) and insets (b') and (c') (Figure 5.15) illustrate the most significant wind events identified over the course of sediment trap deployment. During event (b'), average wind direction was 0 degrees (Northerly, a combination of long-shore and onshore) with wind speeds reaching close to  $8 \text{ m.s}^{-1}$ . During event (c'), average wind direction was 49 degrees (North-east, primarily onshore) Wind speed remained strong for the longest duration during event (b'), with northerly wind speeds remaining mostly above  $4 \text{ m.s}^{-1}$  for a 28 hour period. During event (c') winds reached a higher average than event (b') but blew for a shorter duration. Average predicted sediment deposition rates during events (b') and (c') were  $3.9 \text{ kg.m}^{-1}\text{hr}^{-1}$  and  $4.5 \text{ kg.m}^{-1}\text{hr}^{-1}$  respectively. In accordance with Figure 5.7 inset A, Figure 5.15 shows the strongest winds in the area, expressed as northerlies and north-easterlies, with onshore winds dominating the cross-shore component. Onshore/cross-shore winds contribute to both the cross-shore and the long-shore component of wind, during short term wind events.

#### 5.3.3.3 Third sediment trap deployment

The third sediment trap deployment recorded a substantial amount of aeolian sediment movement. During this phase of deployment, traps were shifted seaward and relocated in the foredune at each site (Figure 5.2). Following their relocation, sediment traps no longer had any vegetation growth on the seaward side. Figure 5.16 illustrates the directional orientation of sediment traps at sample sites A and B as well as the volumes of sediment collected. At site B, both the traps orientated to the north-east collected greater volumes of sediment than those orientated towards the south-west, as seen during the initial and secondary deployments. At site A however, trap 1 collected more sediment than trap 2 despite being orientated in a south west direction. Interestingly, trap 2 was the only trap at sample site A that didn't collect a greater amount of sediment when compared to traps sample site B. This is in direct contrast when compared to observations made during initial trap deployment, but in line with results obtained during the second phase of deployment.

A point to note is that a single plant had grown directly in front, on the seaward side, of trap 2 at site A over the third phase of trap deployment.

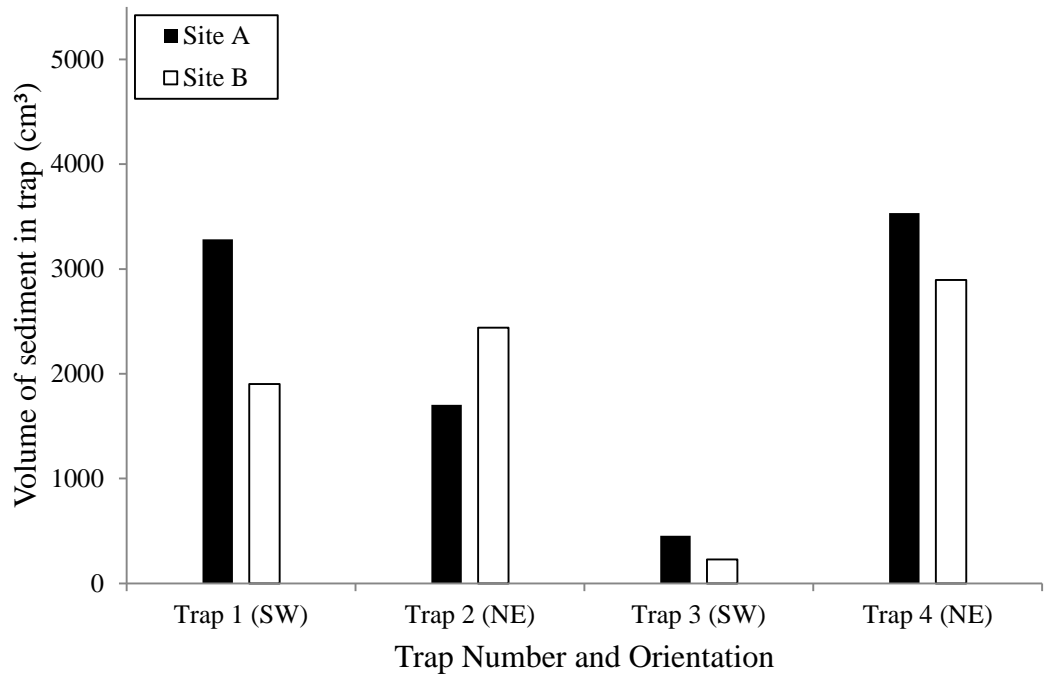


**Figure 5.16:** Volumes of sediment collected from sediment traps deployed in the foredune, landward of the dune crest at sample sites A and B between the 6<sup>th</sup> of October and the 12<sup>th</sup> of November 2010.

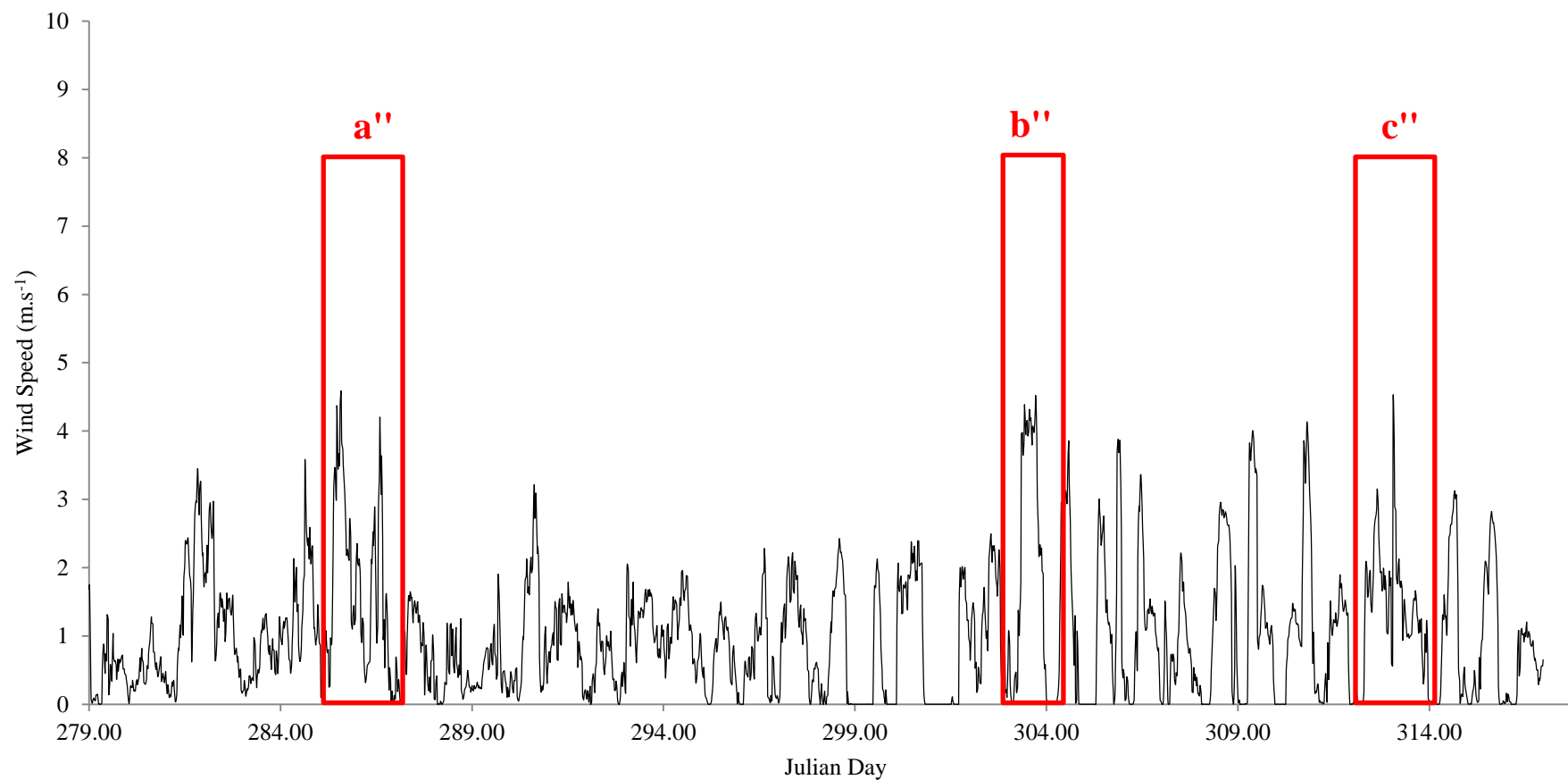


**Figure 5.17:** Sample site wind speeds during the third wave of sand trap deployment between the 6<sup>th</sup> of October and the 12<sup>th</sup> of November 2010. Red boxes (a'', b'' and c'') highlight wind speed events greater than  $4 \text{ m.s}^{-1}$  and are discussed in the text.

On several occasions during the third phase of sediment trap deployment, site wind speeds exceeded  $4 \text{ m.s}^{-1}$ , with speeds never exceeding  $5 \text{ m.s}^{-1}$ . Three instances of high wind speeds have been identified in Figure 5.17 by the red boxes (a''), (b''), and (c''). These areas have again been selected as possible wind events which exceed the specific site threshold velocity for initiating sediment movement. The primary direction of these wind events are outlined in Figure 5.18.

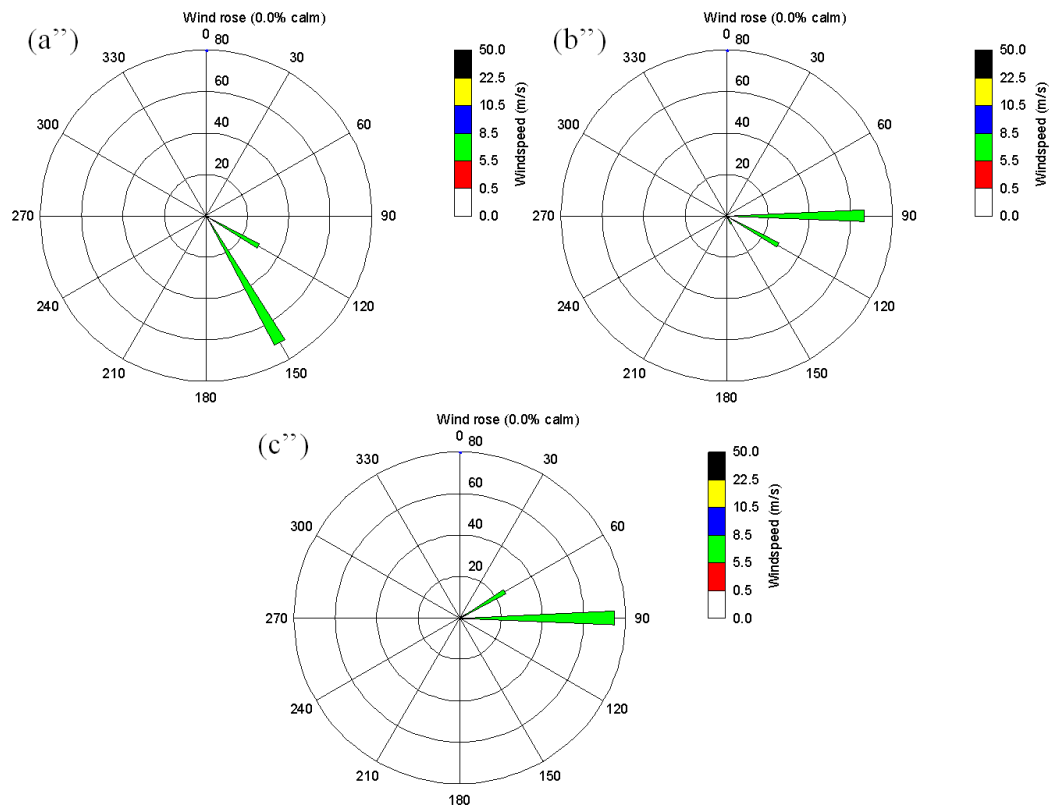


**Figure 5.18:** Wind rose plots showing wind speed and direction for three identified wind events during the course of the third sediment trap deployment from the 6<sup>th</sup> of October to the 12<sup>th</sup> of November. Plots (a''), (b'') and (c'') correspond to the sections (a''), (b'') and (c'') identified in Figure 5.17.

Red box (b'') (Figure 5.17) and inset (b'') (Figure 5.18) illustrate the most significant wind event identified over the course of sediment trap deployment. During this event, average wind direction was 90 degrees (Easterly, a combination of onshore cross-shore). Site wind speed during the third phase of trap deployment never reached speeds seen in the first and second phases of

deployment. Average predicted sediment deposition rate during this event was  $1.91 \text{ kg}\cdot\text{m}^{-1}\cdot\text{hr}^{-1}$  much smaller than seen in earlier deployments. Figure 5.18 shows the strongest winds in the area during trap deployment expressed as easterlies, with onshore winds dominating the cross-shore component. Again, onshore/cross-shore winds contribute to both the cross-shore and the long-shore component of wind, during short term wind events.

Towards the end of the sampling period, wind speed is recorded as 0 more frequently (Figure 5.17). Figure 5.19 compares on site wind speed to wind speed data at Tauranga Aero Club obtained from a Niwa CliFlo station. During periods where site wind speed was recorded as 0, the Tauranga station recorded speeds ranging between 1 and  $10 \text{ m}\cdot\text{s}^{-1}$ . This is mainly caused by south-westerly winds from which the sample site is sheltered. Instrument seizure due to the impact of prolonged exposure to salt may also be partly to blame. The Tauranga station recorded faster wind speed in general as its location is higher above ground (4 m) reducing surface interference.

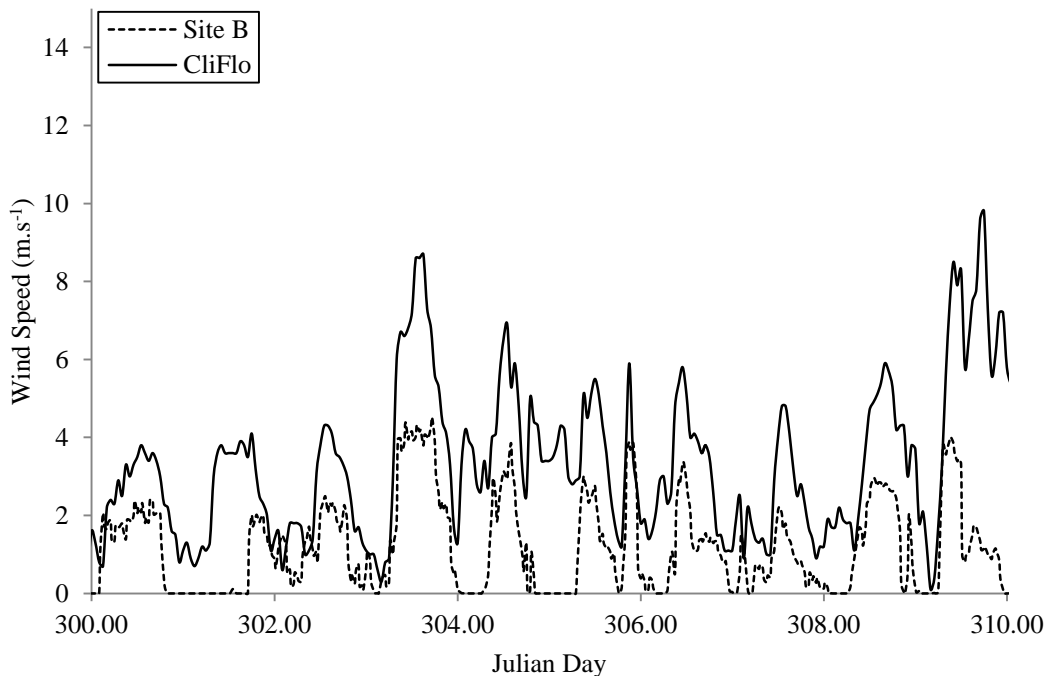


**Figure 5.19:** Comparative wind speeds at site B and Tauranga Aero Club over a 10 day period in 2010. Site B wind speeds were measured at a height of 0.8 m above dune. Aero Club wind speeds were measured at a height of 4 m above mean sea level.

5.3.3.4 Relationship between sediment transport and rainfall

High wind speed events are often a product of localised short period storm events. These short period storms produce localised rainfall events resulting in strong winds most likely accompanied by rainfall. Figure 5.20 shows that over a month long period in 2010, high sample site wind speeds were often accompanied by rainfall events causing a saturation of onsite surface sediment. Saturation of surface sediment reduces potential transport.

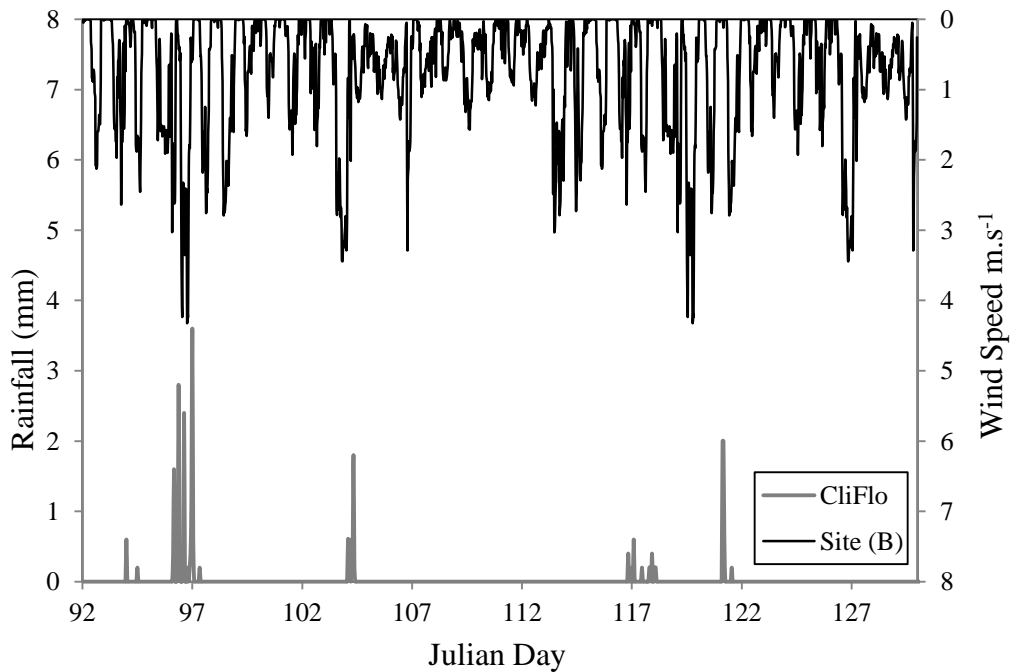


**Figure 5.20:** Wind speed (black) and rainfall (gray) comparison from the 2<sup>nd</sup> of April to the 9<sup>th</sup> of May 2010. Rainfall data is from Niwa’s CliFlo station at Tauranga Aero Club. Wind speed data is from sample site B.

**5.3.4 Aeolian Sediment Characteristics**

Following the collection of sediment trap inserts on the 29<sup>th</sup> of July, sediment samples were collected from the inserts and run through the laser sizer to determine mean grain size and standard deviation (a measure of sorting). Average mean grain size was calculated for each site based on sediment collected from the four site sediment traps. Tables 5.1 & 5.2 show mean grain size of sediment collected in the traps is closest to the mean grain size of sediment sampled from the corresponding swale at sites A and B. Aeolian shifted sediment has a mean

grain size smaller than sample site beach sediment and larger than sample site dune face sediment.

**Table 5.1:** Sediment grain size descriptive statistics for samples collected across the profile at sample sites A & B.

| Sample Location | Median ( $\mu\text{m}$ ) | Mean ( $\mu\text{m}$ ) | Standard Dev ( $\mu\text{m}$ ) | Skewness ( $\mu\text{m}$ ) | Kurtosis ( $\mu\text{m}$ ) |
|-----------------|--------------------------|------------------------|--------------------------------|----------------------------|----------------------------|
| Site A          |                          |                        |                                |                            |                            |
| Beach           | 353.63                   | 394.15                 | 195.55                         | 0.90                       | 0.38                       |
| Site A Dune     |                          |                        |                                |                            |                            |
| Face            | 224.49                   | 239.91                 | 87.07                          | 0.92                       | 0.85                       |
| Site A          |                          |                        |                                |                            |                            |
| Swale           | 252.06                   | 274.98                 | 114.27                         | 1.03                       | 1.03                       |
| Site B          |                          |                        |                                |                            |                            |
| Beach           | 285.59                   | 315.00                 | 139.83                         | 1.03                       | 0.96                       |
| Site B Dune     |                          |                        |                                |                            |                            |
| Face            | 218.14                   | 232.02                 | 81.80                          | 0.86                       | 0.64                       |
| Site B          |                          |                        |                                |                            |                            |
| Swale           | 236.53                   | 253.01                 | 92.58                          | 0.93                       | 0.84                       |

**Table 5.2:** Average Sediment grain size descriptive statistics for samples collected from sediment traps at sample sites A & B on the 29<sup>th</sup> July.

| Sample Location | Median ( $\mu\text{m}$ ) | Mean ( $\mu\text{m}$ ) | Standard Dev ( $\mu\text{m}$ ) | Skewness ( $\mu\text{m}$ ) | Kurtosis ( $\mu\text{m}$ ) |
|-----------------|--------------------------|------------------------|--------------------------------|----------------------------|----------------------------|
| Site A          | 250.56                   | 269.05                 | 101.26                         | 0.93                       | 0.79                       |
| Site B          | 257.69                   | 275.92                 | 102.01                         | 0.91                       | 0.74                       |

## 5.4 DISCUSSION

### 5.4.1 Vegetation and wind interactions

The proximity of site A to site B ensured that unobstructed wind speeds and directions at both sample sites were similar. Figure 5.5 illustrates the relationship between sites A and B where a regression analysis showed a moderate relationship between sites with a  $R^2$  value of 0.766. Differences between sites are attributed to the positioning of instruments. An above ground height difference of 3.2 m between sites resulted in wind speed and direction being more susceptible to the influence of vegetation obstruction (plant roughness) at site B. Due to issues with weather station A, a comparison between wind speeds at plant height was unable to be made. It was therefore assumed that vegetation roughness was the main factor driving the differences between tower wind speed (site A) and vegetation wind speed (site B).

The weaker correlation observed between wind directions at sites A and B is considered partly a result of differences in vegetation roughness between sites, with human and instrument error also suggested as contributors. Site anemometers were orientated by hand, using a compass. If the initial orientation between sites was slightly different or strong winds re-orientated instruments during data collection, then actual direction would be misrepresented, weakening the correlation. The data (Figure 5.6) was corrected to account for an average 30 degree re-orientation of the station site A caused by a strong wind event, but this did not account for smaller interim re-orientations. Instrument issues at site B resulted in some chunks of the data being unusable, which may have also weakened the correlation.

Vegetation roughness affects the movement of aeolian sediment through the slowing of wind velocity, and also increasing the threshold velocity required for sediment particle movement (Bressolier & Thomas, 1977). Vegetation roughness is controlled by plant height, density and species characteristics. It is therefore suggested that vegetation roughness is greater at site A when compared to site B based on the classification of each site established in Chapter 3. Average *Ammophila* height (site A) was greater than *Spinifex* (site B) with the density of *Ammophila* at site A also being greater. It is suggested that the difference in

vegetation roughness between sites led to differences in aeolian sediment deposition as discussed below.

#### **5.4.2 Aeolian sediment movement**

Three phases of sediment trap deployment established aeolian sediment transport patterns in the foredune and dune at both sites A and B. The differences in aeolian sediment deposition are attributed to the differences in vegetation species and density between sites. Figures 5.11 & 5.12 illustrated a wind event identified over the course of the first sediment trap deployment. During this event, average wind direction was 60 degrees (East-north-east, directly onshore) with wind speeds reaching close to  $10 \text{ m.s}^{-1}$ . Wind speed remained strong for the longest duration during this individual event, with onshore wind speeds remaining above  $4 \text{ m.s}^{-1}$  for around 19 hours. Therefore, it is hypothesised that this event is the most significant during this phase of deployment, and is the main contributor to aeolian sediment deposition at both sites A and B. During the initial deployment all sediment traps orientated in a north-easterly direction (offshore) collected greater amounts of sediment than those orientated south-west (onshore). The distribution of sediment around traps and vegetation (Figure 5.10) further suggest the primary depositing wind came from the east-north-east. All traps at site B collected vastly more sediment during the initial deployment compared to traps at site A, suggesting that greater vegetation roughness at site A reduced deposition landward of the foredune. The following two sediment trap deployments strengthened this suggestion.

During the second phase of deployment site B traps were surrounded by bare sediment due to the burial of plants, as opposed to site A where traps remained surrounded by *Ammophila* vegetation. With little vegetation at site B to reduce the wind strength to below the impact threshold, little sand was deposited at the traps and most likely remained in the air stream to be deposited more landward. During this phase, traps at site A caught greater amounts of sediment than those at site B in line with previous studies (Van der Putten, 1989; Moore & Davis, 2004 and Hilton *et al*, 2005) which show *Ammophila* to be an effective sand binding plant and a better option than having no vegetation present.

The third phase of sediment trap deployment saw all four traps at sites A and B shifted into the foredune at each site, with no vegetation on their seaward side at

the time of installation. During this phase the difference in sediment volumes collected at each site was much less than previous deployments, with the reduced difference most likely due to the lack of vegetation seaward of the traps. Traps at site A all collected more sediment than their partner traps at site B with the exception of one north-easterly orientated trap. A single *Ammophila* plant had begun growing directly in front of this trap blocking it from the seaward side and is therefore deemed the reason for this exception. The similar results for the third deployment highlight the influence of vegetation in the first two deployments.

Esler (1970) showed that *Ammophila* dominated dunes tend to have a much steeper foredune than dunes created by native species such as *Spinifex*. It is suggested by Esler (1970) that the steeper dunes can be attributed to the density in which *Ammophila* grows. With a large vegetation roughness, surface wind speed is reduced drastically when it comes into contact with the foredune side of vegetation during onshore winds. This reduces wind speed to below the impact threshold and causes sediment in the air stream to be deposited in clumps at the foredune, rather than being deposited more evenly throughout the dune as seen in *Spinifex* dominated sand dunes. The larger amounts of sediment caught in traps at site A suggest this process is occurring on Matakana Island during onshore wind events.

Average predicted sediment deposition values calculated from wind showed greatest potential transport rate occurring during initial trap deployment. Agreeing with potential rates, actual rates of transport were greatest during initial deployment. However, predicted rates suggested the smallest volumes of deposition occur during the third phase of deployment. Actual rates show least sediment deposition occurring during the second phase of deployment, not the third. Potential rates of transport may differ to actual rates as a result of the wind data used.

Due to instrument issues, site B wind instruments at a height of 0.8m were used to approximate wind conditions at sites A and B. As a result, on site wind data (between 2 and 10 m, as suggested by Davidson-Arnott & Law (1996)) is underestimated suggesting potential transport rates are under predicted. It is however, hypothesised that vegetation roughness and density are the key factors inducing differences in trapped sediment volume between the second and third

trap deployment phases. During the third phase of trap deployment site A and B traps were positioned in the foredune with no vegetation to their seaward side. During the cross-shore component of sediment transport (in this case, onshore), sediment flux landward decreases rapidly from the seaward limit of vegetation cover due to the influence of vegetation on the transport threshold (Lancaster & Baas, 1998; Kuriyama *et al.*, 2005). A greater deposition of sediment in the foredune at each site is therefore expected, when compared to sediment deposition landward of the foredune.

Mean grain size of sediment collected in the traps is closest to the mean grain size of sediment sampled from the corresponding swale (landward of traps) at sites A and B. Aeolian shifted sediment has a mean grain size smaller than beach sediment sampled and larger than dune face sediment sampled. The difference in mean grain sizes between the beach and sediment traps, suggests some sorting of sediment by wind. Bagnold (1960) showed quartz with a grain size of 0.8 mm to be the most readily transported, as threshold shear velocity is at its minimum for this size. Largest mean grain size recorded at the sample site was 0.39 mm with an average of 0.25 mm. Small differences between various sections of the beach may therefore occur with bigger grains more readily shifted. Small grains require higher wind speeds to initiate transportation due to cohesion forces between grains, whilst larger grains offer greater resistance resulting from greater mass/surface ratios (Bagnold, 1960; van der Wal, 1998). Sediment collected in the foredune was well sorted (smaller standard deviation), compared to that collected from the lower beach (Table 5.1). Van der Wal (1998) showed that beach sand with high rates of transport was well to very well sorted. It is therefore suggested that sediment collected in traps has been transported from the section of beach between the swash zone and the dune face, with sorting by wind leading to the smaller mean grain size recorded in sediment traps. The beach sediment samples at both sites were taken from close to the swash zone, so it is likely that these samples represent a section of the beach that is saturated during a proportion of the tidal phase. The saturation of this sediment limits the larger grains availability for transport. Sediment above the high tide line is most prone to transportation during strong onshore winds. Sediment in the swale as well as that recorded in the

sediment traps is likely to be the result of onshore aeolian sediment transport from the beach, above the high tide mark.

Rainfall influences the transport rates of sediment shifted by wind through the saturation of surface sediment (Arens, 1994). Figure 5.20 shows that high on-site wind speeds were often accompanied by rainfall, which would reduce potential aeolian sediment transport rates. Strong local onshore winds are often accompanied by high water levels, resulting in the flooding of much of the beach and causing the surface to become too wet and the cohesiveness between grains too great for the wind to initiate transport. The majority of onshore sediment is therefore considered to take place at the beginning of localised storm events before the surface sediment becomes too wet, or during wind events that were not accompanied by rainfall.

Many naturally eroding surfaces often have higher threshold velocities and lower rates of sediment supply, where total sediment flux is controlled by the ability of the surface to supply sediment grains to the air stream (Arens, 1994; Davidson-Arnott & Law, 1996). On Matakana Island, wind direction directly affects the ability of the surface to supply sediment grains to that air stream. The beach is narrow (refer Chapter 3, section 3.4.2) so during onshore and offshore winds, sediment source and fetch (the horizontal distance of the sediment over which the wind blows) are limited. Aeolian sediment transport rates are known to reach equilibrium when beach width exceeds 10 m (Davidson-Arnott & Law, 1996; Jackson & Cooper, 1999; Kuriyama et al, 2005), in which case fetch becomes irrelevant as wind can become contain no more sediment regardless of an increase in fetch.

The wider the beach, the greater the fetch is. While sample site fetch length was greater than 10 m at profile sampling intervals, actual beach width during strong onshore winds will have been much smaller due to the effects of storm surge and increased wave run-up. Storm surge and wave run-up may have reduced beach width to less than 10 m when coinciding with high tides, reducing potential transport rates.

Although no sediment traps orientated in the long-shore directions were deployed, it is hypothesised that the potential long-shore component of aeolian sediment

transport seaward of the foredune on Matakana Island may exceed the cross-shore component. When wind blows parallel to the beach, then the sediment source and fetch increase to the point where the wind can become saturated with sand (Arens, 1994). Wind speed and direction for the duration of this study is illustrated in Figure 5.7, showing the largest percentage of wind to be coming from the north-west (long-shore). This however, is average wind speed and does not truly represent strong wind speed events that characterise aeolian sediment transport. It is therefore suggested the cross-shore transport rates are of a greater significance.

Assuming that onshore winds are the most significant component of aeolian cross-shore transport rates on Matakana Island, local aeolian sediment deposition is linked to aquifer levels discussed in Chapter 4 through beach source width. Beach width, together with the thickness of beach sediment above the water table, determines the total volume of sediment available for deposition under a given set of conditions (Davidson-Arnott & Law, 1996). Fluctuations in water table height between sample sites, reduces or increases the total volume of sediment available for deposition.

Aquifer levels therefore have the potential to affect cross-shore aeolian sediment deposition. Lower aquifer levels cause the seepage face to occur further seaward towards the swash zone, extending the width of the beach during the ebb tide. The extended beach width results in an increased fetch and a greater sediment source for cross-shore sediment transport. Aquifers that drain more readily therefore, provide a greater sediment source more promptly following events that raise the water table (rainfall, storm surge, flood tide infiltration). In the case of Matakana Island where the onshore component of cross-shore aeolian sediment transport dominates, the more readily draining aquifer caused by *Spinifex serעיus* provides a greater sediment source for onshore aeolian sediment transport. The aquifers drain more readily following storm events and flood tides, increasing the potential sediment budget of the dunes.

### 5.4.3 Limitations with Results

This chapter suggests patterns in aeolian sediment transport on Matakana Island, stemming from differences in vegetation. It is however recognised that the aeolian sediment transport data, and therefore the resulting conclusions are limited. With only three recorded sediment trap deployments, average sediment transport rates during storm events were impossible to deduce. A more developed deployment plan, as well as easier site access would have benefitted data collection and the conclusions made. Higher frequency sampling would have allowed a greater reliability in the coupling of strong wind and sediment transport events. Furthermore, sampling at frequencies as high as hourly intervals would have provided the data required to effectively suggest a more reliable site threshold velocity, primary direction of source sediment and the difference in sediment deposition throughout the dune at each site. A more detailed approach towards the measurement of aeolian sediment transport is recommended for any future work surrounding this process.

### 5.4.4 Further Research

Both *Ammophila* and *Spinifex* are recognised for their effectiveness as sand binders, through their stem and leaf characteristics as well as root growth and density (Van der Putten *et al*, 1989; Maze and Whalley, 1990). Although no exploration into the differences in root densities between species was conducted over the course of this study due to time constraints, root density is recognised as a potential contributor to the compaction of sediment within the dune. In Chapter 3 the growth patterns of *Ammophila* at site A were shown to be greater in density than those of *Spinifex* at site B. Differences in growth densities between species may or may not lead to differences in root densities between sites effecting sediment compaction. At current there appears to be no research comparing the in-situ root densities of *Ammophila* and *Spinifex*. Assessing root densities is a difficult process, with complete root system extraction very laborious and an unknown fraction of roots are lost during the process (Kummerow, 1978). However, it is suggested that quantitative root extractions taken from a number of cores across the cross-shore dune profile at each site would give some indication into differences in root densities between sites. Further research comparing root

densities of *Ammophila* and *Spinifex* are recommended to further establish dune forming mechanisms of each species.

## 5.5 CONCLUSIONS

Analysis of vegetation impacts on aeolian sediment transport rates on Matakana Island displayed results suggested as typical across New Zealand by the literature (Esler, 1970; Maze & Whalley, 1992; Hilton *et al*, 2005). Transport results further distinguished between the two beach types as characterised in Chapter 3, whilst further stressing the complexity of the coastal system and the benefits that can be gained from its understanding. The following conclusions have been drawn from the analysis of aeolian sediment transport rates:

- Aeolian sediment deposition varies greatly across the cross-shore profile. Variations arise from a combination of factors, with wind speed and direction, rainfall, humidity, sediment moisture content and surface vegetation all influencing sediment transport rates.
- The long-shore component of aeolian sediment transport may exceed the cross-shore component but is considered less significant due to the north to east direction that strong local winds predominate.
- A small beach width at high tide combined with storm surge and wave run-up during periods of high winds, led to onshore aeolian transport rates becoming fetch limited. Transport rates were further limited when strong winds coincided with rainfall. In these instances, sediment transport is suggested to have taken place during the beginning of the wind event prior to rainfall.
- Sediment deposition was evenly distributed in the *Spinifex* dominated dune system as opposed to deposition in the *Ammophila* dominated dune, which occurred primarily at the seaward side of vegetation growth in the foredune. This pattern stems from the characteristics of each species, primarily their average height and growth density.
- The different sediment deposition rates between sites explain the differences in sediment compaction observed in Chapter 3 through the more frequent deposition of aeolian sediment. This compaction difference

alters dune porosity and permeability, effecting groundwater movement as discussed in Chapter 4.

The key suggestion surrounding the aeolian sediment transport rates discussed in this chapter is the ability of *Spinifex* to promote a more even distribution of aeolian deposited sediment throughout the dune when compared to *Ammophila*. An even deposition of sediment through the dune helps to create a more porous and permeable dune. Dunes with greater porosity and permeability allow groundwater beneath the dune to drain more readily, with lower groundwater levels increasing swash infiltration and sediment availability for further onshore aeolian transport.

# **CHAPTER SIX**

## **SUMMARY AND RECOMENDATIONS**

---

### **6.1 INTRODUCTION**

The purpose of this investigation was to ascertain if varying species of dune vegetation have an impact on unconfined coastal aquifers, primarily during and directly following, seasonal short term storm events on Matakana Island. A secondary aim of establishing differences in aeolian sediment movement between two neighbouring dune systems comprised of different vegetation species was also investigated. The data set was collected between March and November, 2010. Analysis identified both short-term and longer-term variations between sample sites. The conclusions presented in this chapter relate to the expected outcomes and hypotheses outlined within each previous chapter.

### **6.2 SAND DUNE CLASSIFICATION**

In Chapter 3, each sample site was given an overall classification in order to distinguish between sites; attribute variation in aeolian sediment transport; and aquifer fluctuation to different sand dune classifications. Classification is as follows:

#### Site A

- Narrow intermediate beach comprised of medium sand
- Sediment is more poorly sorted with a larger mean grain size when compared to site B
- Sediment porosity less than site B
- Incipient foredune dominated by *Ammophila arenaria*

#### Site B

- Narrow intermediate beach comprised of medium sand
- Sediment is better sorted with a smaller mean grain size when compared to site A
- Sediment porosity greater than site A
- Incipient foredune dominated by *Spinifex sericeus*

### 6.3 SHORT-TERM AQUIFER FLUCTUATION

Chapter 4 described variation in short-term aquifer fluctuations between sites. The key findings are as follows:

- Matakana Island aquifer levels beneath the dune face were highly variable. Fluctuations were a product and mixture of short-term and long-term change as a result of a range of factors including tide, rainfall and profile shape.
- Short-term fluctuations in aquifer level occurred as a result of tidal forcing. The fluctuations were asymmetrical in the aquifer compared to symmetrical offshore, as their shape is a function of beach drainage capability and the amount of groundwater contained in the upper slope of the profile.
- Longer-term changes in the profile of the beach influenced average aquifer levels, with an accreting beach resulting in an elevating average aquifer level and an eroding beach resulting in a diminishing aquifer level.
- Lower sediment permeability in the *Ammophila* dominated dune system hindered the movement of groundwater, resulting in the *Spinifex* dominated dune system filling and draining more readily.

### 6.4 AEOLIAN SEDIMENT TRANSPORT

Chapter 5 described variations in aeolian sediment transport between sampled sites. The key findings are as follows:

- Aeolian sediment deposition varies greatly through the cross-shore profile. Variations arise from a combination of factors with wind speed and direction; rainfall; humidity; sediment moisture content; and surface vegetation all influencing sediment transport rates.
- The long-shore component of aeolian sediment transport has the potential to exceed the cross-shore component, but is considered less significant due to the north through east direction that strong local winds predominate.
- A small beach width at high tide combined with storm surge and wave run-up during periods of high winds, induce fetch limited onshore aeolian transport rates. Transport rates were further limited where strong winds

coincided with rainfall. In these instances, sediment transport is suggested to have taken place during the beginning of the wind event prior to rainfall.

- Sediment deposition was evenly distributed in the *Spinifex* dominated dune system as opposed to strong deposition at the seaward limit of vegetation in the *Ammophila* dominated dune. This pattern stems from the characteristics of each species, primarily their average height and growth density.
- The different sediment deposition rates between sites explain the differences in sediment compaction observed in Chapter 3 through the more frequent deposition of aeolian sediment. The compaction difference alters dune porosity and permeability, effecting groundwater movement.

## 6.5 SUMMARY

The key suggestion surrounding the beach face groundwater dynamics, discussed in this thesis, is the ability of *Spinifex* to provide a dune that allows more readily flowing groundwater movement beneath the dune when compared to *Ammophila*. This supports the original hypothesis that *Spinifex* is well equipped at creating a more porous and permeable dune. Differences in sediment compaction between sites give rise to these porosity and permeability differences, with the differences suggested to have partially stemmed from variations in aeolian sediment transport rates between dune types.

*Spinifex* showed the ability to promote a more even distribution of aeolian deposited sediment throughout the dune when compared to *Ammophila*, where deposition was primarily seen at the seaward limit of vegetation. *Ammophila* showed a greater restraining effect on sediment around vegetation through its density, further promoting the compaction of its surrounding sediment. *Ammophila* did show its ability as an established sand binder when compared to sites with little to no vegetation, proving its worth in un-vegetated dune where sediment encroachment is problematic.

The superior drainage capabilities of *Spinifex* dune increase the potential for swash infiltration during the flood tide and reduce the potential for sediment

fluidisation during the ebb tide. Lower groundwater levels increase sediment availability for further onshore aeolian transport through the widening of unsaturated beach. These abilities combined make *Spinifex* more adept than *Ammophila* at mitigating and reducing the effects of erosion on Bay of Plenty beaches.

Based on the findings of this thesis, it is recommended that areas of the Bay of Plenty coastline undergoing dune rehabilitation be planted with the native sand binder *Spinifex sericeus*. It has been shown to promote the growth of dunes of a desirable shape and porosity for the area.

## **6.6 RECOMENDATIONS FOR FUTURE RESEARCH**

Results suggested in this thesis prompt the following recommendations for further research:

- Instrument complications saw a comparison between wind speeds at plant height unmanageable. Comparisons between wind speeds at multiple heights through the cross-shore profile of both sample sites would give a greater understanding as to the differences in wind speed induced by sections of vegetation and their density.
- Sampling of in-situ sediment and root density at various depths through the vegetated section of the cross-shore profile would provide a more quantitative approach when determining permeability and porosity differences between dune types. Sampling of root density of each species would reveal possible links between this and sediment density.
- Sampling of aquifer fluctuation was conducted from a single point in the foredune at each site. Greater aquifer sampling both spatially and temporally would provide a more quantitative approach when deducing variations in aquifer fluctuations between sites. Further piezometer deployment in both the cross-shore and long-shore aspects would achieve this, with higher frequency sampling through the beach during and directly following storm events recommended.

- Higher frequency profile sampling coupled with water table fluctuation would provide more insight into the response of average beach water table levels following changes in beach profile shape.
- Aquifer sampling at different sites where the cross-shore profile varied to that presented in this study would determine whether similar behaviour is displayed in all *Spinifex/Ammophila* comparisons.
- It is recognised that aeolian sediment transport data, and therefore transport results and conclusions are limited. Aeolian sediment sampling at a much greater frequency would make attributing sediment deposition to particular wind events, assignment of a threshold velocity and attributing a main source direction more accurate. Thus providing further understanding of differences between *Ammophila* and *Spinifex*.



## REFERENCES

---

- Aagaard, T., Davidson-Arnott, R., Greenwood, B., & Nielsen, J. (2004). Sediment supply from shoreface to dunes: Linking sediment transport measurements and long-term morphological evolution. *Geomorphology*, 60, 205-224.
- Anthony, E.J. (2005). Beach Erosion. *Encyclopaedia of Coastal Science*, 140-145 M.L. Schwartz. The Netherlands, Springer. 1211
- Arens, S.M. (1996). Rates of aeolian sediment transport in a temperate humid climate. *Geomorphology*, 17, 3-18.
- Arens, S.M., & van der Lee, G.E.M. (1993). Saltation sand traps for the measurement of Aeolian transport into the foredunes. *Soil Technology*, 8, 61-74.
- Baas, A.C.W. (2007). Complex systems in aeolian geomorphology. *Geomorphology*, 91, 311-331.
- Bagnold, R.A. (1941 reprinted 1960). *The Physics of Blown Sand and Desert Dunes*. London: Methuen, 265p.
- Baird, A.J., & Horn, D.P. (1996). Monitoring and modelling groundwater behaviour in sandy beaches. *Journal of Coastal Research*, 12 (3), 630-640.
- Bauer, B.O., Davidson-Arnott, R.G.D, Hep, P.A., Namikas, S.L., Ollerhead, J., & Walker, I.J. (2009). Aeolian sediment transport on a beach: Surface moisture, wind fetch, and mean transport. *Geomorphology*, 105, 106-116.
- Bird, E. (2008). *Coastal Geomorphology: An Introduction, Second edition*. John Wiley & Sons, Ltd. The Atrium, Southern Gate, Chichester.
- Bressolier, C., & Thomas, Y. (1977). Studies on wind and plant interactions on French Atlantic coastal dunes. *Journal of Sedimentary Petrology*, 47, (1), 331-338.
- Bruun, P. (1989). The coastal drain: What can it do or not do? *Journal of Coastal Research*, 5 (1), 123-125.
- Buell, A.C., Pickart, A.J., & Stuart, J.D. (1995). Introduction history and invasion patterns of *Ammophila arenaria* on the North Coast of California. *Conservation Biology*, 9, 1587-1593.
- Carter, R.W.G. (1991). Near-future sea level impacts on coastal dune landscapes. *Landscape Ecology*, 6, (1/2), 29-39.
- Carter, R.W.G., & Wilson, P. (1993). Aeolian processes and deposits in northwest Ireland. *Geological society, London, Special publications*, 72, 173-190.

- Chappell, J., Eliot, I.G., Bradshaw, M.P., & Lonsdale, E. (1979). Experimental control of beach face dynamics by water table pumping. *Engineering Geology*, 77, 319-326.
- Clarke, D.J., & Eliot, I.G. (1987). Groundwater-level changes in a coastal dune, sea-level fluctuations and shoreline movement on a sandy beach. *Marine Geology*, 77, 319-326.
- Clements, A., Simmonds, A., Hazelton, P., Inwood, C., Woolcock, C., Markovina, A., & O'Sullivan, P. (2010). Construction of an environmentally sustainable development on a modified coastal sand mined and landfill site – Part 2. Re-Establishing the natural ecosystems on the reconstructed beach dunes. *Sustainability*, 2, 717-741.
- Coastal Engineering Manual. (2008). *Part III, Chapter 4, Wind Blown Sediment Transport*. Report Number: EM1110-2-1100.
- Cockayne, L. (1911). *Report on the dune-areas of New Zealand: Their geology, botany and reclamation*. Department of Lands, Wellington, 76.
- Curry, C., Bennett, R., Hulbert, M., Curry, K., & Faas, R. 2004. Comparative study of sand porosity and a technique for determining porosity of undisturbed marine sediment. *Marine Geosources and Geotechnology*, 22, 4, 231-252.
- Davidson-Arnott, R.G.D., & Law, M.N. (1996). Measurement and prediction of long-term sediment supply to coastal foredunes. *Journal of Coastal Research*, 12, 3, 654-663.
- Dean, R.G. (1977). *Equilibrium beach profiles: U.S. Atlantic and Gulf Coasts*. Ocean Engineering Report. No. 12, Department of Civil Engineering, University of Delaware.
- Duncan, J.R. (1964). The effects of water table and tide cycle on swash-backwash sediment distribution and beach profile development. *Marine Geology*, 2, 186-197.
- Eliot, I.G., & Clarke, D.J. (1988). Semi-diurnal variation in beach face aggradation and degradation. *Marine Geology*, 79, 1-22.
- Esler, A.E. (1970). Manawatu sand dune vegetation. *Proceedings of the New Zealand Ecological Society*, 17, 41-46
- Gadgil, R.L. (2002). Marram Grass (*Ammophila Arenaria*) and coastal stability in New Zealand. *New Zealand Journal of Forestry Science*, 32.
- Gillette, D.A., Marticorea, B., & Bergametti, G. (1998). Change in the aerodynamic roughness height by saltating grains: experimental assessment, test of theory, and operational parameterization. *Journal of Geophysical Research*, 103, 6203-6209.

- Hertling, U.M & Lubke, R.A. (1999b). Indigenous and *Ammophila arenaria* dominated dune vegetation on the South African Cape coast. *Applied Vegetation Science*, 2, 157-168.
- Hilton, M.J., Macauley, U., & Henderson, R. (2000). Inventory of New Zealand's active dune lands. *Science for Conservation*, 157. Wellington, Department of Conservation, 34.
- Hilton, M., Duncan, M., & Jul, A. (2005). Processes of *Ammophila arenaria* (Marram Grass) Invasion and Indigenous Species Displacement, Stewart Island, New Zealand. *Journal of Coastal Research*, 21(1), 175-185
- Hilton, M. (2006). The loss of New Zealand's active dunes and the spread of marram grass (*Ammophila arenaria*). *New Zealand Geographer*, 62, 105-120
- Hope-Simpson, J.F & Jefferies, R.L. (1966). Observations relating to vigour and debility in marram grass (*Ammophila arenaria* (L.) Link). *Journal of Ecology*, 54, 271-275
- Horn, D.P. (2002). Beach groundwater dynamics. *Geomorphology*, 48, 121-146
- Horn, D.P. (2005). Hydrology of the coastline. *Encyclopaedia of Coastal Science*. M.L. Schwartz. The Netherlands, Springer. 1211
- Horn, D.P. (2006). Measurement and modelling of beach groundwater flow in the swash zone: a review. *Continental Shelf Research*, 26 (5), 622-652
- Hsu, S.A. (1974). Computing eolian sand transport from routine weather data. *Proceedings, 14<sup>th</sup> Conference on Coastal Engineering*, ASCE, New York, 1619-1626
- Huiskes, A.H.L. (1980). The effects of habitat perturbation on leaf populations of *Ammophila arenaria* (L.) Link. *Acta Botanica Neerlandica*, 29, 443-450
- Isla, F.I., & Bujalesky, G.G. (2005). Groundwater dynamics on macrotidal gravel beaches of Tierra del Fuego, Argentina. *Journal of Coastal Research*, 21 (1), 65-72.
- Jackson, D.W.T., & Cooper, J.A.G. (1999). Beach fetch distance and aeolian sediment transport. *Sedimentology*, 46, 517-522.
- Jamieson, S.L. (2010). *Sand dune restoration in New Zealand: Methods, Motives and Monitoring*. (unpublished MSc thesis). Victoria University of Wellington, New Zealand.
- Kraus, N.C. (2005). Beach Profile. *Encyclopaedia of Coastal Science*, 169-172 M.L. Schwartz. The Netherlands, Springer. 1211

- Kriebel, D.L., & Dean, R.G. (1985). Numerical simulation of time-dependent beach and dune erosion due to severe storms. *Coastal Engineering*, 9, 221-245
- Kummerow, J., Krause, D., & Jow, W. 1978. Seasonal changes of fine root density in the southern Californian chaparral. *Oecologia*, 37, 201-212.
- Kuriyama, Y., Mochizuki, N., & Nakashima T. (2005). Influence of vegetation on aeolian sand transport rate from a backshore to a foredune at Hasaki, Japan. *Sedimentology*, 52, 1123-1132.
- Lancaster, N., & Baas, A. (1998). Influence of vegetation cover on sand transport by wind: Field studies at Owens Lake, California. *Earth Surface Processes and Landforms*, 23, 69-82.
- Lanyon, J.A., Eliot, I.G., & Clarke, D.J. (1982). Groundwater-level variation during semidiurnal spring tidal cycles on a sandy beach. *Australian Journal of Marine and Freshwater Research*, 33, (3), 377-400.
- Leatherman, S.P. (1978). A new aeolian sand trap design. *Sedimentology*, 25, 303-306.
- Li, L., Barry, D.A., & Pattiaratchi, C.B. (1997). Numerical modelling of tide-induced beach water table fluctuations. *Coastal Engineering*, 30, 105-123.
- Li, L., Horn, D. P., & Baird, A. J. 2006. Tide-Induced variations in surface temperature and water table depth in the intertidal zone of a sandy beach. *Journal of Coastal Research*, 22, 6, 1370-1381
- List, J.H. (2005). Sediment Budget. *Encyclopaedia of Coastal Science*. M.L. Schwartz. The Netherlands, Springer. 1211
- Livingstone, I., & Warren, A. (1996). *Aeolian Geomorphology: An Introduction*. Addison Wesley Longman, Harlow. 211p.
- Macky, G. H., Latimer, G. J., & Smith, R. K. (1995). Wave climate of the western Bay of Plenty, New Zealand, 1991-93. *New Zealand Journal of Marine and Freshwater Research*. 29, 311-327
- Marshall, J.K. (1965). *Corynephorus canescens* (L.) P. Beauv. As a model for the *Ammophila* problem. *Journal of Ecology*, 53, 447-465
- Marui, A., & Yasuhara, M. (1993). Subsurface water movement and transmission of rainwater pressure through a clay layer. *Hydrology of Warm Humid Regions*, (Proceedings of the Yokohama Symposium), 216.
- Maze, K.M., & Whalley, R.D.B. (1990). Resource allocation patterns in *spinifex sericeus* R.Br.: A dioecious perennial grass of coastal sand dunes. *Australian Journal of Ecology*, 15, 145-153.

- Maze, K.M., & Whalley, R.D.B. (1992). Effects of salts spray and sand burial on *Spinifex sericeus* R.Br. *Australian Journal of Ecology*, 17, 9-19
- McEwan, I.K. (1993). Bagnold's kink: a physical feature of a wind velocity profile modified by blown sand. *Earth Surface Processes and Landforms*, 18, 145-156.
- McEwan, I.K., & Willetts, B.B. (1993). Sand transport by wind: a review of the current conceptual model. *The Dynamics and Environmental Context of Aeolian Sedimentary Systems*. Geological Society Special Publication, 72, 7-16.
- Moore, P. & Davis, A. (2004). Marram Grass *Ammophila arenaria* removal and dune restoration to enhance nesting habitat of Chatham Island oyster catcher *Haematopus chathamensis*, Chatham Island, New Zealand. *Conservation Evidence*, 1, 8-9.
- Muasya, A.M., & de Lange, P.J. (2010). *Ficinia siprialis* (Cyperaceae) a new genus and combination for *Desmoschoenus spirialis*. *New Zealand Journal of Botany*, 48, 1, 31-39.
- Nielsen, P. 1990. Tidal dynamics of the water table in beaches. *Water Resources Research*, 26, 2127-2134
- Nygaard, R., Gutierrez, M., Gautam, R., & Hoeg, K. 2004. Compaction behaviour of argillaceous sediments as function of diagenesis. *Marine and Petroleum Geology*, 21, 349-362
- Okoli, R.E. (2003). Wind tunnel study on aeolian saltation dynamics and mass flow. *Journal of Arid Environments*, 53, 569-583.
- Pye, K. (1993). Introduction: the nature and significance of Aeolian sedimentary systems. *The Dynamics and Environmental Context of Aeolian Sedimentary Systems*. Geological Society Special Publication, 72, 1-4.
- Rehbinder, G. 1978. Measurement of the average pore velocity of water flowing through a rock specimen. *Rock Mechanics*, 11, 19-28.
- Rhew, H.S., & Yu, K.B. (2009). Pattern of aeolian sand transport and morphological change in the foredune ridge, Shindu dunefield, Korea: A case study during the winter, December 2000 to March 2001. *Journal of Coastal Research*, 25, (4), 1015-1024.
- Sawyer, J.D. (2004). *Plant conservation strategy: Wellington Conservancy 2004-2010*. Wellington, Department of Conservation.
- Skykes, M.T., & Wilson, J.B. (1991). Vegetation of a coastal sand dune system in Southern New Zealand. *Journal of Vegetation Science*, 2(4), 531-538

- Sherman, D.J., & Hotta, S. (1990). Aeolian sediment transport: theory and measurements. In: *Coastal Dunes: Form and Process*. Nordtrom, K.F., Psuty, N.P., Carter, R.W.G. (Eds). John Wiley & Sons, Chichester, 17-37.
- Sherman, D.J. (2005). Dissipative Beaches. *Encyclopaedia of Coastal Science*, 389-390 M.L. Schwartz. The Netherlands, Springer. 1211
- Short, A.D., & Hesp, P.A. (1982). Wave, beach and dune interactions in South Eastern Australia. *Marine Geology*, 48, 259-284.
- Sonu, C.J., & Van Beek, J.L. (1971). Systematic beach changes on the outer banks, North Carolina. *Journal of Geology*, 79, 416-425.
- Steele, D.A. (1995) *Possible interactions between groundwater, a seawall and coastal processes: Impact on erosion at Waihi Beach, New Zealand*. (unpublished MSc thesis). University of Waikato, New Zealand.
- Svasek, J.N., & Terwindt, J.H.J. (1974). Measurements of sand transport by wind on a natural beach. *Sedimentology*, 21, 311-322
- Taylor, R. & Smith, I. (1997). *The state of New Zealand's environment (1997)*. Ministry for the Environment, Wellington.
- Turner, I. 1993. Water table outcropping on macro-tidal beaches: A simulation model. *Marine Geology*, 115, 227-238
- Turner, I.L. (1998). Monitoring groundwater dynamics in the littoral zone at seasonal, storm, tide and swash frequencies. *Coastal Engineering*, 35, 1-16.
- Turner, I.L., & Leatherman, S.P. (1997). Beach dewatering as a 'soft' engineering solution to coastal erosion – A history and critical review. *Journal of Coastal Research*, 13 (4), 1050-1063.
- Turner, I.L., & Nielsen, P. (1997). Rapid water table fluctuations within the beach face: Implications for swash zone sediment transport. *Coastal Engineering*, 32, 45-59
- Urish, D.W., & McKenna, T.E. (2004). Tidal effects on ground water discharge through a sandy marine beach. *Ground Water*, 42, (7), 971-982.
- van der Putten, W.H., Van der Werf-Klein Breteler, J.T. & Van Dijk, C. (1989). Colonization of the root zone of *Ammophila arenaria* by harmful soil organisms. *Plant and Soil*, 120, 213-223
- van der Wal, D. (1998). The impact of the grain-size distribution of nourishment sand on aeolian sand transport. *Journal of Coastal Research*, 14, 2, 620-631.
- Vesterby, H. (2000). *Modelling groundwater flow in beach profiles for optimising stabilising measures*. International Coastal Symposium. Rotorua, New Zealand.

- Wal, A., & McManus, J. (1993). Wind regime and sand transport on a coastal beach-dune complex, Tentsmuir, eastern Scotland. *The Dynamics and Environmental Context of Aeolian Sedimentary Systems*. Geological Society Special Publication, 72, 159-171.
- Weisman, R.N., Seidel, G.S., & Ogden, M.R. (1995). Effect of water-table manipulation on beach profiles. *Journal of Waterway, Port, Coastal, and Ocean Engineering*, 121 (2), 134-142
- Willis, A.J. (1965). The influence of mineral nutrients on the growth of *Ammophila arenaria*. *Journal of Ecology*, 53, 735-745
- Xun, Z., Chuanxia, R., Yanyan, Y., Bin, F., & Yecheng, O. (2006). Tidal effects of groundwater levels in the coastal aquifers near Beihai, China. *Environmental Geology*, 51, 517-525.



***APPENDIX I***  
***SEDIMENT COMPACTION TABLE***

---

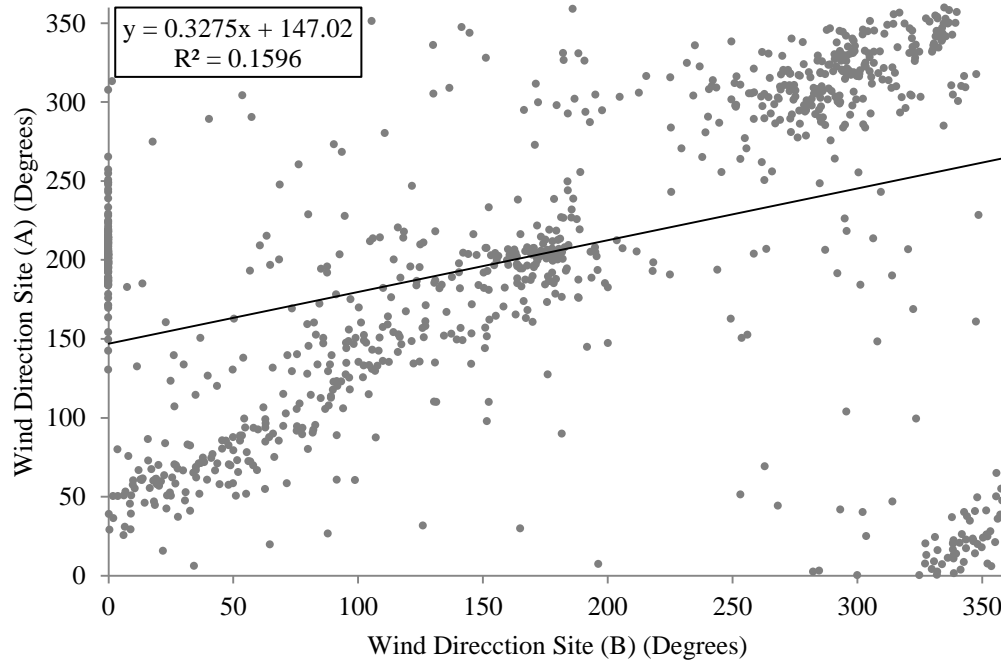
**Table I.1:** Scala Penetrometer penetration averages per one blow, across the swale to beach profile

| <b>Profile</b>    | <b>Swale</b>            | <b>Dune 1</b>           | <b>Dune 2</b>           | <b>Foredune</b>         | <b>Beach</b>            |
|-------------------|-------------------------|-------------------------|-------------------------|-------------------------|-------------------------|
| <b>Position</b>   | <b>Penetration (mm)</b> |
| <b>Marram</b>     |                         |                         |                         |                         |                         |
| <b>Average</b>    | 156                     | 93                      | 111                     | 93                      | 91                      |
| <b>Spinifex</b>   |                         |                         |                         |                         |                         |
| <b>Average</b>    | 156                     | 163                     | 135                     | 86                      | 98                      |
| <b>Difference</b> | 0                       | 70                      | 23                      | 6                       | 6                       |



## APPENDIX II

### WIND DATA



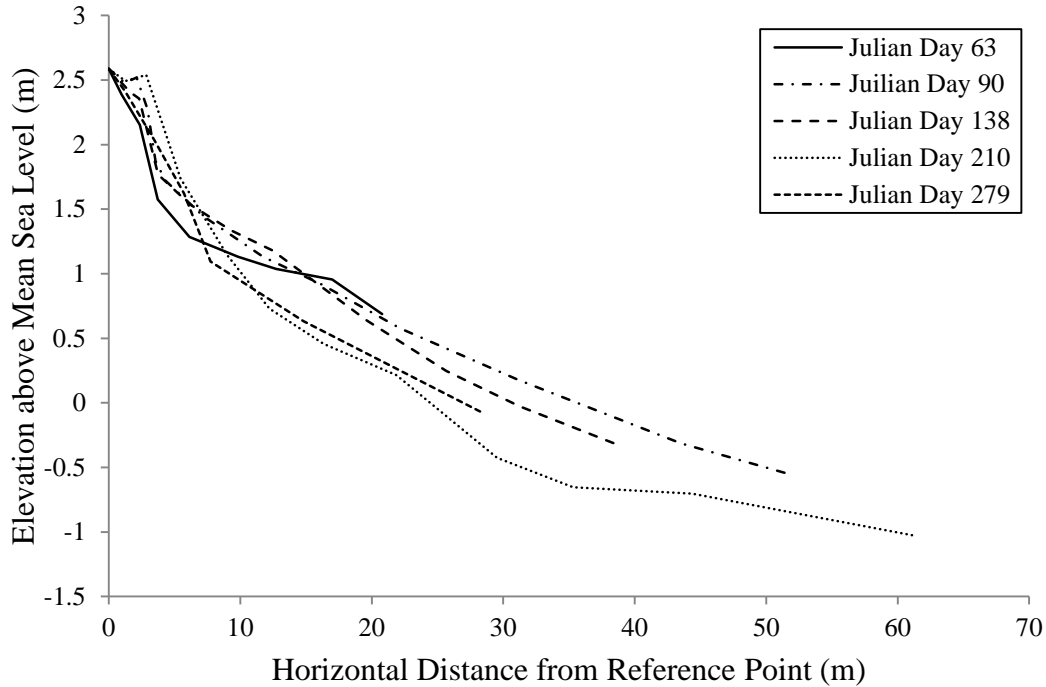
**Figure II.1:** Uncorrected correlation between wind directions at site A and site B. Site A wind directions were measured at a height of 4 metres above dune. Site B wind directions were measured at a height of 0.8 metres above dune. R squared value and equation of the line of best fit are displayed on the figure.

Figure II.1 shows the uncorrected wind correlation plot discussed in Chapter 4. Obvious outliers occur clustered around a wind direction of  $350^\circ$  (x-axis) and  $25^\circ$  (y-axis). This cluster of outliers was attributed to a directional re-orientation of the sampling station at site A. A second set of outliers appear as zero values along the x-axis, with outliers in this case attributed to instrument error.



# APPENDIX III

## PROFILE PLOTS



**Figure III.1:** Beach profiles above mean sea level (MSL) at site A for days 63, 90, 138, 210 and 279, showing beach profile evolution in 2010

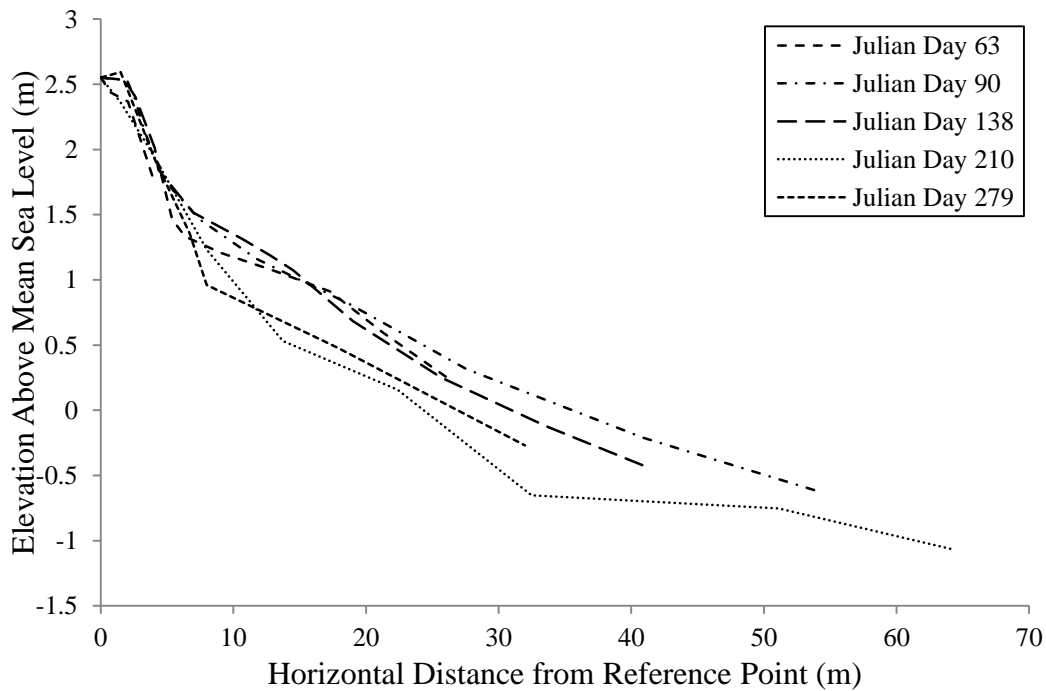


**Figure III.2:** Beach profiles above mean sea level (MSL) at site B for days 63, 90, 138, 210 and 279, showing beach profile evolution in 2010

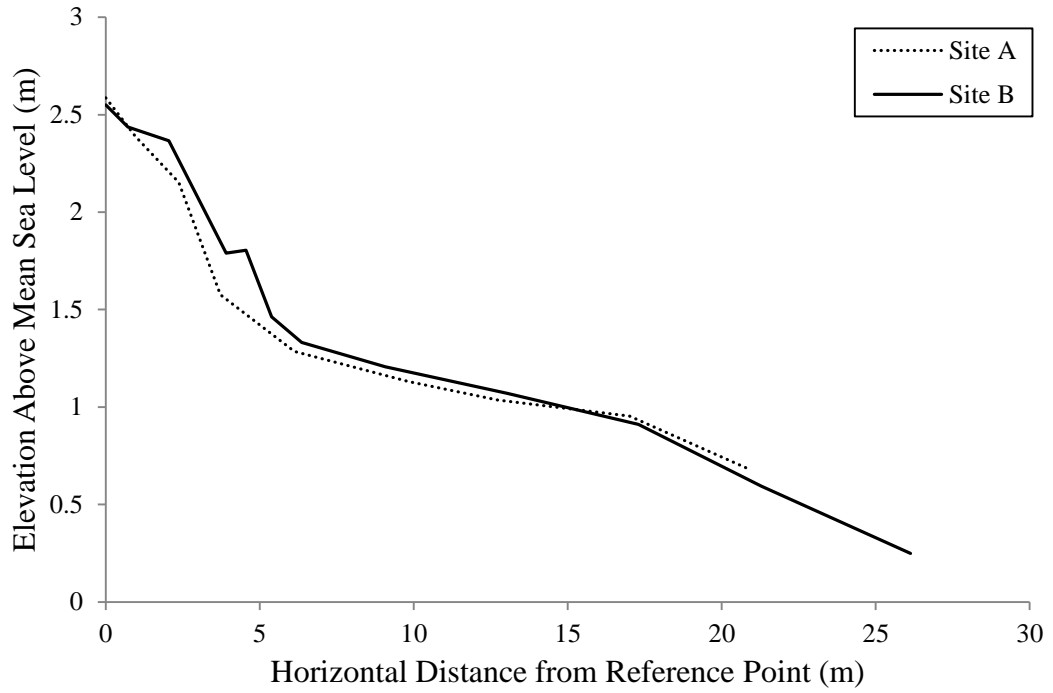


**Figure III.3:** Beach profiles above mean sea level (MSL) at sites A and B for Julian Day 63 in 2010.

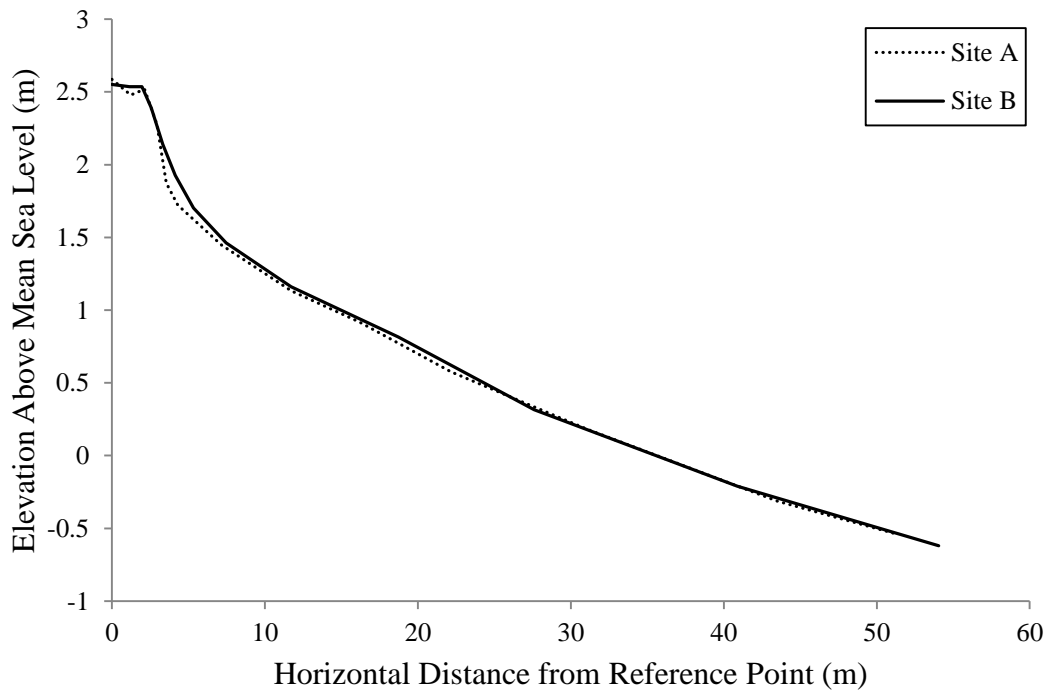


**Figure III.4:** Beach profiles above mean sea level (MSL) at sites A and B for Julian Day 90 in 2010.

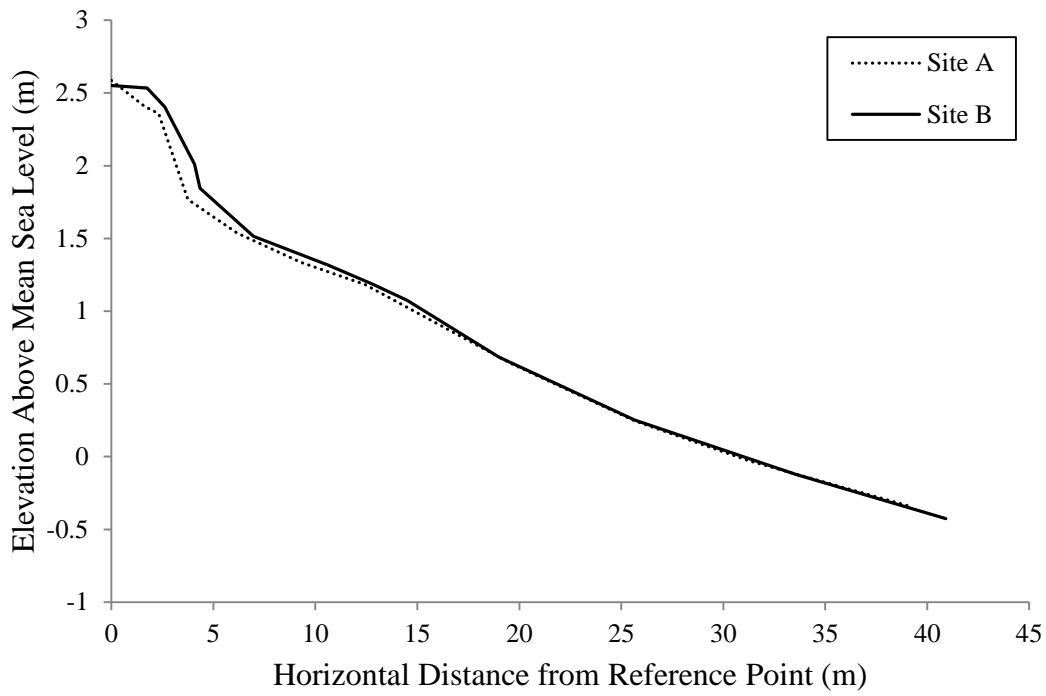


**Figure III.5:** Beach profiles above mean sea level (MSL) at sites A and B for Julian Day 138 in 2010.

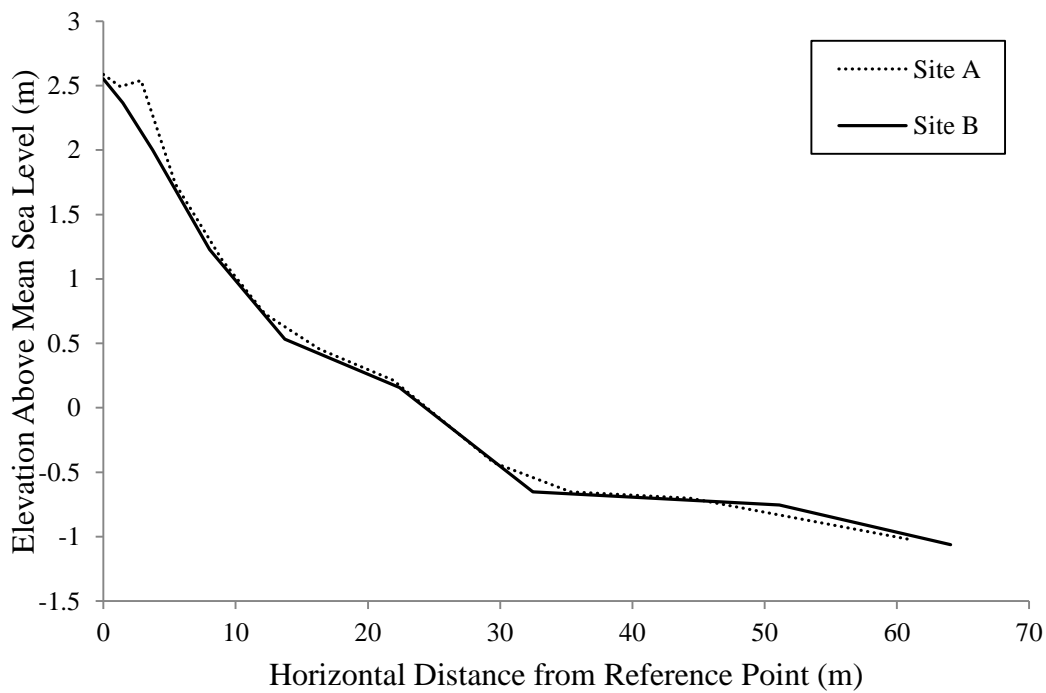


**Figure III.6:** Beach profiles above mean sea level (MSL) at sites A and B for Julian Day 210 in 2010.

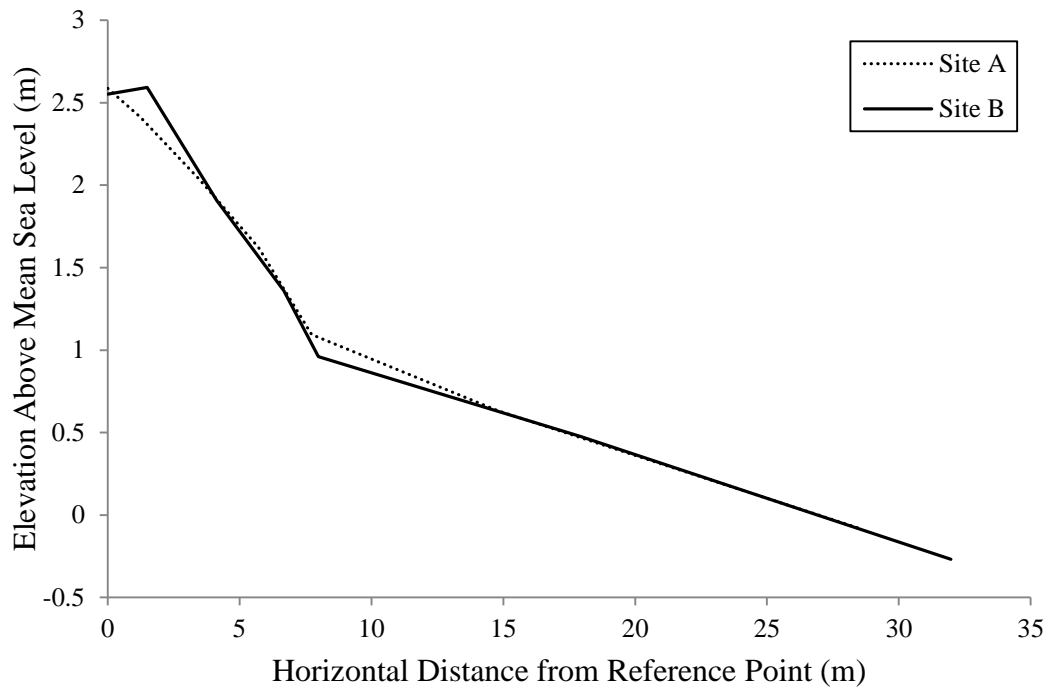


**Figure III.7:** Beach profiles above mean sea level (MSL) at sites A and B for Julian Day 279 in 2010.